Bacterial Transformation of Glyphosate and Related Organophosphonates

Dissertation

der Mathematisch-Naturwissenschaftlichen Fakultät

der Eberhard Karls Universität Tübingen

zur Erlangung des Grades eines

Doktors der Naturwissenschaften

(Dr. rer. nat.)

vorgelegt von

M.Sc. Kleanthi Kourtaki

aus Chania, Griechenland

Tübingen

2025

Gedruckt mit Genehmigung der Mathematisch-Naturwissenschaftlichen Fakultät
der Eberhard Karls Universität Tübingen.

Tag der mündlichen Qualifikation:	24.11.2025
Dekan:	Prof. Dr. Thilo Stehle
1. Berichterstatter/-in:	Prof. Dr. Stefan Haderlein
2. Berichterstatter/-in:	Prof. Dr. Peter Grathwohl

Abstract

Aminophosphonates (APs) are a class of organophosphorus compounds featured by carbon–phosphorus (C–P bond(s)), widely used in agriculture, industry, and domestic products due to their chelating, scale-inhibiting, and herbicidal properties. Among them, glyphosate, used globally as a non-selective herbicide, and its main metabolite, aminomethylphosphonate AMPA, are the most prominent representatives. Aminopolyphosphonates (APPs)-with multiple C–P bonds such as aminotris(methylenephosphonate) (ATMP) and diethylenetriamine penta(methylenephosphonate) (DTPMP)–are commonly applied in water treatment, detergents, and industrial processes. Due to their extensive production and application, APPs, are released into soils, surface waters, and wastewater streams, where they also accumulate as environmental contaminants. The environmental fate of A(P)Ps is determined by their high chemical stability, resistance to hydrolysis, strong affinity for sorption, inefficient removal during wastewater treatment, and poor biodegradability. Of all mitigation processes, biodegradation stands out as the main process, potentially capable of permanently eliminating A(P)Ps from the environment. Research in this field originated with the isolation and characterization of microbial strains capable of using glyphosate, the most prominent AP, as a nutrient source. While the biodegradability of glyphosate and other amino(mono)phosphonates has been well-studied, certain key parameters and environmental conditions have often been overlooked, making it unclear whether these observations hold for real environments that differ significantly in e.g., nutrient availability, microbial diversity, and mineral content. Whether comparable microbial pathways can also drive the transformation or degradation of other A(P)Ps remains unresolved—an issue of growing importance given recent findings that identify APPs as precursors of both glyphosate and its major breakdown product, AMPA. This provides new insights into the biodegradability of A(P)Ps under different conditions, and evaluates how this biodegradability translates to real-world effectiveness in reducing their environmental impact.

The first objective of this study was to evaluate glyphosate biotransformation under conditions where multiple substrates compete, particularly in the presence of another AP with one or two C–P bonds serving as an additional phosphorus (P)-source. Although glyphosate is known for its high biotransformation potential, most previous experiments were conducted under controlled, P-limited laboratory settings. However, in real environments where glyphosate is found in soil and water, it often coexists with other APs, such as AMPA. Batch experiments with two bacterial strains and binary mixtures of glyphosate and another aminomonophosphonate as P-source revealed that glyphosate was consistently the least preferred substrate. Its uptake was slower than that of the other P-source, or occurred only after the second compound was depleted. With diphosphonate compounds as the second P-source, however, bacteria always utilized glyphosate first, and the diphosphonate was taken up sequentially. These results demonstrate that both the presence and the type of co-occurring P-sources significantly affect

glyphosate degradation. As a result, the high biotransformation rates commonly observed in P-limited laboratory experiments with glyphosate as the sole P-source may not accurately represent glyphosate's fate in natural environments where it coexists with a mixture of P-containing compounds.

In the second part of this study, the biotransformation potential of glyphosate and AMPA in the presence of a mineral sorbent was evaluated. In natural environments, microorganisms interact within complex soil–water systems, where ionic APs, such as glyphosate and AMPA, have a strong affinity for binding to positively charged mineral surfaces. This causes these compounds to partition between the aqueous phase and the mineral-bound (sorbed) phase. Sorbed fractions are often considered less bioavailable, which is generally thought to reduce their biotransformation potential. To test this, goethite — a common and environmentally relevant iron (oxyhydr)oxide mineral with high sorption capacity for glyphosate and AMPA – was used as a model sorbent. Batch experiments were conducted with goethite suspensions and glyphosate and/or AMPA, and the results were compared to sorbent-free controls. The presence of goethite did not retard the microbial degradation of either compound, regardless of whether they were introduced individually or together. Contrary to common expectations that AMPA would persist due to sorption, our results indicate that the sorbed fractions remained bioavailable to the tested bacterial strains. No effects on biodegradation rates were observed, suggesting that under the tested conditions, mineral sorption does not necessarily limit the biotransformation of glyphosate and AMPA.

In the third part of this thesis, the biodegradability of higher APPs—containing three or more C–P bonds—in bacterial growth media was critically examined. While earlier studies reported significant biodegradation by bacterial strains using these compounds as P-sources, those experiments were conducted in media containing dissolved manganese (Mn(II)), a known mediator for the abiotic oxidation of higher APPs by molecular oxygen. Batch experiments showed rapid transformation of aminotris(methylenephosphonate) (ATMP) and ethylenediamine–tetramethylenephosphonate (EDTMP) in growth media both with and without bacterial cells. Transformation was primarily driven by even trace levels of dissolved Mn(II), rather than by bacterial activity. The identification of transformation products further confirmed that both compounds underwent abiotic degradation in the absence of cells. A review of the existing literature, together with our findings, revealed a critical flaw in previous biodegradation studies of higher APPs and therefore questions the reported biodegradation potential in common cultivation media containing trace element solution.

Lastly, compound-specific isotope analysis (CSIA) was considered to study isotope effects during the biodegradation of APs such as glyphosate and AMPA. A key challenge for CSIA is the efficient separation of target analytes from abundant organic medium components — particularly glutamate, which is added at high

concentrations as a carbon source. To overcome this, two cleanup approaches were tested prior to CSIA: cation-exchange and surface complexation using aluminum oxide sorbent. The cation exchange method caused substantial losses of glyphosate and AMPA, whereas the aluminum oxide approach successfully reduced glutamate levels while maintaining analyte recovery. This enabled isotope analysis at early time points, although residual glutamate and possible transformation products still interfered with measurements at later stages. While our results represent only partial success, they demonstrate a key step toward establishing CSIA for studying glyphosate and AMPA biodegradation. Achieving the full potential of carbon CSIA will require more selective and efficient cleanup methods to ensure complete sample purification.

Overall, this thesis advances our understanding of the biodegradability of APs and APPs under more complex conditions, addressing important gaps related to environmental relevance and methodological challenges. By systematically investigating bacterial degradation in the presence of co-occurring P-sources, mineral sorbents, and under abiotic influences, this work reveals that critical previous assumptions do not necessarily hold in real-world settings. Altogether, this work provides novel insights that challenge established views on AP and APP degradability and lays the groundwork for more accurate environmental risk assessments and the development of improved analytical tools for studying these persistent pollutants.

Kurzfassung

Aminophosphonate (APs) sind eine Klasse organischer Phosphorverbindungen, die durch Kohlenstoff–Phosphor-Bindungen (C–P-Bindung(en)) gekennzeichnet

sind und aufgrund ihrer komplexbildenden, schuppenhemmenden und herbiziden Eigenschaften in Landwirtschaft, Industrie und Haushaltsprodukten weit verbreitet eingesetzt werden. Unter ihnen ist Glyphosat das bekannteste Beispiel, das weltweit als nicht-selektives Herbizid sowie durch sein Hauptmetabolit Aminomethylphosphonsäure (AMPA) von Bedeutung ist. Darüber hinaus werden Aminopolyphosphonate (APPs) – mit mehreren C–P-Bindungen, wie Aminotris(methylenphosphonat) (ATMP) und Diethylentriaminpenta(methylenphosphonat) (DTPMP) – häufig in der Wasseraufbereitung, in Reinigungsmitteln und in industriellen Prozessen eingesetzt. Aufgrund ihrer umfangreichen Produktion und Anwendung gelangen APPs in Böden, Oberflächengewässer und Abwasserströme, wo sie sich zudem als Umweltkontaminanten anreichern.

Das Umweltverhalten von A(P)Ps wird bestimmt von ihrer hohen chemischen Stabilität, Resistenz gegenüber Hydrolyse, starken Sorptionsaffinität, unvollständigen Entfernung in Kläranlagen und ihrer geringen biologischen Abbaubarkeit. Der biologische Abbau der einzige Prozess, der eine dauerhafte Eliminierung von A(P)Ps aus der Umwelt ermöglicht. Die Forschung in diesem Bereich begann mit der Isolierung und Charakterisierung von Mikroorganismen, die Glyphosat – den prominentesten Vertreter der APs – als Nährstoffquelle nutzen konnten. Während die biologische Abbaubarkeit von Glyphosat und anderen Amino(mono)phosphonaten bereits umfassend untersucht wurde, wurden bestimmte Schlüsselparameter und Umweltbedingungen häufig vernachlässigt. Daher ist unklar, ob diese Befunde auch für reale Umweltsysteme gelten, die sich z. B. in Nährstoffverfügbarkeit, mikrobieller Diversität und Feststoffgehalt deutlich unterscheiden. Ob vergleichbare mikrobielle Stoffwechselwege auch den Abbau anderer A(P)Ps ermöglichen können, ist bislang ungeklärt – eine Fragestellung, die zunehmend an Bedeutung gewinnt, da jüngste Studien APPs als Vorläufer von sowohl Glyphosat als auch dessen Hauptabbauprodukt AMPA identifiziert haben. Ziel dieser Arbeit war es daher, neue Erkenntnisse zur biologischen Abbaubarkeit von A(P)Ps unter verschiedenen Bedingungen zu gewinnen und deren Relevanz für eine wirksame Reduzierung der Umweltbelastung zu bewerten.

Der erste Schwerpunkt dieser Studie war die Untersuchung der Glyphosat-Biotransformation unter Bedingungen, bei denen mehrere P-haltige Substrate konkurrieren – insbesondere in Anwesenheit eines weiteren AP mit einer oder zwei C–P-Bindungen, das als zusätzliche Phosphorquelle dient. Obwohl Glyphosat für sein hohes Biotransformationspotenzial bekannt ist, basierte ein Großteil der bisherigen Forschung auf kontrollierten, phosphorlimitierten Laborsystemen mit Glyphosat als Einzelsubstanz. In natürlichen Umgebungen, in denen Glyphosat in Boden und Wasser vorkommt, tritt es jedoch häufig gemeinsam mit anderen APs, wie AMPA, auf. In Batch-Experimenten mit zwei Bakterienstämmen zeigte sich, dass Glyphosat im Wettbewerb mit einem anderen Aminomonophosphonat

durchweg die am wenigsten bevorzugte Phosphorquelle war. Seine Aufnahme erfolgte langsamer als die des Vergleichssubstrats oder erst nach dessen vollständigem Verbrauch. War die alternative P-Quelle hingegen ein Aminodiphosphonat, wurde Glyphosat stets zuerst abgebaut, während der Diphosphonat-Aufnahmeprozess sequenziell folgte. Diese Ergebnisse verdeutlichen, dass sowohl die Anwesenheit als auch die Art konkurrierender P-Quellen die Glyphosat-Degradation maßgeblich beeinflussen. Daraus folgt, dass die hohen Abbauraten, die in phosphorlimitierten Laborexperimenten beobachtet werden, nicht zwangsläufig das Verhalten von Glyphosat in natürlichen Systemen widerspiegeln, in denen es mit einer Vielzahl phosphorhaltiger Verbindungen koexistiert.

Im zweiten Teil dieser Studie wurde das Biotransformationspotenzial von Glyphosat und AMPA in Anwesenheit eines Mineralsorbenten untersucht. In natürlichen Umweltsystemen interagieren Mikroorganismen mit komplexen Boden-Wasser-Matrizes, in denen ionische APs wie Glyphosat und AMPA eine starke Affinität zu positiv geladenen Mineraloberflächen aufweisen. Dadurch verteilen sich die Verbindungen zwischen wässriger Phase und sorbierter Phase. Sorbierte Fraktionen gelten häufig als weniger bioverfügbar, was allgemein mit einer verringerten Biotransformation assoziiert wird. Zur Überprüfung dieser Annahme nutzten wir Goethit – ein häufiges und umweltrelevantes Eisen-(Oxyhydr)oxid-Mineral mit hoher Sorptionskapazität für Glyphosat und AMPA – als Modellphase. Batch-Experimente mit Goethit-Suspensionen, die mit Glyphosat und/oder AMPA im Gleichgewicht standen, wurden mit mineralfreien Kontrollen verglichen. Die Ergebnisse zeigten, dass die Anwesenheit von Goethit den mikrobiellen Abbau beider Substanzen nicht hemmte, unabhängig davon, ob sie einzeln oder gemeinsam vorlagen. Entgegen der gängigen Erwartung, dass AMPA durch Sorption länger persistieren würde, blieben die sorbierten Fraktionen für die getesteten Bakterienstämme gut bioverfügbar. Es wurde kein verminderter Abbau beobachtet, was darauf hinweist, dass Mineralsorption unter den getesteten Bedingungen (insbesondere geringe Partikelgröße) die Biotransformation von Glyphosat und AMPA nicht zwangsläufig einschränkt.

Im dritten Teil der Studie wurde die biologische Abbaubarkeit höherer APPs – mit drei oder mehr C–P-Bindungen – in bakteriellen Nährmedien kritisch untersucht. Während frühere Studien einen signifikanten Abbau durch Bakterien berichteten, die diese Verbindungen als Phosphorquelle nutzen. Allerdings wurden diese Experimente in Nährmedien durchgeführt, die gelöstes Mangan (Mn(II)) enthielten – ein bekannter Mediator für die abiotische Oxidation höherer APPs durch molekularen Sauerstoff. Batch-Experimente zeigten in solchen Medien eine rasche Transformation von Aminotris(methylenphosphonat) (ATMP) und Ethylendiamintetramethylenphosphonat (EDTMP) sowohl in Anwesenheit als auch in Abwesenheit von Bakterien. Die Transformation wurde primär durch Spuren von gelöstem Mn(II) und nicht durch bakterielle Aktivität verursacht.

Durch den Nachweis der Transformationsprodukte konnte klar gezeigt werden, dass beide Verbindungen auch ohne mikrobielle Beteiligung abiotisch abgebaut wurden. Eine Literaturrecherche zusammen mit den neuen experimentellen Ergebnissen deckte somit einen grundlegendes Manko früherer Studien zum APP-Abbau auf und stellt die bisher angenommene mikrobielle Abbaubarkeit in üblichen Kultivierungsmedien mit Spurenelementlösungen in Frage.

Abschließend wurde versucht, die verbindungsspezifische Isotopenanalyse (CSIA) als Methode zur Charakterisierung des biologischen Abbaus von Aminophosphonaten wie Glyphosat und AMPA anzuwenden. Eine zentrale Herausforderung der CSIA ist die effiziente Abtrennung der Zielanalyten von reichlich vorhandenen Matrixkomponenten – insbesondere von Glutamat, das in hohen Konzentrationen als Kohlenstoffquelle zugesetzt wird. Hierfür wurden zwei Aufreinigungsverfahren getestet: Kationenaustausch und Oberflächenkomplexierung mit Aluminiumoxid. Während der Kationenaustausch zu erheblichen Verlusten von Glyphosat und AMPA führte, konnte die Aluminiumoxid-Methode die Glutamatgehalte effektiv reduzieren, ohne die Wiederfindung der Analyten zu beeinträchtigen. Dadurch war die Isotopenanalyse in frühen Probenahmephasen erfolgreich, während in späteren Stadien verbliebenes Glutamat und mögliche Transformationsprodukte die Messungen beeinträchtigten. Auch wenn die Ergebnisse nur einen Teilerfolg darstellen, markieren sie einen wichtigen Schritt zur Etablierung der CSIA für die Untersuchung des biologischen Abbaus von Glyphosat und AMPA. Um das volle Potenzial der Kohlenstoff-CSIA auszuschöpfen, sind jedoch selektivere und effizientere Aufreinigungsmethoden erforderlich, die eine vollständige Probenreinigung ermöglichen.

Insgesamt trägt diese Arbeit dazu bei, das Verständnis der biologischen Abbaubarkeit von APs und APPs unter komplexeren Bedingungen zu vertiefen und bestehende Forschungslücken in Bezug auf Umweltrelevanz und methodische Herausforderungen zu schließen. Durch die systematische Untersuchung bakterieller Abbauprozesse unter gleichzeitiger Berücksichtigung konkurrierender P-Quellen, Mineralsorption und abiotischer Einflüsse zeigt diese Arbeit, dass kritische bisherige Annahmen nicht uneingeschränkt auf reale Umweltsysteme übertragbar sind. Insgesamt liefert diese Arbeit entscheidende neue Erkenntnisse, die etablierte Sichtweisen zur Abbaubarkeit von APs und APPs in Frage stellen, und schafft die Grundlage für genauere Umwelt-Risikoabschätzungen sowie für die Entwicklung verbesserter analytischer Werkzeuge zur Untersuchung dieser persistenten Schadstoffe.

Table of Contents

List of Figures

List of Schemes

List of Tables

Statement of authorship

I hereby declare that I have independently written the submitted thesis. All sources and references used, as well as any passages quoted verbatim or adapted from other works, are clearly identified as such. For each chapter, I have explicitly stated my own contributions, as well as the contributions of others who were involved in this work.

Hiermit erkläre ich, dass ich die vorliegende Dissertation selbstständig verfasst habe. Alle verwendeten Quellen und Referenzen sowie alle wörtlich übernommenen oder sinngemäß angepassten Passagen aus anderen Werken sind als solche kenntlich gemacht. Für jedes Kapitel habe ich meine eigenen Beiträge sowie die Beiträge anderer, die an dieser Arbeit beteiligt waren, ausdrücklich angegeben.

Kleanthi Kourtaki

1 General Introduction

1.1 Organophosphonates in the environment

Organic pollutants comprise a diverse group of synthetic compounds that are widely distributed in the environment due to their extensive industrial and agricultural use. Among them, organophosphonates (OPs), derivatives of phosphonic acid, are a diverse class of organic compounds distinguished by the presence of the phosphonate functional group ($R–C–P(+III)O_3H_2$), where the phosphorus atom is directly bound to a carbon atom. Furthermore, OPs may also contain amine and carboxylic acid group(s). They can be of either biogenic (e.g., 2-aminoethylphosphonate acid (AEP), phosphonoacetate, or phosphonopyruvate) or of synthetic origin (Kamat and Raushel, 2013). Among the broad class of synthetic OPs, glyphosate stands out as a well-known representative as one of the most intensively applied agrochemicals worldwide, and its major metabolite aminomethylphosphonate (AMPA). Glyphosate is a broad-spectrum non-selective herbicide, owing its effectiveness to its ability to inhibit 5-enolpyruvylshikimate-3-phosphate synthase (EPSPS) – an essential enzyme in the biosynthesis of aromatic amino acids such as tryptophan and tyrosine – primarily in plants (Giesy et al., 2000). Its widespread use was further expanded with the development of genetically modified glyphosate-tolerant crops, which enabled efficient weed control without damaging the crop. Besides glyphosate, OPs also include synthetic (amino)polyphosphonates ((A)PPs) containing more than one C–P bond(s) and are widely used complexing agents such as the diphosphonate 1-hydroxyethane-1,1-diphosphonate (HEDP) and the APPs diethylenetriamine penta(methylene phosphonate) (DTPMP) or ethylenediamine tetra (methylenephosphonate) (EDTMP) as well as their transformation products such as iminodi(methylene phosphonate) (IDMP) (Nowack, 2003; Grandcoin et al., 2017; Kuhn et al., 2017; Röhnelt et al., 2023). The introduction of these compounds to the market was driven by the demand for more efficient and environmentally friendly chelating agents to replace traditional polyphosphates and polycarboxylates such as ethylenediaminetetraacetate (EDTA) (Knepper, 2003; Jaworska et al., 2002). Their ability to form stable complexes with di- and trivalent metal ions makes them valuable in applications requiring control of metal-catalyzed reactions or prevention of mineral deposits. Their effectiveness at concentrations an order of magnitude lower than polyphosphates further underpins their broad application and commercial relevance (Studnik et al., 2015). They are used in a wide range of industrial and household applications, such as detergents for reducing water hardness and bleach stabilizer, corrosion inhibitors and antiscalants in water boilers, as well as flame retardants (Nowack, 2003; Jaworska

et al., 2002). In 2012, the global application of OPs, including APPs, was estimated at 94,000 t in 2012 (EPA, 2013). Extensive use of synthetic OPs has led to frequent detection in surface waters, soils, crop products, and even organisms reliant on those environments, raising concerns about their environmental fate and potential adverse effects (Tauchnitz et al., 2020). The release of synthetic OPs is strongly associated with human activities: glyphosate and its metabolites primarily enter soils and surface waters through agricultural runoff following field application, while APPs are mainly introduced into aquatic systems via wastewater discharges from municipal and industrial sources. Although the sorption of (A)PPs onto sewage sludge is an important removal pathway, an estimated 9,000–18,600 t/a still enter surface waters via wastewater treatment plant (WWTP) effluents, reflecting municipal, agricultural, and industrial contributions in Europe (Nowack, 2003; Rott et al., 2018). Recent studies also identify WWTPs as a significant source of glyphosate and AMPA in European rivers (Schwientek et al., 2024). This occurs through the abiotic transformation of diethylenetriamine penta(methylene phosphonate) (DTPMP), a commonly used scale inhibitor, challenging the assumption that agricultural applications are the primary source of glyphosate in surface waters and raising new questions about its environmental fate (Venditti et al., 2023; Schwientek et al., 2024; Röhnelt et al., 2025). Despite the European Union's regulatory limit for glyphosate in environmental waters set at 0.1 µg/L, glyphosate and AMPA are frequently detected in European waters at concentrations far exceeding this limit, reaching up to 2.5 µg/L in some cases, while in soils even higher concentrations of up to 2 mg/kg have been reported (Sanchís et al., 2012; Silva et al., 2018; Huntscha et al., 2018).

1.2 Environmental health and significance

APPs are believed to have low acute toxicity to mammals as well as aquatic biota, such as invertebrates and fish. However, the release of toxic metabolites like glyphosate and AMPA – known environmental contaminants – raises concerns (Knepper, 2003; HERA, 2004). In addition, due to their strong chelating abilities, they can have indirect effects by binding essential trace metals, reducing their bioavailability, and indirectly compromising growth by altering nutrient dynamics (Schowanek et al., 1996). As a result, their release into aquatic environments can disrupt ecosystems, affecting microbial competition for these essential minerals. While (A)PPs are not regulated and are mostly subject to restrictions aiming at limiting P-content in consumer detergents, mainly for preventing eutrophication risks, glyphosate has been classified as "probably carcinogenic to humans-Group 2A" by the International Agency for Research on Cancer (IARC) (IARC, 2015). Since then, glyphosate's regulatory status has been marked by extensive evaluations, controversies, and legal challenges in Europe. In 2023, the European Commission renewed glyphosate's approval for an additional 10 years, authorizing its use in the EU until December 15, 2033, but under specific conditions and

restrictions aimed at minimizing risks. This decision faced criticism from several EU member states, and in 2025, in response to scientific data, the European Chemical Agency (ECHA) formally requested its Committee for Risk Assessment (RAC) to reassess glyphosate's classification for carcinogenicity, mutagenicity, and reproductive toxicity under the EU classification, labelling, and packaging (CLP) Regulation. AMPA is also under debate as it has been shown to exhibit environmental (eco–)toxicological risks, similar or even higher to glyphosate (Barreto et al., 2023). Importantly, biomonitoring campaigns monitoring internal exposure to glyphosate and AMPA frequently detect both compounds in human samples (Connolly et al., 2022). For example, screenings conducted in Germany between 2001 and 2015 found glyphosate and AMPA in 30–40% of urine samples, at concentrations equal to or exceeding the limit of quantification (0.1 µg/L), underscoring the need for ongoing evaluation of the human health risks associated with these substances (Conrad et al., 2017). In aquatic systems, AMPA can adversely affect the growth and reproduction of various organisms, including algae, invertebrates, and fish, potentially affecting the function of aquatic life communities or even reducing biodiversity (Hembach et al., 2023). While environmental concentrations of AMPA are typically well below levels causing acute toxicity, its chronic effects and synergistic interactions with other agrochemicals may represent subtler but ecologically significant risks. It has also been shown to be a transformation product of glyphosate, but also of aminopolyphosphonates such as DTPMP, further raising concerns about its potential impacts on both aquatic biota and the environment (Röhnelt et al., 2025).

1.3 Environmental chemistry and fate

Understanding the impacts of their widespread use and significance demands a comprehensive characterization of their environmental chemistry and fate, which remains unresolved due to the complexity of environmental systems. The chemical structure of OPs, containing one or more C–P bonds, amine and carboxylic acid groups, leads to high solubility in water (e.g., 11.6 g/L for glyphosate and 500 g/L for aminotris(methylenephosphonate) (ATMP) @25°C), low volatility (Henry's constant 2.1 $x10^{-12}$ atm m^3/mol for glyphosate and 8 $x10^{-18}$ atm m^3/mol for ATMP), and low solubility in organic solvents ($logK_{ow}$ < -3.4 for both glyphosate and ATMP) (HERA, 2004; Pallett, 2018). Despite their high solubility, they also demonstrate strong adsorption to mineral surfaces such as aluminum, iron, and manganese (oxyhydr)oxides in soils and sediments, with sorption coefficients (K_d values) varying depending on the soil, pH, ionic strength, and competing ions (Pessagno and Afonso, 2005). For glyphosate, K_d values were reported ranging from 0.6 to 303 L/kg for organic-rich soil and muddy soils, respectively (Vereecken, 2005). Due to its strong tendency to sorb onto soil particles, glyphosate and other OPs primarily accumulate in the upper soil layers. However, processes such as surface runoff, spray drift, and vertical movement through the

soil profile can transport them into groundwater, surface water bodies, and sediments (Borggaard & Gimsing, 2008; Silva et al., 2018). The fate of glyphosate in soil is influenced both by its intrinsic properties—such as molecular structure, adsorption behavior, solubility—and by the soil's physicochemical and biological characteristics, including organic carbon content, pH, moisture, microbial biomass, bioavailability, pore connectivity, and clay fraction (Borggaard & Gimsing, 2008; Okada et al., 2019). The presence of phosphate has already been identified as a significant factor leading to the remobilization of glyphosate, leading to its detection in surface and groundwaters (De Gerónimo & Aparicio, 2022). The environmental fate of OPs and other organic pollutants is mainly determined by their degradation rates. Half-life times for OPs are highly variable, typically ranging from several days to months, depending on site-specific factors such as pH, redox potential, and microbial activity. Reported half-lives for glyphosate range from 2 to 91 days in water, while in soil environments, it can reach up to 215 days. AMPA is generally more persistent than glyphosate, with half-lives often extending beyond 240 days in soil environments (Battaglin et al., 2014). For APPs such as ATMP in water, half-life times are reported to be approximately 400 days, while in soil, 120 days (HERA, 2004). Studies have suggested that abiotic degradation processes, including photolysis, can efficiently break APPs and other OPs down (Lesueur et al., 2005; Kuhn et al., 2018; Marks et al., 2023). They also undergo oxidation processes, notably oxidation by Mn(III/IV)-(hydr)oxides and Mn(II)-catalyzed oxidation by molecular oxygen, leading to the cleavage of either their C–P or C–N bond (Nowack & Stone, 2000; Barrett & McBride, 2005; Martin et al., 2022; Röhnelt et al., 2023). Their abiotic degradation often limits their long-term accumulation but releases phosphate and other P-containing transformation products, which influence nutrient cycling and may contribute to eutrophication. During waste treatment, their removal is primarily achieved through sorption and chemical oxidation, because biodegradation is often regarded as negligible. This is due to the high phosphate content preventing the induction of enzymes like C–P lyases – key enzymes for breaking down OPs (McGrath et al., 1997; Kononova & Nesmeyanova, 2002; Santos-Beneit, 2015; Stosiek & Klimek-ochab, 2020).

1.4 Biodegradation of glyphosate and other OPs

While OPs were previously considered resistant to degradation due to their resilient C–P bond (Ternan et al., 1998), numerous studies demonstrate biotransformation to be the main elimination process for glyphosate and other OPs under environmentally relevant conditions. However, the factors that influence this process in such conditions remain largely unexplored (Masotti et al., 2023; Padilla & Selim, 2020). In natural environments, microorganisms often face P-scarcity, making phosphorus (P) a critical growth-limiting nutrient. P is an essential macronutrient for microbes, required for structural and metabolic functions like

energy transfer and the synthesis of phospholipids, nucleotides, nucleic acids, and proteins (Santos-Beneit, 2015). While bacteria typically prefer P in the form of inorganic phosphate (Pi) or (organo-)phosphate esters (O=P(+V)(OR)3), under Pi-limiting conditions, a mechanism to respond to P-starvation and maintain P-homeostasis is to acquire P from OPs (R–C–P(+III)O3H2) (Kamat and Raushel, 2013). OPs constitute a substantial portion of the environmental P-pool–up to 25% in oceans–and as a response to their adaptability in the presence of xenobiotics, bacteria have evolved pathways to utilize them, converting these compounds into more bioavailable P-forms (Kolowith et al., 2001; McGrath et al., 2013; Kamat and Raushel, 2013; Feng et al., 2020; Stosiek and Klimek-ochab, 2020). This biodegradation process is notably complex and significant, involving diverse microbial taxa and environmental interactions, underscoring the urgent need for detailed study. Key bacterial and fungal taxa involved in glyphosate biodegradation include well-studied genera such as *Pseudomonas*, *Bacillus*, *Ochrobactrum*, *Agrobacterium*, *Achromobacter*, and *Rhizobium* (Schowanek and Verstraete, 1990; Ermakova et al., 2017; Rossi et al., 2021; Acosta-Cortés et al., 2019) among bacteria, while fungi primarily include species of *Aspergillus*, *Penicillium*, *Fusarium*, *Trichoderma,* and *Purpureocillium* (Krzyśko-Lupicka et al., 1997; Castro et al., 2007; Spinelli et al., 2021; Wirsching et al., 2022). These microorganisms degrade OPs by utilizing them as a source of carbon, nitrogen, or phosphorus. Biodegradation rates are strongly influenced by environmental factors, including bioavailability, sorption to soil particles or minerals, microbial community interactions, as well as environmental parameters such as pH, temperature, nutrients, and oxygen availability (Kebede et al., 2021; Liu et al., 2025). Because bacterial cell membranes are largely impermeable to ionic compounds like OPs, their uptake depends on membrane transport proteins that actively import them for intracellular metabolism (Ruffolo et al., 2023). Thus, the bacterial utilization of OPs involves the upregulation of genes encoding enzymes responsible for their transport across the cell membrane, as well as those capable of cleaving their hydrolytically stable C–P bond (Metcalf and Wanner, 1993; Rizk et al., 2006). Depending on the structure of the OP, different enzymatic systems can be responsible for their breakdown and transformation (i.e., phosphonatase, phosphonoacetate and phosphonopyruvate hydrolase, C–P lyase, and a glyphosate oxidoreductase (GOX) (Kamat & Raushel, 2013; Kononova & Nesmeyanova, 2002). The mechanism of bacterial-driven glyphosate transformation has been mostly attributed to the activity of the C–P lyase that shows a broad substrate range (McGrath et al., 1997; Kulakova et al., 2001; McMullan and Quinn, 1994). A recent work evidenced that biotransformation of other OPs, such as AMPA or IDMP, can also occur via the cleavage of the C–P bond by the C–P lyase (Riedel et al., 2024). The genetic characterization has shown that the C–P lyase is encoded by the phn operon, part of the phosphate regulon, a mechanism by which the cells respond to the scarcity of exogenous phosphate (Santos-Beneit, 2015). The phn operon is a multienzyme system composed of 14 genes responsible for either the binding, transport, uptake, and/or metabolism of

the OPs and their transformation products (Metcalf and Wanner, 1993; Rizk et al., 2006). Under phosphate deficiency conditions, the phnJ from the activated C–P lyase enzyme complex (PhnG, PhnH, PhnI, PhnJ, PhnK, PhnL, PhnM) cleaves the C–P bond of the OPs, and after various enzymatic steps, they are converted into 5-phosphoribosyl-a-1diphosphate, a substrate which can be easily assimilated by the microorganisms (Wackett et al., 1987; Kamat & Raushel, 2015).

1.5 Methodological approaches

Biotransformation of OPs is commonly investigated using a variety of methodological approaches designed to elucidate the role of microorganisms in their environmental fate. Unraveling biotransformation pathways and dynamics in complex environmental matrices remains challenging due to low transformation rates, strong sorption limiting bioavailability, and the difficulty of distinguishing biotic processes from abiotic transformations. Pure culture experiments, in which selected microbial strains are cultivated under controlled laboratory conditions, provide critical insights into specific metabolic pathways, enabling the identification of genes and enzymes directly involved in biotransformation. Although such studies fail to account for community-level interactions and environmental heterogeneity – making it challenging to extrapolate results to natural ecosystems – they offer high mechanistic resolution at a molecular level, linking enzymatic reactions to observed changes in substrate. While mixed microbial co-cultures are often reported to enhance organic pollutant degradation, a recent meta-analysis has found monocultures to be more effective in some cases, likely due to differences in incubation durations (Liu et al., 2025). Analytical methods play a crucial role in these investigations, ranging from conventional chromatographic and spectrometric approaches to advanced isotope-based techniques. However, the quantification of compounds such as glyphosate, AMPA, and polyphosphonates (PPs) remains challenging due to their complex physicochemical properties. These include zwitterionic character, formation of multiple ionic species, and the absence of chromophore groups, which limit options for direct detection. To address these challenges, a variety of analytical approaches optimized for sensitivity and selectivity are employed. High-performance liquid chromatography (HPLC) after derivatization – typically using agents like fluorenylmethyloxycarbonyl chloride FMOC-Cl targeting the amine group – coupled with ultraviolet (UV), fluorescence (FLD), or (tandem) mass spectrometric detection (MS/MS, time of flight MS (TOF-MS), or triple quadrupole, QQQ) remains the preferred method for accurate, low-level detection in complex environmental samples (Koskinen et al., 2016). Ion chromatography (IC) utilizes the ionic character of OPs and allows separation without prior derivatization. Detection can be realized by inductively coupled plasma mass spectrometry (ICP-MS), conductivity detection (CD), or integrated pulsed amperometric detection (IPAD), which leverages the electroactive nature of OPs (Schmidt et al., 2013; Dovidauskas et al., 2020; Athmer et al., 2025). While

traditionally applied to glyphosate and AMPA, recent advances now allow simultaneous quantification of PPs, overcoming the need for derivatization (Röhnelt et al., 2025). This expands research possibilities that were previously limited to tracking inorganic phosphate after chemical conversion of APPs (Riedel et al., 2024). Such developments are particularly important, as recent findings indicate that PO_4^{3-} quantification can be biased by matrix interferences in samples with high levels of higher APPs (Guo et al., 2025).

Despite advancements in the detection and quantification of OPs, distinguishing between biotic and abiotic processes remains challenging. Carbon compound specific stable isotope analysis (carbon-CSIA) is an advanced analytical technique that has emerged as a powerful tool for investigating the transformation of contaminants by allocating sources, but also distinguishing between abiotic and biotic pathways, as mass balances are often not possible or inconclusive (Elsner & Imfeld, 2016). This method allows researchers to measure the isotopic composition of specific compounds, providing insights into their sources and (bio)degradation pathways in complex environmental systems. By analyzing the stable isotope ratios of carbon within individual molecules, CSIA can reveal subtle changes in isotopic signatures that occur during (bio-) transformation, enabling the identification and quantification of degradation processes that may not be detectable through conventional concentration measurements alone (Elsner, 2010). This technique is based on the principle that bond cleavage occurs more easily in molecules containing lighter isotopes, as their activation energies are lower and they react faster, resulting in an enrichment of heavier isotopes in the remaining contaminant pool (Elsner, 2010). Consequently, during transformation, molecules containing the light isotope (e.g., for carbon ^{12}C) at the reactive position possess slightly higher reaction rates compared to the molecules containing the heavy isotope (e.g., for carbon ^{13}C) (Elsner et al., 2005). The relative abundances of two stable isotopes in a molecule are usually expressed as isotopic ratios R (e.g. for carbon $^{13}C/^{12}C$, for nitrogen $^{14}N/^{15}N$) or typically converted into a δ-value by normalizing R against an internationally recognized standard (Coplen et al., 2002). In closed systems, this isotopic fractionation can be described using the Rayleigh distillation equation (see Equation 1.1), which allows for the calculation of ε-values from measured isotope ratios and the remaining fraction of the reactant (expressed as normalized concentration) (Elsner, 2010).

$$ln\left(\frac{R_t}{R_0}\right) = ln\left(\frac{\delta^{13}C_t + 1}{\delta^{13}C_0 + 1}\right) = \varepsilon * \ln(f_t) \qquad (1.1)$$

where R_0 and $\delta^{13}C_0$ is the initial, R_t and $\delta^{13}C_t$ the actual measured (normalized) isotope ratio and the remaining substrate fraction (i.e., $c_t\,/c_0$).

Negative ε-values indicate a preferential transformation of a lighter isotopologue at the reactive site, while positive ε-values (less common) describe preferential

removal of a heavier isotopologue, enriching the lighter isotopes in the residual contaminant pool. Measured ε-values reflect the changes in isotope ratios that occur during physical, chemical, or biological transformations under specific conditions. By comparing these to theoretical or experimentally determined ε-values for specific reaction mechanisms, it is possible to identify and differentiate between various (bio-)transformation processes. Kujawinski et al. (2013) developed a method to accurately determine glyphosate and AMPA δ-values. They observed highly variable glyphosate δ-values across different manufacturers (-24 to -34 ‰), underscoring the potential of carbon-CSIA for source allocation (Kujawinski et al., 2013; Mogusu et al., 2015). Abiotic degradation of glyphosate to sarcosine and AMPA by MnO_2 yielded ε_C of -3.5 ± 0.5‰, indicating an enrichment of the heavy isotopologue in the remaining glyphosate pool (Mogusu E. Dissertation, 2015). Notably, during biodegradation by *Ochrobactrum* sp. FrEM, isotope effects were also observed, resulting in an ε_C-value of –4.5 ± 0.5‰, demonstrating the potential of carbon-CSIA in distinguishing degradation processes (Ehrl et al., 2018).

Despite its strengths, the application of carbon-CSIA to the study of glyphosate and its primary degradation product, AMPA, remains limited due to several analytical challenges. One key reason for the scarcity of CSIA-based studies lies in the method's stringent prerequisites. Accurate carbon-CSIA requires complete chromatographic peak separation, exhibits low sensitivity compared to conventional MS, and demands the use of carbon-free eluents to minimize background CO_2 signals (Bakkour et al., 2024; Kujawinski et al., 2013). These limitations are particularly pronounced in environmental samples, where polar contaminants like glyphosate and AMPA are typically present in aqueous concentrations ranging from nM to low µM – well below the detection limits of conventional CSIA techniques which are typically in the high µM range (Sanchís et al., 2012; Battaglin et al., 2014). As a result, extensive enrichment and purification procedures are often necessary, with the effectiveness of these steps largely linked to the analytes' ionic properties and the complexity of the sample matrix.

To address these challenges, a variety of sample preparation strategies aimed at minimizing matrix interferences without altering the isotopic composition of the target compounds were explored. These strategies include the use of organic solvent extraction, solid-phase extraction (SPE), cation exchange resins, and derivatization techniques (Shamsi et al., 2025). Among these, SPE-based methods are the most widely used. The choice of sorbent in SPE is critical and is typically based on desired interaction mechanisms – such as ionic exchange, van der Waals forces, π–π interactions or hydrogen bonding – between the sorbent and the compound to be retained or removed. In addition to analytical constraints, studying degradation processes in environmental samples presents further challenges. These include the slow pace of degradation and the coexistence of multiple degradation

pathways. As a result, laboratory-based studies are often used to investigate associated isotope effects under simplified conditions –isolating single transformation processes while excluding non-reactive processes that do not contribute to the actual removal of the contaminant load.
However, such laboratory experiments frequently require the addition of highly concentrated organic buffers or other carbon-containing components, which can compromise isotope analysis. Specifically, microbially mediated transformation studies of organophosphonates typically involve an excess of nutrients – often including organic buffers with high C-content. For example, glutamic acid is commonly used as a carbon source in such studies, often at concentrations 100 times greater than those of glyphosate or AMPA, which serve as P-sources. These high concentrations can significantly interfere with chromatographic separation and may obscure subtle isotopic shifts that are essential for accurately assessing biodegradation. Given the complexity of these systems, studies focusing on the purification of samples containing complex growth media remain limited. Nevertheless, the development of highly selective purification techniques is essential to enable reliable isotope analysis while investigating the biodegradation of pollutants such as glyphosate and AMPA.

1.6 Scope and objectives of the thesis

The biotransformation of OPs is environmentally significant, and the factors controlling their degradation remain insufficiently understood. This study provides fundamental insights into the biodegradability of OPs containing one or more C–P bonds, through laboratory batch experiments with isolated bacterial strains possessing the enzymes required for C–P bond cleavage. Numerous studies report high levels of OP biodegradation under P-limiting conditions in liquid batch cultures. Nevertheless, OPs—particularly glyphosate—are still detected at elevated concentrations in soils and aquatic environments. To address this discrepancy, the overall goal of this work is to systematically investigate the biodegradability of glyphosate and other amino(poly)phosphonates (A(P)Ps) under systematically controlled laboratory conditions, to identify key factors that influence their transformation dynamics in the environment. To this end, this study i) assesses the influence of OPs as competing P-sources on the biodegradation potential of glyphosate, ii) examines the biodegradability of glyphosate and its primary metabolite AMPA under sorbed conditions in the presence of the ironoxyhydroxide goethite as environmentally relevant model sorbent, iii) evaluates the biodegradability of higher APPs using approaches applied for other OPs and critically examines the impact of medium composition on their degradation behavior, and iv) develops a cleanup method to provide an analytical foundation for applying carbon CSIA to glyphosate and AMPA during biotransformation experiments. Collectively, these objectives establish a

framework for advancing the understanding of OP biodegradation and support future investigations on their environmental fate in more complex matrices.

This dissertation is structured into six chapters. **Chapter 1** provides an overview of the environmental chemistry and occurrence of OPs as environmental contaminants and presents the significance of OP biotransformation. It discusses key factors influencing this process and outlines the methodological approaches employed to study it. Furthermore, it describes the concept of carbon-CSIA of organic pollutants and highlights the need for a cleanup technique to enable its application. **Chapter 2** explores the impact of aminomono- and diphosphonates on the biodegradation potential of glyphosate in laboratory batch cultures using pure strains capable of utilizing OPs as P-sources. Amino(mono)phosphonates such as AMPA, which are frequently detected alongside glyphosate in soils and waters, can act as alternative P-sources and may affect glyphosate degradation. To investigate this, a series of batch experiments was conducted in which AMPA and other commonly occurring amino(mono)phosphonates were supplied in parallel with glyphosate as P-sources for selected bacterial strains. **Chapter 3** examines the influence of sorbents on the bacterial transformation of glyphosate and AMPA, simulating interactions with mineral phases commonly found in the environment. Both glyphosate and AMPA exhibit strong sorption to soil matrices, particularly mineral surfaces, which can substantially reduce their bioavailability and, consequently, their microbial biotransformation. This chapter specifically investigates how the presence of iron(oxy)hydroxide minerals, such as goethite, affects the biodegradation potential of glyphosate and AMPA by creating bioavailability constraints. **Chapter 4** focuses on the biodegradability of higher APPs, using methods previously applied to OPs such as glyphosate and examining the influence of cultivation medium composition on their degradation. Although higher APPs have traditionally been regarded as non-biodegradable, recent evidence points to the possibility of microbially mediated breakdown. Furthermore, manganese(II) (Mn(II))—commonly added as a trace element in biodegradation studies—can catalyze abiotic degradation of higher APPs in the presence of oxygen. This chapter, therefore, investigates Mn(II)'s role in shaping the observed biodegradation processes. **Chapter 5** focuses **o**n developing purification techniques to reduce matrix effects, enabling carbon-CSIA of glyphosate and AMPA during biodegradation experiments. Isotope effects linked to the biodegradation of OPs, including glyphosate and AMPA, remain poorly understood due to matrix interferences from growth media that hinder isotope analysis. Determining enrichment factors (ε values) for glyphosate and AMPA biodegradation is crucial, as such data are scarce and could significantly improve the interpretation of isotope signatures in complex environmental settings where multiple transformation processes coexist. Finally, **Chapter 6** summarizes the main findings, discusses their environmental implications, and outlines recommendations for future research.

1.7 References

Acosta-Cortés, A. G., Martinez-Ledezma, C., López-Chuken, U. J., Kaushik, G., Nimesh, S., & Villarreal-Chiu, J. F. (2019). Polyphosphate recovery by a native Bacillus cereus strain as a direct effect of glyphosate uptake. *ISME Journal*, *13*(6), 1497–1505. https://doi.org/10.1038/s41396-019-0366-3

Athmer, M., Röhnelt, A. M., Maas, T. J., Haderlein, S. B., & Karst, U. (2025). Comprehensive IC-ICP-MS analysis of polyphosphonates and their transformation products. *Journal of Chromatography A*, *1748*(February). https://doi.org/10.1016/j.chroma.2025.465843

Bakkour, R., Wabnitz, C., & Glöckler, D. (2024). Lack of selectivity in sample preparation – An achilles heel of compound-specific isotope analysis for environmental micropollutants. *TrAC - Trends in Analytical Chemistry*, *180*(March). https://doi.org/10.1016/j.trac.2024.117908

Barreto, L. S., Souza, T. L. de, Morais, T. P. de, & Oliveira Ribeiro, C. A. de. (2023). Toxicity of glyphosate and aminomethylphosphonic acid (AMPA) to the early stages of development of Steindachneridion melanodermatum, an endangered endemic species of Southern Brazil. *Environmental Toxicology and Pharmacology*, *102*(January). https://doi.org/10.1016/j.etap.2023.104234

Barrett, K. A., & McBride, M. B. (2005). Oxidative degradation of glyphosate and aminomethylphosphonate by manganese oxide. *Environmental Science and Technology*, *39*(23), 9223–9228. https://doi.org/10.1021/es051342d

Battaglin, W. A., Meyer, M. T., Kuivila, K. M., & Dietze, J. E. (2014). Glyphosate and its degradation product AMPA occur frequently and widely in U.S. soils, surface water, groundwater, and precipitation. *Journal of the American Water Resources Association*, *50*(2), 275–290. https://doi.org/10.1111/jawr.12159

Borggaard, O. K., & Gimsing, A. L. (2008). Fate of glyphosate in soil and the possibility of leaching to ground and surface waters: A review. *Pest Management Science*, *64*(4), 441–456. https://doi.org/10.1002/ps.1512

Castro, J. V., Peralba, M. C. R., & Ayub, M. A. Z. (2007). Biodegradation of the herbicide glyphosate by filamentous fungi in platform shaker and batch bioreactor. *Journal of Environmental Science and Health - Part B Pesticides, Food Contaminants, and Agricultural Wastes*, *42*(8), 883–886. https://doi.org/10.1080/03601230701623290

Connolly, A., Koch, H. M., Bury, D., Koslitz, S., Kolossa-Gehring, M., Conrad, A., Murawski, A., McGrath, J. A., Leahy, M., Brüning, T., & Coggins, M. A. (2022). A Human Biomonitoring Study Assessing Glyphosate and Aminomethylphosphonic Acid (AMPA) Exposures among Farm and Non-Farm Families. *Toxics*, *10*(11). https://doi.org/10.3390/toxics10110690

Conrad, A., Schröter-Kermani, C., Hoppe, H. W., Rüther, M., Pieper, S., & Kolossa-Gehring, M. (2017). Glyphosate in German adults – Time trend (2001 to 2015) of human exposure to a widely used herbicide. *International*

Journal of Hygiene and Environmental Health, *220*(1), 8–16. https://doi.org/10.1016/j.ijheh.2016.09.016

Coplen, T. B., Böhlke, J. K., De Bièvre, P., Ding, T., Holden, N. E., Hopple, J. A., Krouse, H. R., Lamberty, A., Peiser, H. S., Révész, K., Rieder, S. E., Rosman, K. J. R., Roth, E., Taylor, P. D. P., Vocke, R. D., & Xiao, Y. K. (2002). Isotope-abundance variations of selected elements (IUPAC technical report). *Pure and Applied Chemistry*, *74*(10), 1987–2017. https://doi.org/10.1351/pac200274101987

De Gerónimo, E., & Aparicio, V. C. (2022). Changes in soil pH and addition of inorganic phosphate affect glyphosate adsorption in agricultural soil. *European Journal of Soil Science*, *73*(1), 1–16. https://doi.org/10.1111/ejss.13188

Dovidauskas, S., Okada, I. A., & dos Santos, F. R. (2020). Validation of a simple ion chromatography method for simultaneous determination of glyphosate, aminomethylphosphonic acid and ions of Public Health concern in water intended for human consumption. *Journal of Chromatography A*, *1632*, 461603. https://doi.org/10.1016/j.chroma.2020.461603

Ehrl, B. N., Mogusu, E. O., Kim, K., Hofstetter, H., Pedersen, J. A., & Elsner, M. (2018). High Permeation Rates in Liposome Systems Explain Rapid Glyphosate Biodegradation Associated with Strong Isotope Fractionation. *Environmental Science and Technology*, *52*(13), 7259–7268. https://doi.org/10.1021/acs.est.8b01004

Elsner, M. (2010). Stable isotope fractionation to investigate natural transformation mechanisms of organic contaminants: Principles, prospects and limitations. *Journal of Environmental Monitoring*, *12*, 2005–2031. https://doi.org/10.1039/c0em00277a

Elsner, M., & Imfeld, G. (2016). Compound-specific isotope analysis (CSIA) of micropollutants in the environment - current developments and future challenges. *Current Opinion in Biotechnology*, *41*(Table 1), 60–72. https://doi.org/10.1016/j.copbio.2016.04.014

Elsner, M., Zwank, L., Hunkeler, D., & Rene P Schwarzenbach. (2005). A New Concept Linking Observable Stable Isotope Fractionation to Transformation Pathways of Organic Pollutants. *Environmental Science and Technology*, *39*, 6896–6916.

EPA, 2013. Phosphonates in Detergents. EPA Detergent Phosphonates Dossier. European Phosphonate Association.

Ermakova, I. T., Shushkova, T. V., Sviridov, A. V., Zelenkova, N. F., Vinokurova, N. G., Baskunov, B. P., & Leontievsky, A. A. (2017). Organophosphonates utilization by soil strains of Ochrobactrum anthropi and Achromobacter sp. *Archives of Microbiology*, *199*(5), 665–675. https://doi.org/10.1007/s00203-017-1343-8

Feng, D., Soric, A., & Boutin, O. (2020). Treatment technologies and degradation pathways of glyphosate: A critical review. *Science of the Total Environment*, *742*, 140559.

https://doi.org/10.1016/j.scitotenv.2020.140559
Giesy, J. P., Dobson, S., & Solomon, K. R. (2000). Ecotoxicological risk assessment for Roundup® herbicide. *Reviews of Environmental Contamination and Toxicology*, *167*, 35–120. https://doi.org/10.1007/978-1-4612-1156-3_2
Grandcoin, A., Piel, S., & Baurès, E. (2017). AminoMethylPhosphonic acid (AMPA) in natural waters: Its sources, behavior and environmental fate. *Water Research*, *117*, 187–197. https://doi.org/10.1016/j.watres.2017.03.055
Guo, R., Röhnelt, A. M., Martin, P. R., & Haderlein, S. B. (2025). Limitations of the molybdenum blue method for phosphate quantification in the presence of organophosphonates. *Analytical and Bioanalytical Chemistry*, *0123456789*. https://doi.org/10.1007/s00216-025-05850-y
Hembach, N., Drechsel, V., Sobol, M., Kaster, A. K., Köhler, H. R., Triebskorn, R., & Schwartz, T. (2023). Effect of glyphosate, its metabolite AMPA, and the glyphosate formulation Roundup® on brown trout (Salmo trutta f. fario) gut microbiome diversity. *Frontiers in Microbiology*, *14*(January), 1–15. https://doi.org/10.3389/fmicb.2023.1271983
HERA. (2004). Human & Environmental Risk Assessment on ingredients of European household cleaning products Phosphonates. *Assessment*, 1–114.
Huntscha, S., Stravs, M. A., Bühlmann, A., Ahrens, C. H., Frey, J. E., Pomati, F., Hollender, J., Buerge, I. J., Balmer, M. E., & Poiger, T. (2018). Seasonal Dynamics of Glyphosate and AMPA in Lake Greifensee: Rapid Microbial Degradation in the Epilimnion during Summer. *Environmental Science and Technology*, *52*(8), 4641–4649. https://doi.org/10.1021/acs.est.8b00314
International Agency for Research on Cancer. IARC Monographs Volume 112: Evaluation of Five Organophosphate Insecticides and Herbicides. 2015. Available online: www.iarc.fr/en/media-centre/ iarcnews/pdf/MonographVolume112.pdf
Jaworska, J., Van Genderen-Takken, H., Hanstveit, A., Van de Plassche, E., & Feijtel, T. (2002). Environmental risk assessment of phosphonates, used in domestic laundry and cleaning agents in the Netherlands. *Chemosphere*, *47*(6), 655–665. https://doi.org/10.1016/S0045-6535(01)00328-9
Kamat, S. S., & Raushel, F. M. (2013). The enzymatic conversion of phosphonates to phosphate by bacteria. *Current Opinion in Chemical Biology*, *17*(4), 589–596. https://doi.org/10.1016/j.cbpa.2013.06.006
Kamat, S. S., & Raushel, F. M. (2015). PhnJ – A novel radical SAM enzyme from the C–P lyase complex. *Perspectives in Science*, *4*, 32–37. https://doi.org/10.1016/j.pisc.2014.12.006
Kebede, G., Tafese, T., Abda, E. M., Kamaraj, M., & Assefa, F. (2021). Factors Influencing the Bacterial Bioremediation of Hydrocarbon Contaminants in the Soil: Mechanisms and Impacts. *Journal of Chemistry*, *2021*. https://doi.org/10.1155/2021/9823362
Knepper, T. P. (2003). Synthetic chelating agents and compounds exhibiting

complexing properties in the aquatic environment. *TrAC - Trends in Analytical Chemistry*, *22*(10), 708–724. https://doi.org/10.1016/S0165-9936(03)01008-2

Kolowith, L. C., Ingall, E. D., & Benner, R. (2001). Composition and cycling of marine organic phosphorus. *Limnology and Oceanography*, *46*(2), 309–320. https://doi.org/10.4319/lo.2001.46.2.0309

Kononova, S. V, & Nesmeyanova, M. A. (2002). *Phosphonates and their degradation by microorganisms*. *67*(2), 184–195. doi: 10.1023/a:1014409929875. PMID: 11952414

Koskinen, W. C., Marek, L. J., & Hall, K. E. (2016). Analysis of glyphosate and aminomethylphosphonic acid in water, plant materials and soil. *Pest Management Science*, *72*(3), 423–432. https://doi.org/10.1002/ps.4172

Krzyśko-Lupicka, T., Strof, W., Kubś, K., Skorupa, M., Wieczorek, P., Lejczak, B., & Kafarski, P. (1997). The ability of soil-borne fungi to degrade organophosphonate carbon-to-phosphorus bonds. *Applied Microbiology and Biotechnology*, *48*(4), 549–552. https://doi.org/10.1007/s002530051095

Kuhn, R., Jensch, R., Bryant, I. M., Fischer, T., Liebsch, S., & Martienssen, M. (2018). The influence of selected bivalent metal ions on the photolysis of diethylenetriamine penta(methylenephosphonic acid). *Chemosphere*, *210*, 726–733. https://doi.org/10.1016/j.chemosphere.2018.07.033

Kuhn, R., Tóth, E., Geppert, H., Fischer, T., Liebsch, S., & Martienssen, M. (2017). Identification of the Complete Photodegradation Pathway of Ethylenediaminetetra(methylenephosphonic acid) in Aqueous Solution. *Clean - Soil, Air, Water*, *45*(5). https://doi.org/10.1002/clen.201500774

Kujawinski, D. M., Wolbert, J. B., Zhang, L., Jochmann, M. A., Widory, D., Baran, N., & Schmidt, T. C. (2013). Carbon isotope ratio measurements of glyphosate and AMPA by liquid chromatography coupled to isotope ratio mass spectrometry. *Analytical and Bioanalytical Chemistry*, *405*(9), 2869–2878. https://doi.org/10.1007/s00216-012-6669-0

Kulakova, A. N., Kulakov, L. A., Akulenko, N. V., Ksenzenko, V. N., Hamilton, J. T. G., & Quinn, J. P. (2001). Structural and functional analysis of the phosphonoacetate hydrolase (phnA) gene region in Pseudomonas fluorescens 23F. *Journal of Bacteriology*, *183*(11), 3268–3275. https://doi.org/10.1128/JB.183.11.3268-3275.2001

Lesueur, C., Pfeffer, M., & Fuerhacker, M. (2005). Photodegradation of phosphonates in water. *Chemosphere*, *59*(5), 685–691. https://doi.org/10.1016/j.chemosphere.2004.10.049

Liu, S., Guo, L., Xiang, C., Zhu, B., Huang, W., Tian, L., Tang, J., Dai, Z., Filimonenko, E., Mekhalif, R., Jia, H., & Kuzyakov, Y. (2025). Factors of microbial degradation of organic pollutants: Two meta-analyses. *Journal of Cleaner Production*, *486*(December 2024), 144459. https://doi.org/10.1016/j.jclepro.2024.144459

Marks, R. G. H., Drees, F., Rockel, S., Kerpen, K., Jochmann, M. A., & Schmidt,

T. C. (2023). Mechanistic investigation of phosphonate photolysis in aqueous solution by simultaneous LC-IRMS and HRMS analysis. *Journal of Photochemistry and Photobiology A: Chemistry*, *439*(September 2022), 114582. https://doi.org/10.1016/j.jphotochem.2023.114582

Martin, P. R., Buchner, D., Jochmann, M. A., Elsner, M., & Haderlein, S. B. (2022). Two Pathways Compete in the Mn(II)-Catalyzed Oxidation of Aminotrismethylene Phosphonate (ATMP). *Environmental Science and Technology*, *56*(7), 4091–4100. https://doi.org/10.1021/acs.est.1c06407

Masotti, F., Garavaglia, B. S., Gottig, N., & Ottado, J. (2023). Bioremediation of the herbicide glyphosate in polluted soils by plant-associated microbes. *Current Opinion in Microbiology*, *73*, 102290. https://doi.org/10.1016/j.mib.2023.102290

McGrath, J. W., Ternan, N. G., & Quinn, J. P. (1997). Utilization of organophosphonates by environmental microorganisms. *Letters in Applied Microbiology*, *24*(1), 69–73. https://doi.org/10.1046/j.1472-765X.1997.00350.x

McGrath, John W., Chin, J. P., & Quinn, J. P. (2013). Organophosphonates revealed: New insights into the microbial metabolism of ancient molecules. *Nature Reviews Microbiology*, *11*(6), 412–419. https://doi.org/10.1038/nrmicro3011

McMullan, G., & Quinn, J. P. (1994). In vitro characterization of a phosphate starvation-independent carbon- phosphorus bond cleavage activity in Pseudomonas fluorescens 23F. *Journal of Bacteriology*, *176*(2), 320–324. https://doi.org/10.1128/jb.176.2.320-324.1994

Metcalf, W. W., & Wanner, B. L. (1993). Evidence for a fourteen-gene, phnC to phnP locus for phosphonate metabolism in Escherichia coli. *Gene*, *129*(1), 27–32. https://doi.org/10.1016/0378-1119(93)90692-V

Mogusu E. Dissertation. (2015). *Compound Specific Isotopic Analysis To Investigate Sources and Degradation of Glyphosate*.

Mogusu, E. O., Wolbert, J. B., Kujawinski, D. M., Jochmann, M. A., & Elsner, M. (2015). Dual element (15N/14N, 13C/12C) isotope analysis of glyphosate and AMPA by derivatization-gas chromatography isotope ratio mass spectrometry (GC/IRMS) combined with LC/IRMS. *Analytical and Bioanalytical Chemistry*, *407*, 5249–5260. https://doi.org/10.1007/s00216-015-8721-3

Nowack, B., & Stone, A. T. (2000). Degradation of nitrilotris(methylenephosphonic acid) and related (amino)phosphonate chelating agents in the presence of manganese and molecular oxygen. *Environmental Science and Technology*, *34*(22), 4759–4765. https://doi.org/10.1021/es0000908

Nowack, Bernd. (2003). Environmental chemistry of phosphonates. *Water Research*, *37*(11), 2533–2546. https://doi.org/10.1016/S0043-1354(03)00079-4

Okada, E., Costa, J. L., & Bedmar, F. (2019). Glyphosate Dissipation in Different

Soils Under No-Till and Conventional Tillage. *Pedosphere*, *29*(6), 773–783. https://doi.org/10.1016/S1002-0160(17)60430-2

Padilla, J. T., & Selim, H. M. (2020). Environmental behavior of glyphosate in soils. In *Advances in Agronomy* (1st ed., Vol. 159). Elsevier Inc. https://doi.org/10.1016/bs.agron.2019.07.005

Pallett, K. (2018). Special issue of outlooks focussing on glyphosate. *Outlooks on Pest Management*, *29*(6), 245–246. https://doi.org/10.1564/v29_dec_02

Pessagno, R. C. ;, Dos, S., & Afonso, M. (2005). N-(Phosphonomethyl)Glycine Interactions With Soils. *The Journal of the Argentine Chemical Society*, *93*(6), 97–106.

Riedel, R., Commichau, F. M., Benndorf, D., Hertel, R., Holzer, K., Hoelzle, L. E., Mardoukhi, M. S. Y., Noack, L. E., & Martienssen, M. (2024). Biodegradation of selected aminophosphonates by the bacterial isolate Ochrobactrum sp. BTU1. *Microbiological Research*, *280*, 127600. https://doi.org/10.1016/j.micres.2024.127600

Riedel, R., Meißner, K., Kaschubowski, A., Benndorf, D., Martienssen, M., & Braun, B. (2024). Laundry Isolate Delftia sp. UBM14 Capable of Biodegrading Industrially Relevant Aminophosphonates. *Microorganisms*, *12*(8), 1–20. https://doi.org/10.3390/microorganisms12081664

Rizk, S. S., Cuneo, M. J., & Hellinga, H. W. (2006). Identification of cognate ligands for the Escherichia coli phnD protein product and engineering of a reagentless fluorescent biosensor for phosphonates . *Protein Science*, *15*(7), 1745–1751. https://doi.org/10.1110/ps.062135206

Röhnelt, A. M., Martin, P. R., Athmer, M., Bieger, S., Buchner, D., Karst, U., Huhn, C., Schmidt, T. C., & Haderlein, S. B. (2025). Glyphosate is a transformation product of a widely used aminopolyphosphonate complexing agent. *Nature Communications* , *16*(1), 1–11. https://doi.org/10.1038/s41467-025-57473-7

Röhnelt, A. M., Martin, P. R., Buchner, D., & Haderlein, S. B. (2023). Transformation of Iminodi(methylene phosphonate) on Manganese Dioxides - Passivation of the Mineral Surface by (Formed) Mn2+. *Environmental Science and Technology*, *57*(32), 11958–11966. https://doi.org/10.1021/acs.est.3c01838

Röhnelt, A. M., Martin, P. R., Marks, R. G. H., Buchner, D., Weiss, J., Schmidt, T. C., & Haderlein, S. B. (2025). Green quantification of amino(poly)phosphonates using ion chromatography coupled to integrated pulsed amperometric detection. *Analytical and Bioanalytical Chemistry*, *417*(8), 1581–1594. https://doi.org/10.1007/s00216-025-05747-w

Rossi, F., Carles, L., Donnadieu, F., Batisson, I., & Artigas, J. (2021). Glyphosate-degrading behavior of five bacterial strains isolated from stream biofilms. *Journal of Hazardous Materials*, *420*(July), 126651. https://doi.org/10.1016/j.jhazmat.2021.126651

Rott, E., Steinmetz, H., & Metzger, J. W. (2018). Organophosphonates: A review on environmental relevance, biodegradability and removal in wastewater

treatment plants. *Science of the Total Environment*, *615*, 1176–1191. https://doi.org/10.1016/j.scitotenv.2017.09.223

Ruffolo, F., Dinhof, T., Murray, L., Zangelmi, E., Chin, J. P., Pallitsch, K., & Peracchi, A. (2023). *Phosphonates*. *Molecules*. 2023 Sep 29;28(19):6863. doi: 10.3390/molecules28196863.

Sanchís, J., Kantiani, L., Llorca, M., Rubio, F., Ginebreda, A., Fraile, J., Garrido, T., & Farré, M. (2012). Determination of glyphosate in groundwater samples using an ultrasensitive immunoassay and confirmation by on-line solid-phase extraction followed by liquid chromatography coupled to tandem mass spectrometry. *Analytical and Bioanalytical Chemistry*, *402*(7), 2335–2345. https://doi.org/10.1007/s00216-011-5541-y

Santos-Beneit, F. (2015). The Pho regulon: A huge regulatory network in bacteria. *Frontiers in Microbiology*, *6*(APR), 1–13. https://doi.org/10.3389/fmicb.2015.00402

Schmidt, C. K., Raue, B., Brauch, H. J., & Sacher, F. (2013). Trace-level analysis of phosphonates in environmental waters by ion chromatography and inductively coupled plasma mass spectrometry. *International Journal of Environmental Analytical Chemistry*, 94(4), 385–398. https://doi.org/10.1080/03067319.2013.831410

*S*chowanek, D., & Verstraete, W. (1990). Phosphonate utilization by bacterial cultures and enrichments from environmental samples. *Applied and Environmental Microbiology*, *56*(4), 895–903. https://doi.org/10.1128/aem.56.4.895-903.1990

Schowanek, Diederik, McAvoy, D., Versteeg, D., & Hanstveit, A. (1996). Effects of nutrient trace metal speciation on algal growth in the presence of the chelator [S,S]-EDDS. *Aquatic Toxicology*, *36*(3–4), 253–275. https://doi.org/10.1016/S0166-445X(96)00807-7

Schwientek, M, Rügner, H., Haderlein, S. B., Schulz, W., Wimmer, B., Engelbart, L., Bieger, S., & Huhn, C. (2024). Glyphosate contamination in European rivers not from herbicide application? *Water Research*, *263*, 122140. https://doi.org/https://doi.org/10.1016/j.watres.2024.122140

Shamsi, Z., Buchner, D., & Haderlein, S. B. (2025). Trends in Analytical Chemistry Methods for pre-concentration and clean-up of glyphosate and aminomethylphosphonic acid from water samples : A review. *Trends in Analytical Chemistry*, *193*(September), 118459. https://doi.org/10.1016/j.trac.2025.118459

Silva, V., Montanarella, L., Jones, A., Fernández-Ugalde, O., Mol, H. G. J., Ritsema, C. J., & Geissen, V. (2018). Distribution of glyphosate and aminomethylphosphonic acid (AMPA) in agricultural topsoils of the European Union. *Science of the Total Environment*, *621*, 1352–1359. https://doi.org/10.1016/j.scitotenv.2017.10.093

Spinelli, V., Ceci, A., Dal Bosco, C., Gentili, A., & Persiani, A. M. (2021). Glyphosate-eating fungi: Study on fungal saprotrophic strains' ability to tolerate and utilise glyphosate as a nutritional source and on the ability of

purpureocillium lilacinum to degrade it. *Microorganisms*, *9*(11). https://doi.org/10.3390/microorganisms9112179

Stosiek N, Talma M, Klimek-Ochab M. Carbon-Phosphorus Lyase-the State of the Art. *Appl Biochem Biotechnol*. 2020 Apr;190(4):1525-1552. doi: 10.1007/s12010-019-03161-4.

Studnik, H., Liebsch, S., Forlani, G., Wieczorek, D., Kafarski, P., & Lipok, J. (2015). Amino polyphosphonates - chemical features and practical uses, environmental durability and biodegradation. *New Biotechnology*, *32*(1), 1–6. https://doi.org/10.1016/j.nbt.2014.06.007

Tauchnitz, N., Kurzius, F., Rupp, H., Schmidt, G., Hauser, B., Schrödter, M., & Meissner, R. (2020). Assessment of pesticide inputs into surface waters by agricultural and urban sources - A case study in the Querne/Weida catchment, central Germany. *Environmental Pollution*, *267*. https://doi.org/10.1016/j.envpol.2020.115186

Ternan, N. G., Mc Grath, J. W., Mc Mullan, G., & Quinn, J. P. (1998). Review: Organophosphonates: Occurrence, synthesis and biodegradation by microorganisms. *World Journal of Microbiology and Biotechnology*, *14*(5), 635–647. https://doi.org/10.1023/A:1008848401799

Venditti, S., Kiesch, A., & Hansen, J. (2023). Fate of glyphosate and its metabolite AminoMethylPhosponic acid (AMPA) from point source through wastewater sludge and advanced treatment. *Chemosphere*, *340*(July), 139843. https://doi.org/10.1016/j.chemosphere.2023.139843

Vereecken, H. (2005). Mobility and leaching of glyphosate: A review. *Pest Management Science*, *61*(12), 1139–1151. https://doi.org/10.1002/ps.1122

Wackett, L. P., Wanner, B. L., Venditti, C. P., & Walsh, C. T. (1987). Involvement of the phosphate regulon and the psiD locus in carbon-phosphorus lyase activity of Escherichia coli K-12. *Journal of Bacteriology*, *169*(4), 1753–1756. https://doi.org/10.1128/jb.169.4.1753-1756.1987

Wirsching, J., Wimmer, B., Ditterich, F., Schlögl, J., Martin-Laurent, F., Huhn, C., Haderlein, S., Kandeler, E., & Poll, C. (2022). 13C assimilation as well as functional gene abundance and expression elucidate the biodegradation of glyphosate in a field experiment. *Environmental Pollution*, *306*(March). https://doi.org/10.1016/j.envpol.2022.119382

Chapter 2

2 Influence of Organophosphonates as Alternative P-sources on Bacterial Transformation of Glyphosate

Kleanthi Kourtaki[1], Daniel Buchner[1*], Philipp R. Martin[1‖], Katharine J. Thompson[2], Stefan B. Haderlein[1]

[1]Department of Geosciences, Eberhard Karls University Tübingen, Germany

[2]Institute of Sanitary Engineering, Water Quality and Solid Waste Management (ISWA), University of Stuttgart, Germany

[‖]Present Address: Division for Environmental Geosciences, Centre for Microbiology and Environmental Systems Science, University of Vienna, Austria

Author	Author position	Scientific ideas	Data generation*	Analysis & interpretation	Paper writing
K. Kourtaki	1	50	75	50	50
D. Buchner	2	20	0	15	15
P. Martin	3	10	0	15	15
K. Thompson	4	10	0	10	10
S. Haderlein	5	10	0	10	10

Title of the paper:
Influence of organophosphonates as alternative P-sources on bacterial transformation of glyphosate

Status in the publication process:
Manuscript published in Environmental Pollution

*Experiments were conducted with the help of Martin Richter, Tamara Pruneddu, and Larissa Werle (see acknowledgements)

Chapter 2

Kleanthi Kourtaki, Daniel Buchner, Philipp R. Martin, Katharine J. Thompson, Stefan B. Haderlein,
Influence of organophosphonates as alternative P-sources on bacterial transformation of glyphosate,
Environmental Pollution, Volume 371, 2025, 125872, ISSN 0269-7491,
https://doi.org/10.1016/j.envpol.2025.125872.

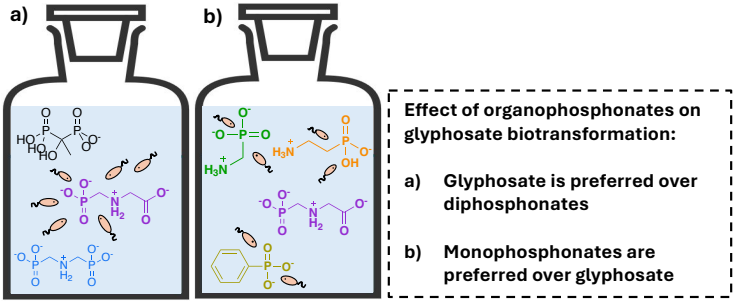

Scheme 2. 1. Graphical abstract summarizing the main findings and methodological approach of chapter 2.

Chapter 2

Keywords: Synthetic phosphonates; AMPA; P-cycling; C–P bond cleavage; C–P lyase; *Achromobacter*; *Ochrobactrum*

Highlights:

- N-(phosphonomethyl)glycine (glyphosate) transforming bacteria also utilized other mono- or diphosphonates as P-sources.
- Glyphosate was the least preferred monophosphonate utilized as sole P-source.
- Biotransformation of aminomethylphosphonate (AMPA) and 2-aminoethylphosphonate (AEP) can hinder glyphosate biotransformation.
- Glyphosate was a preferred P-source over the diphosphonates iminodi(methylene phosphonate) (IDMP) and 1-hydroxyethane-1,1-diphosphonate (HEDP).
- HEDP retarded glyphosate biotransformation and was weakly utilized as P-source.
- Organophosphonates (OPs) can adversely affect glyphosate biotransformation.

Chapter 2

2.1 Abstract

Glyphosate biotransformation under phosphorus (P)-limiting conditions has been demonstrated for numerous bacterial strains. However, besides glyphosate bacteria can utilize a broad spectrum of other biogenic and synthetic organophosphorus compounds (e.g., organophosphonates, OPs) as P-source. The ubiquity of OPs in the environment reduces the likelihood that bacteria will encounter conditions where glyphosate is the only P-containing compound. To study the impact of co-existing OPs on the biotransformation of glyphosate, we conducted batch cultivation experiments with the bacterial strains *Achromobacter insolitus* Kg 19 (*A*. Kg 19) and *Ochrobactrum pituitosum* GPr1-13 (*O*. GPr1-13) in which glyphosate and an additional OP were simultaneously provided as P-sources. Experiments with glyphosate and one additional monophosphonate (aminomethylphosphonate (AMPA), 2-aminoethylphosphonate (AEP), or phenylphosphonate (PPA)) showed that glyphosate was the least preferred P-source. Furthermore, the repeated supply of excess AMPA or AEP hindered the biotransformation of glyphosate. For strain *A*. Kg 19, AEP and AMPA threshold concentrations above which no glyphosate transformation occurred were approximately 40 and 120 μM, respectively. Conversely, in the presence of a synthetic diphosphonate (iminodi(methylene phosphonate) (IDMP) or 1-hydroxyethane 1,1-diphosphonate (HEDP)), strain *A*. Kg 19 preferred glyphosate as P-source. While IDMP was transformed after the depletion of glyphosate, HEDP concentration remained constant throughout the experiment and its presence retarded both cell growth and transformation of glyphosate. In light of the ubiquitous presence of AMPA and other OPs in the environment, our findings indicate that the presence of OPs may compromise the biotransformation potential of glyphosate, leading to lower transformation rates than those reported in previous studies.

2.2 Introduction

Phosphorus (P) is an essential macronutrient for microorganisms, required for various structural and metabolic processes (energy transport, synthesis of cellular material such phospholipids, nucleotides or nucleic acids, proteins, etc.) (Santos-Beneit, 2015). In the environment, microorganisms often encounter P-scarce conditions making P a major limiting factor for growth. Bacteria typically prefer P in the form of inorganic phosphate (Pi) or (organo-)phosphate esters ($O=P(+V)(OR)_3$). Under Pi-limiting conditions, however, organophosphonates (OPs) ($R–C–P(+III)O_3H_2$) that comprise a significant fraction of the environmental P-pool (e.g., up to 25% in oceans) can also serve as P-sources (Kolowith et al., 2001; Kamat and Raushel, 2013; McGrath et al., 2013).

OPs are anionic derivatives of phosphonic acid with one or more C–P bond(s). They can be of either biogenic (e.g., 2-aminoethylphosphonate acid (AEP),

phosphonoacetate or phosphonopyruvate) or of synthetic origin (Kamat and Raushel, 2013). Well-known synthetic OPs are the herbicide N-(phosphonomethyl)glycine (glyphosate) and its major metabolite aminomethylphosphonate (AMPA). Notably, also a biogenic origin of AMPA was recently demonstrated (Zhang et al., 2022). OPs also include synthetic polyphosphonates (PPs) containing more than one C–P bond(s) and are widely used complexing agents such as the diphosphonate 1-hydroxyethane-1,1-diphosphonate (HEDP) and the aminopolyphosphonates (APPs) diethylenetriamine penta(methylene phosphonate) (DTPMP) or ethylenediamine tetra (methylenephosphonate) (EDTMP) and their transformation products such as iminodi(methylene phosphonate) (IDMP) (Nowack, 2003; Grandcoin et al., 2017; Kuhn et al., 2017; Röhnelt et al., 2023; Röhnelt et al., 2025). PPs are used in a wide range of industrial and household applications, such as detergents, corrosion inhibitors and flame retardants (Nowack, 2003; Jaworska et al., 2002). While sorption onto sewage sludge is considered to be a significant removal process, approximately 9,000 to 18,600 t/a PPs enter surface waters through waste water treatment plant (WWTP) effluents accounting for municipal, agricultural and industrial contributions in Europe (Nowack, 2003; Rott et al., 2018). Synthetic OPs enter the environment via point sources, e.g., WWTP effluents or diffuse sources, such as the glyphosate application (Botta et al., 2009; Grandcoin et al., 2017). Recent studies identified WWTP as a major source of glyphosate in European rivers challenging the assumption that agricultural applications are the main origin of glyphosate in surface waters (Venditti et al., 2023; Schwientek et al., 2024; Röhnelt et al., 2025). These findings suggest that APPs are not only precursors for AMPA, but also of glyphosate, raising new questions about the processes involved in its environmental fate.

Bacteria have developed pathways to utilize OPs and convert them into more bioavailable P-containing compounds (Kamat and Raushel, 2013; Feng et al., 2020; Stosiek and Klimek-ochab, 2020). However, bacterial cell membranes are relatively impermeable to ionic compounds such as OPs. As a consequence, membrane transporting proteins are required for their uptake into the cell prior to metabolization (Ruffolo et al., 2023). The bacterial utilization of OPs involves the upregulation of genes encoding proteins and enzymes with a high binding affinity for the transport across the cell membrane as well as such capable of cleaving their hydrolytically stable C–P bond (Metcalf and Wanner, 1993; Rizk et al., 2006). Several enzymatic systems have been described for the transformation of OPs (e.g., phosphonoacetaldehyde, phosphonoacetate and phosphonopyruvate hydrolase, C–P lyase, glyphosate oxidoreductase (GOX)) (McMullan and Quinn, 1994; Kulakova et al., 2001; Kononova and Nesmeyanova, 2002; Villarreal-Chiu et al., 2012; Kamat and Raushel, 2013). Interestingly, Wang et al. (2016) reported that the predominant enzymatic system responsible for glyphosate transformation can change depending on nutrient conditions.

While numerous studies have shown that biotransformation is the main elimination process for glyphosate in the environment, studies on PPs transformation are scarce (Padilla and Selim, 2020; Masotti et al., 2023). Bacterial-driven glyphosate transformation has been mostly attributed to the activity of the C–P lyase (Kishore and Jacob, 1987; Pipke et al., 1987; Rossi et al., 2021; Sviridov et al., 2021; Riedel et al., 2024). The genetic characterization has shown that the C–P lyase is encoded by the *phn* operon, part of the phosphate (Pho) regulon, a mechanism by which the cells respond to the scarcity of exogenous phosphate (Pi) (Santos-Beneit, 2015). In *Escherichia coli*, the *phn* operon encodes a multi-enzyme system comprising 17 genes (*phnA* to *phnQ*) of which 14 (*phnC* to *phnP*) are involved in either the binding, uptake, or transformation of the OPs (Metcalf & Wanner,1993; Rizk et al., 2006). Through a series of enzymatic steps, OPs are converted into 5-phosphoribosyl-a- 1-diphosphate, a vital substrate for various cellular metabolic processes (Wackett et al., 1987; Kamat and Raushel, 2015; Seweryn et al., 2015).

Numerous laboratory studies on bacterial glyphosate transformation have been published in the last decades, mainly focusing on glyphosate as the only P-source (Pipke and Amrhein, 1988; Ermakova et al., 2008; Shushkova et al., 2012; Hadi et al., 2013; Shushkova et al., 2016; Ermakova et al., 2017; Sviridov et al., 2021; Rossi et al., 2021). In environmental systems, such as soils, glyphosate is often detected alongside other OPs such as AMPA (Skark et al., 1998; Botta et al., 2009; Daouk et al., 2013; Huntscha et al., 2018; Silva et al., 2018; Schwientek et al., 2024). The biogenic AEP is also likely to be found in environmental soils and waters and therefore coexist with glyphosate. Schowanek et al. (1990) found that among various strains capable of transforming AEP and other OPs, AEP was always transformed either by the phosphonoacetaldehyde hydrolase pathway encoded by the *phnX* gene (as part of the phosphonatase pathway also including the AEP aminotransferase encoded by the *phnW* gene) or exhibiting C–P lyase activity (Kim et al., 2002; Villarreal-Chiu et al., 2012). A recent work showed that biotransformation of OPs other than glyphosate (e.g., AMPA or IDMP) can also occur via the cleavage of the C–P bond by the C–P lyase (Riedel et al., 2024). These findings highlight the broad substrate range of C–P lyase, which includes glyphosate and other OPs, such as PPs, which were previously considered poorly biodegradable (Studnik et al., 2015).

To date, no systematic laboratory investigations have been conducted to determine the extent to which the presence of an additional OP, which can serve as a source of P, influences bacterial glyphosate transformation. To evaluate this effect, we conducted batch cultivation experiments with two bacterial strains – *Achromobacter insolitus* strain Kg 19 (VKM B-3295), and *Ochrobactrum pituitosum sp.* strain GPr1-13 – in which glyphosate and a second OP were simultaneously provided as P-sources. The selected strains belong to the phylum *Proteobacteria*, but differ in their class, order, family, and genus, providing an opportunity to compare glyphosate transformation dynamics across strains of various taxonomic levels. Genera such as *Pseudomonas*, *Agrobacterium*, *Rhizobium*, *Arthrobacter*, *Achromobacter*, and *Ochrobactrum* are commonly

reported among bacteria known to transform glyphosate (I. T. Ermakova et al., 2008; Hadi et al., 2013; A. V. Sviridov et al., 2015; I. T. Ermakova et al., 2017; Rossi et al., 2021). Studies isolating glyphosate-transforming bacterial strains from contaminated sites have consistently shown that among a large number of isolates, the most efficient strains typically belong to *Achromobacter* or *Ochrobactrum* genera (I. T. Ermakova et al., 2017; Masotti et al., 2021). They are widely distributed across diverse environmental settings, including agricultural soils where glyphosate is commonly found. Their high metabolic versatility enables them to adapt to various environments, and metabolize a wide range of substrates, including OPs. As alternative P-sources, we chose a suite of structurally related monophosphonates of natural and anthropogenic origin with varying functional groups such as carboxylic, amine or phenolic groups: AMPA, AEP and phenylphosphonate (PPA) (see Figure 2.1). Furthermore, we investigated the influence of the diphosphonates IDMP and HEDP on glyphosate transformation (see Figure 2.1). The results of these experiments will allow a better understanding of glyphosate biotransformation, accounting for the presence of further OPs – a factor of environmental relevance that has been largely overlooked in previous studies.

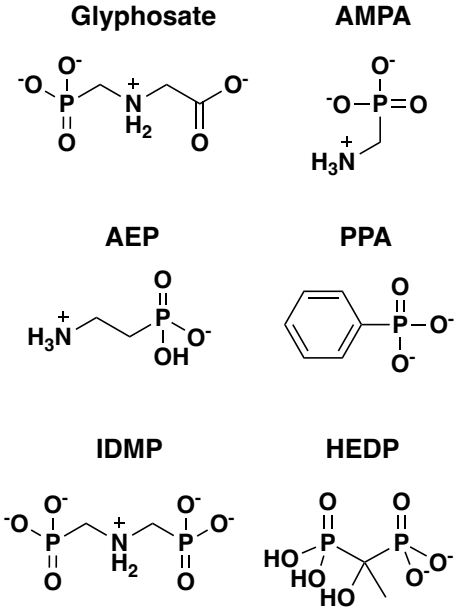

Figure 2.1 Chemical structures of OPs used in this study: N-(phosphonomethyl)glycine (glyphosate), aminomethylphosphonate (AMPA), 2-aminoethylphosphonate (AEP), phenylphosphonate (PPA),

iminodi(methylenephosphonate (IDMP), 1-hydroxyethane-1,1-diphosphonate (HEDP). Shown is the speciation at pH 7 (Boss et al., 2000; Franz, 2001; Popov et al., 2001; Kim et al., 2002; Skeff et al., 2018).

2.3 Materials and methods

Chemicals and materials

Glyphosate (>98%), AMPA (99%), AEP (>99%), PPA (>98%), IDMP (97%) and HEDP (95%) were all purchased from Sigma Aldrich (Steinheim, Germany). MOPS buffer (99.5%) was bought from Carl Roth (Karlsruhe, Germany) and sodium acetate (>99.5%) from Chemsolute (Renningen, Germany). Additional chemicals used for the experiments were purchased from Merck in their highest purity (Darmstadt, Germany). Purified water was used for all experiments obtained by a Barnstead GenPure system (Thermo Fischer Scientific, Germany).

Bacterial strains and cultivation conditions

Two rod-shaped bacterial strains representing species of different genera were used as model microorganisms (for SEM images see Figure A3 in the SI). A freeze-dried culture of *Achromobacter insolitus* strain Kg 19 (VKM B-3295) (hereafter will be referred to as *A*. Kg 19), originally isolated from the Krasnodar region in Russia (45°03’10.8’’N, 38°52’22.8’’E) was obtained from the Russian Centre of Microorganisms (VKM) (Tarlachkov et al., 2020). *Ochrobactrum pituitosum strain* GPr1-13 (hereafter will be referred to as *O*. GPr1-13) was isolated from the area of Poltringen, SW Germany (48°32'33.1"N 8°57'05.8"E). The cultures were maintained in a carbon – and nitrogen–rich medium, buffered with 50 mM MOPS and supplemented with glyphosate as the sole P-source. For each experiment, a fresh inoculum was prepared by cultivating each strain individually for 5 to 6 days, until a dense culture was obtained (optical density (OD) >> 1). On the day the experiment was started, 5 mL of each growing culture was harvested and centrifuged for 10 minutes at 7,000 rcf. The resulting cell pellets were washed twice by resuspension in centrifugation tubes using each time 5 mL sterile P-free medium. After the second washing step, the cell pellets were resuspended in 2.5 mL of the P-free medium, from which 100 µL served as inoculum for each living culture. All experiments were standardized to begin with a similar starting cell number, resulting in a cell density of approximately 10^6 cells mL^{-1}. The media composition for each strain, *A*. Kg 19 and *O*. GPr1-13, is summarized in the SI in Tables A1 and A2, respectively.

Setup of transformation batch experiments

For all experiments, 100 mL glass serum bottles, sterilized by dry heat at 180°C for 4.5 hours were used. The experiments were conducted at room temperature (21 ± 1 °C), with the bottles continuously shaken on a rotary shaker at 150 rpm. Each culture was prepared under sterile conditions, filled with 100 mL of sterile medium, and adjusted to the desired OP concentration by adding a sterile-filtered stock solution prepared in the respective media. The serum bottles were sealed with sterile, oxygen-permeable cotton stoppers. The experiment was initiated by inoculating bottles with the living cells. Each experiment consisted of two or three living replicates, one biotic control (P-free medium) and one abiotic control to assess potential interactions with the OPs and the medium. Organophosphates were excluded from our experimental setup, due to their instability in the media matrix, which led to release of Pi. For each sampling point, 1 mL of sample was withdrawn under sterile conditions with a transfer pipette and transferred to a 1 cm PP cuvette for monitoring growth via optical density measurement with a UV5Bio spectrophotometer (Mettler Toledo, Germany). For consistency and comparability with existing literature for strain *A*. Kg 19, a wavelength of 560 nm was used, while for strain *O*. GPr1-13 all measurements were conducted at 600 nm, which is the common practice for bacterial strains (A. V. Sviridov et al., 2021; T. Ermakova et al., 2017; Rossi et al., 2021; Castledine et al., 2024). Additional 5 mL of sample was withdrawn and transferred to a 5 mL centrifugation tube (Eppendorf, Hamburg, Germany) for centrifugation (10 minutes at 12,000 rcf). The biomass-free supernatant was separated from the cell pellet and stored in 2 mL centrifugation tubes at -20 °C in the dark till concentration analysis, if not analyzed directly. The storage procedure had no adverse effect with respect to the stability of the OPs. During the experiment, the pH was maintained between 6.8 and 7.5 by the addition of 20% sterile H_2SO_4. Transformation rates were determined by performing a linear regression between the timepoints that showed the highest transformation and are summarized in the SI Tables A7, A8, and A9.

Analytical methods
Quantification of orthophosphate

Samples containing orthophosphate were diluted 1:5 with ultrapure water in a 1 cm PP cuvette prior to analysis. Orthophosphate was determined with the molybdenum-blue method adapted from Murphy and Riley (1962) at 710 nm with a UV5Bio spectrophotometer (Mettler Toledo, Germany).

Quantification of glyphosate, AMPA, AEP, IDMP and HEDP
The analytes were quantified with a 930 Compact Flex ion chromatograph equipped with an amperometric detector operated in integrated pulsed amperometric detection (iPAD) mode (Metrohm, Herisau, Switzerland) (see SI, Table A3). Separation of the analytes was realized on an anion-exchange column (Metrosep Carb 2, 100 x 4.0 mm). The analysis of glyphosate, AMPA and AEP included a flow gradient (see SI, Table A4) using 290 mM sodium acetate + 10

mM NaOH as eluent, while IDMP or HEDP separation was achieved with 345 mM sodium acetate + 15 mM NaOH (for flow gradient see SI, Table A5). Prior to the analysis, all samples were diluted with ultrapure water and quantified with external standards in a concentration range 0 to 20 µM. Exemplary chromatograms are available in the SI (see Figure A1).

Quantification of phenylphosphonate (PPA)
PPA was quantified by a LC-20 HPLC system (Shimadzu Germany, Duisburg, Germany) equipped with a binary pump and a UV/Vis detector operated at a wavelength of 210 nm. Chromatographic separation of the analytes was realized on a Triart C18 column (150 mm x 2 mm, 5 µm particle) + guard column (10 mm x 2 mm, 5 µm particle, both YMC Europe, Dinslaken, Germany) with a flow rate of
0.5 mL min^{-1} applying a gradient elution of 5% acetonitrile + 0.1% H_3PO_4 (eluent A) and 5% water + 0.1% H_3PO_4 in acetonitrile (eluent B) (for gradient see SI, Table A6). Quantification was achieved by external standards at a concentration range of 10 to 120 µM. A dilution factor of 5 was applied in all samples prior to their analysis. An exemplary chromatogram is available in the SI (see SI, Figure A2).

2.4 Results and Discussion

To investigate the effect of OPs as alternative P-sources on the bacterial glyphosate (GP) transformation, four sets of batch experiments were performed with the glyphosate transforming bacterial strains *A*. Kg 19 and *O*. GPr1-13 in a carbon- and nitrogen-rich medium under oxic conditions. In the first set, we investigate the ability of the strains to utilize selected monophosphonates as sole P-sources. To examine their influence on the bacterial transformation of glyphosate, we conducted experiments with glyphosate and a second monophosphonate as P-sources at equimolar concentrations. Further on, experiments with continuous monophosphonate-addition as well as in excess supply were conducted to investigate concentration-dependent effects. Lastly, the impact of diphosphonates on the glyphosate transformation was studied. For each experiment, pure cultures of each strain, pre-grown with glyphosate were used as inoculum. Changes in optical densities as a proxy for bacterial growth as well as the OPs concentrations were monitored over time for each experiment. No bacterial growth or transformation was observed in biotic P-free or abiotic P-supplemented controls in any of the setups tested (data provided in the SI in Figures A5, A7, A9, A10, and A11). Calculated transformation rates are summarized in the SI (see Table A7, A8, and A9).

Chapter 2

Ability of the strains to utilize and transform selected monophosphonates as P-sources

Initially, the transformation of four monophosphonates (GP, AMPA, PPA & AEP) as P-sources by the strains *A*. Kg 19 and *O*. GPr1-13 was investigated individually. For comparison, an experiment with orthophosphate (Pi) was conducted for each strain and used as positive control.
Single compound incubations with 0.5 mM of either GP, AMPA, PPA, AEP or Pi resulted in significant growth which was coupled to the transformation of each P-source for both strains (see SI, Figures A4A, B for growth profiles; Figures A4C, D for concentration). Pi was identified as the preferred P-source and exhibited the fastest depletion in setups with either strain, as expected, since Pi requires only uptake and direct utilization. In contrast, the OPs must first be transformed before their P can be utilized. Strain *O*. GPr1-13 showed minor differences in the growth and transformation kinetics of the OP-tested, whereas strain *A*. Kg 19 utilized AEP faster than AMPA, PPA or glyphosate (see SI, Figures A4,D, for transformation rates see Table A7). By the end of the experiment, total P-removal ranged from 84 to 100% for *O*. GPr1-13 and 61 to 100% for *A*. Kg 19. The lowest removal efficiencies were observed for setups with glyphosate for both strains. Although glyphosate was transformed to a lesser extent compared to the other OPs, both strains efficiently transformed AMPA and glyphosate as sole P-sources. While certain bacterial strains within the genera *Achromobacter* or *Ochrobactrum* were demonstrated to transform glyphosate and AMPA, it is not a universal trait shared. *Ochrobactrum sp*. strain GDOS for instance was shown to be capable of transforming glyphosate but not AMPA indicating that the ability of AMPA transformation is not a feature shared among strains within this genus (Hadi et al., 2013). The thermophilic strain *Geobacillus caldoxylosilyticus* T20 was shown to transform AMPA as a metabolite of glyphosate transformation. However, the strain failed to utilize AMPA when it was supplied extracellularly as sole P-source (Obojska et al., 2002). This suggests that the strain's ability to transform AMPA may be regulated or limited at the binding or uptake level (e.g., due to the absence of transport proteins or constraints in AMPA binding to the transport protein) rather than by the substrate specificity of the catalyzing enzyme. The common ability of the strains *A*. Kg 19 and *O*. GPr1-13 to utilize the provided OPs indicates that the strains carry genes encoding enzymes facilitating the binding, transport and the C–P bond cleavage of the tested OPs. Due to lack of genomic data, the pathway by which the strain *O*. GPr1-13 transforms glyphosate and other OPs remains unidentified. Genome analysis of strain *A*. Kg 19 has shown, the strain carries the *phnX* gene, which encodes phosphonoacetaldehyde hydrolase, an enzyme primarily involved in AEP transformation (A. V. Sviridov et al., 2012; Tarlachkov et al., 2020; Sviridov et al., 2021; Epiktetov et al., 2024). Additionally, genome analysis revealed that *A*. Kg 19 does not encode a GOX pathway for glyphosate transformation (Epiktetov et al., 2024). Instead, it contains a putative C–P lyase multi-enzyme complex, which facilitates the utilization of P through the

conversion of glyphosate, and possibly of AMPA and PPA as well (Tarlachkov et al., 2020; Epiktetov et al., 2024). However, further research is needed using molecular biology to identify all specific enzymes involved in the transformation of the OPs tested by the two strains.
Overall, these results demonstrated that both strains effectively transformed all OPs-tested as alternative P-sources in the absence of P.

Biotransformation of glyphosate in presence of monophosphonates as P-sources

To investigate the effects of OPs as alternative P-sources on glyphosate biotransformation, the monophosphonates AMPA, PPA or AEP were provided together with glyphosate in equimolar concentrations (c = 0.25 mM each, $c(P_{tot})$ = 0.5 mM) and compared to an experiment containing solely glyphosate (c = $c(P_{tot})$ = 0.5 mM). A positive control with glyphosate and Pi was also included. The glyphosate concentration profiles obtained from all setups are summarized in Figure 2.2. Both strains started metabolizing glyphosate directly after inoculation when it was the sole P-source. By day 2, strain *O*. GPr1-13 exhibited 22% transformation of glyphosate, while 40% transformation was shown by strain *A*. Kg 19 during the same time. By the end of the experiment, the glyphosate transformation extent reached 88% for both strains (for transformation rates, see SI, Table A8). In contrast, no glyphosate transformation occurred the first 2 days in setups with either of the two strains in the positive control. Interestingly, when glyphosate was provided alongside other OPs, only minor or no glyphosate transformation occurred within the first 2 days of cultivation for both strains as well. This indicates that the presence of all tested OPs retarded the transformation of glyphosate. Nonetheless, by the end of the experiment, glyphosate transformation percentages ranged from 78 to 100% in all setups. Growth in setups with either glyphosate as the sole phosphorus source or in combination with a second OP was comparable to the control setups with Pi, indicating that both strains grew equally well in all setups, regardless of P-source combination (see SI, Figure A6).

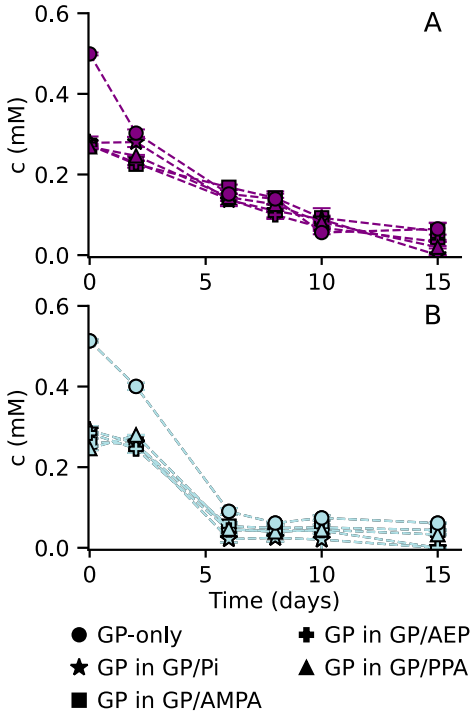

Figure 2.2 Glyphosate concentration over time in competition experiments with A) *A*. Kg 19 (dark- purple symbols) and B) *O*. GPr1-13 (light-green symbols). Glyphosate (GP) was either the sole P-source (c=0.5 mM) (circles connected by lines) or provided in a mixture with equimolar concentrations
(c=0.25 mM) of either Pi (stars connected by lines), AMPA (squares connected by lines), AEP (crosses connected by lines), or PPA (triangles connected by lines). Error bars represent the standard deviation of duplicate cultures (if not visible, error bars are smaller than the data points).

To shed further light on the dynamics of glyphosate biotransformation in presence of an OP as alternative P-source, the changes in concentrations of both compounds (glyphosate and second monophosphonate) as well as the respective growth profiles are visualized for each setup in Figure 2.3. Both strains exhibited growth coupled to the transformation of the P-sources with no lag phase. The concentration profiles revealed that among the OPs tested, glyphosate was the least

preferred P-source. In binary experiments with glyphosate and AEP, both strains completely transformed AEP within 2 days of cultivation. Similarly, in the glyphosate/PPA setups, PPA transformation ranged from 85 to 100% by strains *O*. GPr1-13 and *A*. Kg 19, respectively, by day 2. In the glyphosate/AMPA setup, AMPA transformation preceded glyphosate transformation, with strains *A*. Kg 19 and *O*. GPr1-13 removing 67% and 71% of AMPA, respectively, by day 2. Across all binary setups, glyphosate removal remained below 20% during this period, while in the control setup with solely glyphosate, glyphosate transformation exceeded 22% with either of the two strains. However, subsequent transformation in binary setups eventually resulted in at least 80% total glyphosate removal. Overall, both strains showed substantial transformation of each OP across the different setups, resulting in total P-removal ranging from 88% to 100% within the 15-day experimental run-time. These findings reveal a clear hierarchy in the utilization of AMPA, PPA and AEP by the bacterial strains, which were consistently preferred over glyphosate, retarding its transformation. In the presence of Pi, as seen with other bacteria, no glyphosate transformation occurred. As the enzymes required for glyphosate transformation-–regulated by the Pho regulon (e.g., C–P lyase multi-enzyme system)–are likely not induced, no glyphosate transformation was expected in the positive control until Pi was depleted (e.g., by strain *A*. Kg 19). A recent study has shown that glyphosate can also enter bacterial cells via unspecific glutamate transport proteins, also in the presence of Pi (Wicke et al., 2019). However, Stosiek and Klimek-Ochab (2020) noted that the *de novo* synthesis of proteins from the *phn* operon is suppressed when extracellular Pi levels exceed 4 µM. Amongst others, Kononova and Nesmeyanova, (2002) investigated the cultivation of different bacterial strains with Pi and OPs (methylphosphonate, PPA or AEP) and observed that Pi uptake was always preferred and, in most cases, transformation of OPs started only after Pi was depleted (Roseberg and La Nauze, 1967). Additionally, glyphosate was a less favored P-source in the presence of AEP as alternative P-source. As strain *A*. Kg 19 harbours the *phnX* gene, preferential transformation of AEP over glyphosate might occur via the PhnX pathway. Schowanek et al. (1990) also identified AEP as the most readily accessible OP compared to others, including glyphosate, across different strains. This preference was consistent regardless of the type of pathways (PhnX or C–P lyase) for AEP transformation, which may also apply to the strains in this study. Further supporting this, Rizk et al., (2006) showed that the periplasmic phosphonate-binding PhnD, a component of the *phn* operon, exhibits higher affinity for AEP compared to other OPs like glyphosate and AMPA, as indicated by its lower dissociation constant ($K_{d,AEP}$=0.005 µM vs $K_{d,AMPA}$=5 and $K_{d,glyph}$=650 µM). This likely drives the preferential transformation of AEP compared to other OPs by the C–P lyase pathway. Finally, AMPA was clearly preferred over glyphosate, which contrasts with some previous studies that suggested AMPA typically transforms more slowly than glyphosate (Aparicio et al., 2013; Grandcoin et al., 2017). However, other studies involving *Achromobacter* or *Ochrobactrum* strains also reported a high efficiency in

transforming both glyphosate and AMPA when provided separately by the C–P lyase pathway, likely due to PhnD's high affinity for OPs (for example $K_{d,AMPA}$=5 µM) (Rizk et al., 2006; Masotti et al., 2021; Riedel et al., 2024). Given that the C–P lyase system is present in the genome of strain *A*. Kg 19, but the GOX gene was not identified, the transformation of AMPA and glyphosate is likely mediated solely by enzymes encoded by genes in the *phn* operon. Overall, all findings presented here demonstrate that AMPA undergoes bacterial transformation more favorably than glyphosate. As a transformation product of both glyphosate and APPs, AMPA typically occurs at higher environmental concentrations than glyphosate. In European soils, glyphosate and AMPA typically range from 10 to 80 µg/kg and 30 to 2,100 µg/kg, respectively, though higher concentrations have been reported in some cases (Silva et al., 2018; Wimmer et al., 2022). Similar trends are observed in surface waters like lakes and rivers, where glyphosate and AMPA concentrations generally do not exceed 0.2 µg/L (Poiger et al., 2017). However, in water bodies receiving discharges from wastewater treatment plants, both glyphosate and AMPA are found at much higher levels (Schwientek et al., 2024). Considering the higher concentrations of AMPA compared to glyphosate, along with their observed dynamics on bacterial transformation, AMPA is likely to undergo biotransformation before glyphosate and prolong the residence time of glyphosate in the environment.

In summary, across all experiments, both strains primarily utilized the second OP (AMPA, PPA, AEP). Glyphosate was either slowly transformed alongside the second OP or sequentially after its depletion, leading to a delay in its transformation.

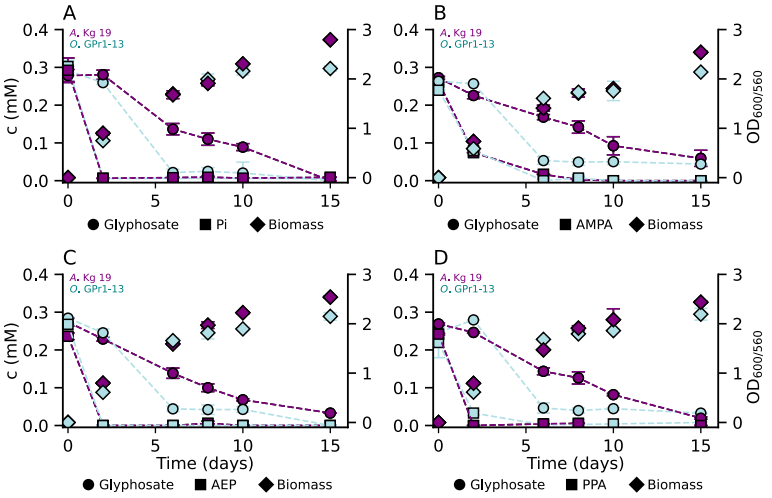

Figure 2.3 Glyphosate, AMPA, AEP, and Pi concentrations, as well as optical density over time in competition experiments with *A*. Kg 19 (dark-purple symbols) and *O*. GPr1-13 (light-green symbols). Glyphosate was provided at 0.25 mM in parallel with equimolar concentrations of (A) Pi, B) AMPA, C) AEP, or (D) PPA. Diamonds represent optical density, circles (connected by lines) represent glyphosate concentration, and squares (connected by lines) represent Pi, AMPA, AEP, or PPA. Error bars represent the standard deviation of duplicate cultures (if not visible, error bars are smaller than the data points).

Biotransformation of glyphosate in presence of excess monophosphonates as P-sources

To study the effect of prolonged exposure of additional P-sources on the biotransformation of glyphosate, cultivation experiments were performed in which the second OP was initially provided at concentrations twice as high as glyphosate. We selected AEP and AMPA as the second monophosphonates, as they exhibited the highest and lowest transformation rates, respectively, among the previously tested OPs (c(GP) = 0.25 mM and c(AEP/AMPA) = 0.5 mM). To avoid depletion as well as to ensure a prolonged presence of AEP or AMPA, the cultures were periodically re-spiked with about 0.25 mM of AEP/AMPA each pulse. Cultures with glyphosate and AEP were re-spiked with AEP after 2, 3.5 and 8 days of cultivation, while two additions of AMPA after 2 and 3.5 days were sufficient to avoid the depletion of AMPA. The results visualized in Figure 2.4 indicate that both strains exclusively transformed AEP or AMPA as P-sources, while glyphosate concentration remained constant throughout the experimental run-time. Consistent with previous experiments for the two strains, AEP and AMPA were continuously transformed by *A*. Kg 19 with rates of 0.116 and 0.058 mM day^{-1}, resulting in a total removal of 95 and 90%, respectively. However, their transformation stagnated by day 22, with concentrations reaching approximately 60 µM for AEP and 100 µM for AMPA (see Figure 2.4A, B). Similarly, strain *O*. GPr1-13 transformed AEP and AMPA with almost identical rates equal to 0.073 and 0.071 mM day^{-1}, respectively. After 42% AEP and 43% AMPA removal, transformation stagnated and about 700 µM AEP and 500 µM AMPA were left in the solution (see Figures 2.4C, D). Overall, the results presented here highlight the metabolic preferences of strains *A*. Kg 19 and *O*. GPr1-13 which exclusively utilized AEP and AMPA when present at excess concentrations, hindering the transformation of glyphosate. These findings provide valuable insights into the hierarchies that govern OP utilization in these strains under the tested conditions. The results underscore the complexity of substrate preference and highlight the importance of considering these dynamics, especially in environmental contexts where OPs are abundant in high concentrations.

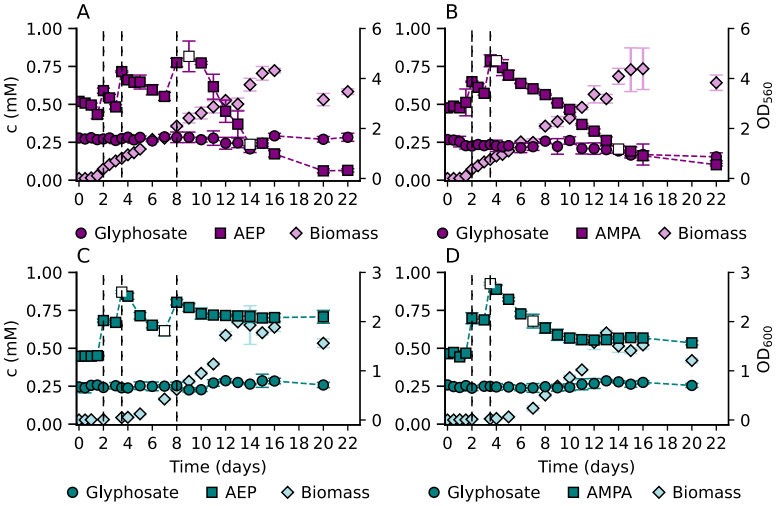

Figure 2.4 Glyphosate, AEP, AMPA concentrations, and optical density over time in spiking experiments with *A*. Kg 19 (purple symbols) and O. GPr1-13 (green symbols). Glyphosate (GP) was provided at 0.25 mM in parallel with (A), (C) AEP or (B), (D) AMPA. Diamonds represent optical density, circles (connected by lines) represent glyphosate concentration, and squares (connected by lines) represent AEP or AMPA concentration. Dashed vertical lines indicate the days when cultures were spiked with the respective compounds of AEP or AMPA. After three pulses of AEP and two pulses of AMPA, the total concentrations of AEP and AMPA introduced were 1.25 mM and 1 mM, respectively. Data points marked with white symbols indicate the time points used to calculate the transformation rates of the OPs. Error bars represent the standard deviation of triplicate cultures (if not visible, error bars are smaller than the data points).

To explore the AEP or AMPA concentration-dependent effect on the restriction of glyphosate transformation, additional experiments were performed. In two separate setups, the alternative P-sources were provided at concentrations twice as high as the initial glyphosate concentration (glyphosate c = 0.25 mM, AEP or AMPA c = 0.5 mM), however, no further re-spike of AEP or AMPA took place. As in the previous experiments, strain *A*. Kg 19 and strain *O*. GPr1-13 primarily transformed AEP or AMPA for 8 to 9 days with rates of 0.113 (AEP) and 0.039 (AMPA) mM day^{-1} and 0.071 (AEP) and 0.059 (AMPA) mM day^{-1}, respectively (see Figures 2.5A, B, transformation and growth profiles for strain *O*. GPr1-13 are available in SI, Figures A8A, B). The growth as well as the transformation of AEP and AMPA by strain *O*. GPr1-13 stagnated on day 12, with 86 µM of AEP and 155

µM AMPA remaining in the solution (see Figures A8A, B). For this strain, minor glyphosate transformation was observed over the course of 15 days. Conversely, strain *A*. Kg 19 showed diauxic metabolism and started sequentially transforming glyphosate after 8 to 9 days, when AEP and AMPA concentrations reached 28 µM and 120 µM, respectively. After an experimental run-time of 15 days, over 75% of glyphosate was transformed in both setups, whereas in re-spike experiments, the respective glyphosate transformation by strain *A*. Kg 19 did not exceed 20% (see Figures 2.4A, B). Notably, glyphosate transformation proceeded at almost identical rates compared to the additionally provided OP (glyphosate rates equaled 0.106 mM day^{-1} for the AEP setup and 0.061 mM day^{-1} for AMPA setup). However, for effective glyphosate biotransformation by strain *A*. Kg 19, we estimated threshold concentrations of 120 µM for AMPA and 28 µM for AEP, respectively. In contrast, the absence of glyphosate transformation in the setups with strain *O*. GPr1-13 prevented the determination of a threshold concentration for AEP and AMPA.

In summary, all findings support that when AMPA and AEP are present in excess, they are preferentially transformed by both strains, hindering glyphosate biotransformation. However, as shown by data from strain *A*. Kg 19, once their concentration reaches a threshold, glyphosate can be sequentially transformed. The results provide experimental evidence of the concentration-dependent effects of OPs on bacterial glyphosate transformation. While the role of Pi as a limiting factor in glyphosate transformation is well known, the intricate dynamic of OPs like AEP or AMPA as alternative P-sources as well as their role as potential suppressors of glyphosate bacterial transformation was not shown before.

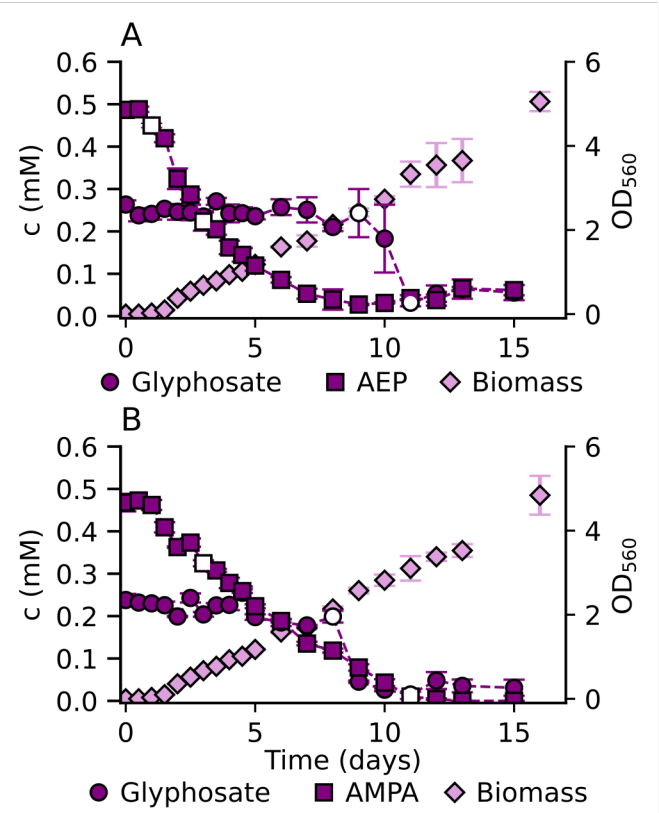

Figure 2.5 Glyphosate, AEP, AMPA concentrations, and optical density over time of *A*. Kg 19. Glyphosate (GP) was provided at 0.25 mM in parallel with (A) AEP or (B) AMPA at c=0.5 mM. Diamonds represent optical density, circles (connected by lines) represent glyphosate concentration, and squares (connected by lines) represent changes in AEP or AMPA concentration. Data points marked with white symbols indicate the time points used to calculate the transformation rates of the OPs. Error bars represent the standard deviation of triplicate cultures (if not visible, error bars are smaller than the data points).

Biotransformation of glyphosate in the presence of diphosphonates as P sources

OPs with more than one C–P bond(s) have been considered poorly biodegradable in the past, but recent studies indicate that these compounds can also serve as P-

sources for bacteria under P-limiting conditions (Forlani et al., 2011; Riedel et al., 2023; Riedel et al., 2024). So far, no study has investigated how the presence of diphosphonates affects the biotransformation of glyphosate. To this end, we carried out experiments with strain *A*. Kg 19, supplying an equimolar concentration (0.25 mM) of glyphosate and one synthetic diphosphonate (IDMP or HEDP). An experiment with glyphosate as sole P-source (c=0.25 mM) was used as control setup (see Figures 2.6A, B and C). Transformation of glyphosate was observed in the control experiment as well as in the glyphosate/IDMP setup with rates 0.082 and 0.057 mM day^{-1}, respectively (see Figure 2.6A). Following the depletion of glyphosate, IDMP was completely transformed within 16 days of cultivation with a rate of 0.028 mM day^{-1}, accompanied by bacterial growth (see Figure 2.6B). Conversely, in the glyphosate/HEDP setup, glyphosate transformation started after a 7-day lag phase with a rate approximately half that of the control glyphosate setup (equal to 0.035 mM day^{-1}). A subsequent HEDP transformation was not observed (see Figure 2.6C). The presence of HEDP resulted in a clear retardation in both growth and glyphosate transformation indicating that HEDP exerts a temporary inhibitory effect.

In line with these findings, significant growth and IDMP transformation was observed when IDMP (c=0.5 mM) was provided to strain *A*. Kg 19 as sole P-source (see SI, Figure A10A). However, when HEDP was the sole P-source (c=0.5 mM), no growth and HEDP transformation were observed for 12 days. Afterward, HEDP transformation started and led to maximum removal of 24% of the total HEDP, which was accompanied by weak growth (OD <2), over the 21-day experimental period. These results suggest the strain exhibits a lower transformation potential for HEDP compared to IDMP, as indicated by the delayed growth and incomplete HEDP transformation (see SI, Figure A10B). Similarly to our observations, Riedel et al., (2023) demonstrated that *Ochrobactrum* sp. strain BTU1, which can successfully transform OPs like IDMP or AMPA and utilize them as P-sources via the C–P lyase pathway, was unable to transform HEDP. The authors attributed this to the C–P lyase's inability to cleave the C–P bond in this compound. Nitrogen-free OPs such as HEDP are found to be more resilient towards bacterial-driven transformation compared to APPs, and are mainly transformed via abiotic processes (Fischer, 1993; Schowanek & Verstraete, 1990; Rott et al., 2018). Studies on the bacterial transformation of OPs with more than one C–P bonds are scarce. Notably, in the subsequent study by Riedel et al., (2024), the *Ochrobactrum* sp. strain BTU1 exhibited higher transformation activity for IDMP compared to glyphosate. However, the data presented in our study indicates that glyphosate was transformed more rapidly than IDMP. This finding, along with the observed differences in the transformation of glyphosate and AMPA between *Ochrobactrum sp*. strain GDOS and *O*. GPr1-13, as reported by Hadi et al. (2013), further highlight the variability within this genus regarding the utilization of OPs as P-source. These findings emphasize the significance of strain-specific characteristics in determining transformation preferences and affinities for OPs.

In summary, our results demonstrate that strain *A*. Kg 19 preferentially transformed glyphosate over the diphosphonates contrary to observations with monophosphonates as second P-sources. The ability of the strain *A*. Kg 19 to transform a diphosphonate as P-source was documented for the first time. These findings imply that bacterial strains capable of transforming glyphosate as P-source in the absence of other OPs with a single C–P bond can also transform OPs with more C–P bond(s) and contribute to their elimination from the environment.

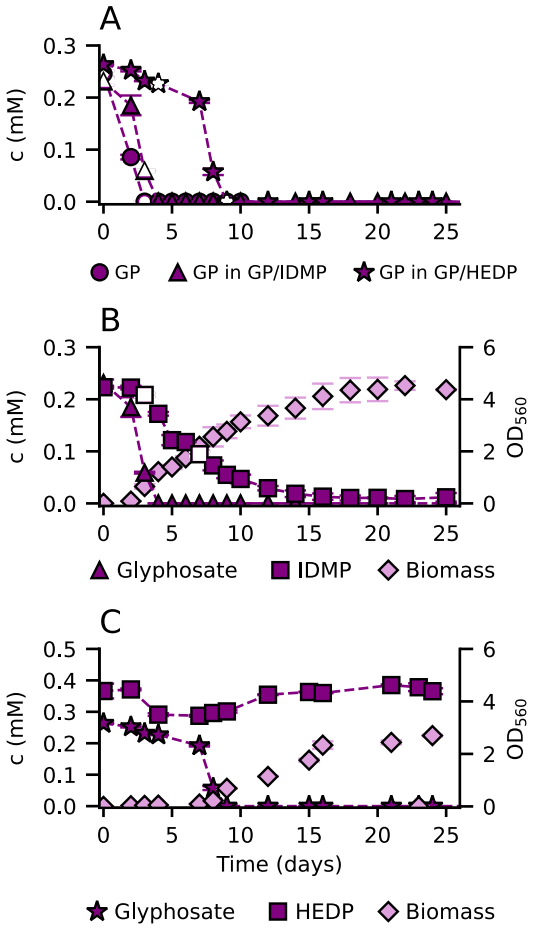

Figure 2.6 (A) Glyphosate (GP) concentration over time when provided to *A*. Kg 19 as sole P-source at c=0.25 mM (circles connected by lines), in a mixture with

0.25 mM IDMP (triangles connected by lines) or in a mixture with 0.25 mM HEDP (stars connected by lines). B) Glyphosate (triangles connected by lines) and IDMP (squares connected by lines) concentration over time when provided in equimolar concentrations (c=0.25 mM) to *A*. Kg 19. C) Glyphosate (stars connected by lines) and HEDP (squares connected by lines) concentration over time when provided in equimolar concentrations (c=0.25 mM) to *A*. Kg 19. Diamonds represent changes in optical density over time of *A*. Kg 19. Data points marked with white symbols indicate the time points used to calculate the transformation rates of the OPs. Error bars represent the standard deviation of triplicate cultures (if not visible, error bars are smaller than the data points).

2.5 Environmental implications

Overall, the results of this study suggest that the presence of OPs as alternative P-sources can hinder the bacterial transformation of glyphosate by two distinct bacterial strains (*A*. Kg 19 and *O*. GPr1-13). Even though glyphosate was preferably taken up when it was supplied simultaneously with a diphosphonate, we observed a retardation of glyphosate biotransformation when provided in a mixture with HEDP. Furthermore, we demonstrated that under the tested conditions, among the monophosphonates AEP, AMPA, or PPA, glyphosate was the least preferred one. Additionally, we showed that when monophosphonates like AEP or AMPA exceed a certain concentration-threshold, they are exclusively transformed, leaving glyphosate unaffected.

These findings highlight the metabolic versatility of the tested bacterial strains capable of utilizing a range of OPs as P-sources and clearly demonstrate their influence on the biotransformation of glyphosate. While the potential of glyphosate transformation by bacteria utilizing it as P-source has been widely proposed based on laboratory experiments particularly under P-deficiency conditions, our results suggest that bacterial glyphosate biotransformation is also significantly affected by coexisting OPs. Although it is well documented that glyphosate biotransformation is impeded in phosphate-rich environments, the role of OPs has not been previously investigated. The findings presented here are of high environmental relevance as glyphosate sinks are rarely OP-free environments. Field studies in basins and water bodies have consistently shown that the detection of glyphosate is often accompanied by high concentrations of other OPs, such as AMPA (Skark et al., 1998; Jaworska et al., 2002; Botta et al., 2009; Coupe et al., 2012; Aparicio et al., 2013, Poiger et al., 2017; Schwientek et al., 2024). Consequently, the presence of AMPA alongside with its higher transformation potential compared to glyphosate, may facilitate glyphosate accumulation and potentially pose environmental risks. Therefore, it is essential to consider the presence of OPs when evaluating the fate and residence times of glyphosate in the environment, despite the high biotransformation potential that has been reported for it under P-limiting conditions.

Although our study was carried out on a limited number of strains under controlled laboratory conditions and in concentration ranges that are typically higher than those encountered in most environmental contexts, it provides new insights. We present the first comprehensive data set on substrate competition and varying availability in the context of glyphosate biotransformation which provides a new dimension to a deeper understanding of these processes. Thus, our research can inform future research studying how these transformation processes occur in more complex environments, where the dynamics of diverse microbial communities, enzymatic pathways, varying OP concentration ranges, and the maintenance of metabolism all come into play, and help bridge the gap between laboratory findings and real-world scenarios.

2.6 References

Aparicio, V. C., De Gerónimo, E., Marino, D., Primost, J., Carriquiriborde, P., & Costa, J. L. (2013). Environmental fate of glyphosate and aminomethylphosphonic acid in surface waters and soil of agricultural basins. *Chemosphere*, *93*(9), 1866–1873. https://doi.org/10.1016/j.chemosphere.2013.06.041

Boss, E. A., Moolenaar, S. H., Massuger, L. F. A. G., Boonstra, H., Engelke, U. F. H., De Jong, J. G. N., & Wevers, R. A. (2000). Aminomethylphosphonate and 2-aminoethylphosphonate as 31P-NMR pH markers for extracellular and cytosolic spaces in the isolated perfused rat liver. *NMR in Biomedicine*, *13*(5), 289–296. https://doi.org/10.1002/1099-1492(200008)13:5<289::AID-NBM647>3.0.CO;2-G

Botta, F., Lavison, G., Couturier, G., Alliot, F., Moreau-Guigon, E., Fauchon, N., Guery, B., Chevreuil, M., & Blanchoud, H. (2009). Transfer of glyphosate and its degradate AMPA to surface waters through urban sewerage systems. *Chemosphere*, *77*(1), 133–139. https://doi.org/10.1016/j.chemosphere.2009.05.008

Castledine, M., Pennycook, J., Newbury, A., Lear, L., Erdos, Z., Lewis, R., Kay, S., Sanders, D., Sünderhauf, D., Buckling, A., Hesse, E., & Padfield, D. (2024). Characterizing a stable five-species microbial community for use in experimental evolution and ecology. *Microbiology*, *170*(9), 1–11. https://doi.org/10.1099/mic.0.001489

Coupe, R. H., Kalkhoff, S. J., Capel, P. D., & Gregoire, C. (2012). Fate and transport of glyphosate and aminomethylphosphonic acid in surface waters of agricultural basins. *Pest Management Science*, *68*(1), 16–30. https://doi.org/10.1002/ps.2212

Daouk, S., Copin, P. J., Rossi, L., Chèvre, N., & Pfeifer, H. R. (2013). Dynamics and environmental risk assessment of the herbicide glyphosate and its metabolite AMPA in a small vineyard river of the Lake Geneva catchment.

Environmental Toxicology and Chemistry, *32*(9), 2035–2044. https://doi.org/10.1002/etc.2276

Epiktetov, D. O., Sviridov, A. V., Tarlachkov, S. V., Shushkova, T. V., Toropygin, I. Y., & Leontievsky, A. A. (2024). Glyphosate-Induced Phosphonatase Operons in Soil Bacteria of the Genus Achromobacter. *International Journal of Molecular Sciences*, *25*(12), 1–22. https://doi.org/10.3390/ijms25126409

Ermakova, I. T., Shushkova, T. V., & Leont'evskii, A. A. (2008). Microbial degradation of organophosphonates by soil bacteria. *Microbiology*, *77*(5), 615–620. https://doi.org/10.1134/S0026261708050160

Ermakova, Inna T., Shushkova, T. V., Sviridov, A. V., Zelenkova, N. F., Vinokurova, N. G., Baskunov, B. P., & Leontievsky, A. A. (2017). Organophosphonates utilization by soil strains of Ochrobactrum anthropi and Achromobacter sp. *Archives of Microbiology*, *199*(5), 665–675. https://doi.org/10.1007/s00203-017-1343-8

Feng, D., Soric, A., & Boutin, O. (2020). Treatment technologies and degradation pathways of glyphosate: A critical review. *Science of the Total Environment*, *742*, 140559. https://doi.org/10.1016/j.scitotenv.2020.140559

Fischer, K. (1993). Distribution and elimination of HEDP in aquatic test systems. *Water Research*, *27*(3), 485–493. https://doi.org/10.1016/0043-1354(93)90049-N

Forlani, G., Prearo, V., Wieczorek, D., Kafarski, P., & Lipok, J. (2011). Phosphonate degradation by Spirulina strains: Cyanobacterial biofilters for the removal of anticorrosive polyphosphonates from wastewater. *Enzyme and Microbial Technology*, *48*(3), 299–305. https://doi.org/10.1016/j.enzmictec.2010.12.005

Franz, R. G. (2001). Comparisons of pKa and Log P values of some carboxylic and phosphonic acids: Synthesis and measurement. *AAPS PharmSci*, *3*(2). https://doi.org/10.1208/ps030210

Grandcoin, A., Piel, S., & Baurès, E. (2017). AminoMethylPhosphonic acid (AMPA) in natural waters: Its sources, behavior and environmental fate. *Water Research*, *117*, 187–197. https://doi.org/10.1016/j.watres.2017.03.055

Hadi, F., Mousavi, A., Noghabi, K. A., Tabar, H. G., & Salmanian, A. H. (2013). New bacterial strain of the genus Ochrobactrum with glyphosate-degrading activity. *Journal of Environmental Science and Health - Part B Pesticides, Food Contaminants, and Agricultural Wastes*, *48*(3), 208–213. https://doi.org/10.1080/03601234.2013.730319

Huntscha, S., Stravs, M. A., Bühlmann, A., Ahrens, C. H., Frey, J. E., Pomati, F., Hollender, J., Buerge, I. J., Balmer, M. E., & Poiger, T. (2018). Seasonal Dynamics of Glyphosate and AMPA in Lake Greifensee: Rapid Microbial Degradation in the Epilimnion during Summer. *Environmental Science and Technology*, *52*(8), 4641–4649. https://doi.org/10.1021/acs.est.8b00314

Jaworska, J., Van Genderen-Takken, H., Hanstveit, A., Van de Plassche, E., & Feijtel, T. (2002). Environmental risk assessment of phosphonates, used in domestic laundry and cleaning agents in the Netherlands. *Chemosphere*, *47*(6), 655–665. https://doi.org/10.1016/S0045-6535(01)00328-9

Kamat, S. S., & Raushel, F. M. (2013). The enzymatic conversion of phosphonates to phosphate by bacteria. *Current Opinion in Chemical Biology*, *17*(4), 589–596. https://doi.org/10.1016/j.cbpa.2013.06.006

Kamat, S. S., & Raushel, F. M. (2015). PhnJ – A novel radical SAM enzyme from the C–P lyase complex. *Perspectives in Science*, *4*, 32–37. https://doi.org/10.1016/j.pisc.2014.12.006

Kim, A. D., Baker, A. S., Dunaway-Mariano, D., Metcalf, W. W., Wanner, B. L., & Martin, B. M. (2002). The 2-aminoethylphosphonate-specific transaminase of the 2-aminoethylphosphonate degradation pathway. *Journal of Bacteriology*, *184*(15), 4134–4140. https://doi.org/10.1128/JB.184.15.4134-4140.2002

Kishore, G. M., & Jacob, G. S. (1987). Degradation of glyphosate by Pseudomonas sp. PG2982 via a sarcosine intermediate. *Journal of Biological Chemistry*, *262*(25), 12164–12168. https://doi.org/10.1016/s0021-9258(18)45331-8

Kolowith, L. C., Ingall, E. D., & Benner, R. (2001). Composition and cycling of marine organic phosphorus. *Limnology and Oceanography*, 46(2), 309–320. https://doi.org/10.4319/lo.2001.46.2.0309

Kononova, S.V., Nesmeyanova, M.A. Phosphonates and Their Degradation by Microorganisms. *Biochemistry (Moscow)* **67**, 184–195 (2002). https://doi.org/10.1023/A:1014409929875

Kuhn, R., Tóth, E., Geppert, H., Fischer, T., Liebsch, S., & Martienssen, M. (2017). Identification of the Complete Photodegradation Pathway of Ethylenediaminetetra(methylenephosphonic acid) in Aqueous Solution. *Clean - Soil, Air, Water*, *45*(5). https://doi.org/10.1002/clen.201500774

Kulakova, A. N., Kulakov, L. A., Akulenko, N. V., Ksenzenko, V. N., Hamilton, J. T. G., & Quinn, J. P. (2001). Structural and functional analysis of the phosphonoacetate hydrolase (phnA) gene region in Pseudomonas fluorescens 23F. *Journal of Bacteriology*, *183*(11), 3268–3275. https://doi.org/10.1128/JB.183.11.3268-3275.2001

Masotti, F., Garavaglia, B. S., Gottig, N., & Ottado, J. (2023). Bioremediation of the herbicide glyphosate in polluted soils by plant-associated microbes. *Current Opinion in Microbiology*, *73*, 102290. https://doi.org/10.1016/j.mib.2023.102290

Masotti, F., Garavaglia, B. S., Piazza, A., Burdisso, P., Altabe, S., Gottig, N., & Ottado, J. (2021). Bacterial isolates from Argentine Pampas and their ability to degrade glyphosate. *Science of the Total Environment*, *774*, 145761. https://doi.org/10.1016/j.scitotenv.2021.145761

McGrath, J. W., Chin, J. P., & Quinn, J. P. (2013). Organophosphonates revealed: New insights into the microbial metabolism of ancient molecules. *Nature Reviews Microbiology*, *11*(6), 412–419.

https://doi.org/10.1038/nrmicro3011

McMullan, G., & Quinn, J. P. (1994). In vitro characterization of a phosphate starvation-independent carbon- phosphorus bond cleavage activity in Pseudomonas fluorescens 23F. *Journal of Bacteriology*, *176*(2), 320–324. https://doi.org/10.1128/jb.176.2.320-324.1994

Metcalf, W. W., & Wanner, B. L. (1993). Evidence for a fourteen-gene, phnC to phnP locus for phosphonate metabolism in Escherichia coli. *Gene*, *129*(1), 27–32. https://doi.org/10.1016/0378-1119(93)90692-V

Murphy J., Riley. J. P. (1962). A modified single solution method for the determination of phosphate in natural waters. *Analytica Chimica Acta*, *8*(1), 11–16. https://doi.org/10.18393/ejss.477560

Nowack, B. (2003). Environmental chemistry of phosphonates. *Water Research*, *37*(11), 2533–2546. https://doi.org/10.1016/S0043-1354(03)00079-4

Obojska, A., Ternan, N. G., Lejczak, B., Kafarski, P., & McMullan, G. (2002). Organophosphonate utilization by the thermophile Geobacillus caldoxylosilyticus T20. *Applied and Environmental Microbiology*, *68*(4), 2081–2084. https://doi.org/10.1128/AEM.68.4.2081-2084.2002

Padilla, J. T., & Selim, H. M. (2020). Environmental behavior of glyphosate in soils. In *Advances in Agronomy* (1st ed., Vol. 159). Elsevier Inc. https://doi.org/10.1016/bs.agron.2019.07.005

Pipke, R., & Amrhein, N. (1988). Degradation of the phosphonate herbicide glyphosate by arthrobacter atrocyaneus ATCC 13752. *Applied and Environmental Microbiology*, *54*(5), 1293–1296. https://doi.org/10.1128/aem.54.5.1293-1296.1988

PIPKE, R., AMRHEIN, N., JACOB, G. S., SCHAEFER, J., & KISHORE, G. M. (1987). Metabolism of glyphosate in an Arthrobacter sp. GLP-1. *European Journal of Biochemistry*, *165*(2), 267–273. https://doi.org/10.1111/j.1432-1033.1987.tb11437.x

Poiger, T., Buerge, I. J., Bächli, A., Müller, M. D., & Balmer, M. E. (2017). Occurrence of the herbicide glyphosate and its metabolite AMPA in surface waters in Switzerland determined with on-line solid phase extraction LC-MS/MS. *Environmental Science and Pollution Research*, *24*(2), 1588–1596. https://doi.org/10.1007/s11356-016-7835-2

Popov, K., Rönkkömäki, H., & Lajunen, L. (2002). Critical evaluation of stability constants of phosphonic acids (IUPAC Technical Report). *Pure and Applied Chemistry - PURE APPL CHEM*, *74*, 2227. https://doi.org/10.1351/pac200274112227

Riedel, R., Commichau, F. M., Benndorf, D., Hertel, R., Holzer, K., Hoelzle, L. E., Mardoukhi, M. S. Y., Noack, L. E., & Martienssen, M. (2024). Biodegradation of selected aminophosphonates by the bacterial isolate Ochrobactrum sp. BTU1. *Microbiological Research*, *280*, 127600. https://doi.org/10.1016/j.micres.2024.127600

Riedel, R., Krahl, K., Buder, K., Böllmann, J., Braun, B., & Martienssen, M. (2023). Novel standard biodegradation test for synthetic phosphonates.

Journal of Microbiological Methods, *212*(June). https://doi.org/10.1016/j.mimet.2023.106793

Rizk, S. S., Cuneo, M. J., & Hellinga, H. W. (2006). Identification of cognate ligands for the Escherichia coli phnD protein product and engineering of a reagentless fluorescent biosensor for phosphonates . *Protein Science*, *15*(7), 1745–1751. https://doi.org/10.1110/ps.062135206

Röhnelt, A. M., Martin, P. R., Buchner, D., & Haderlein, S. B. (2023). Transformation of Iminodi(methylene phosphonate) on Manganese Dioxides - Passivation of the Mineral Surface by (Formed) Mn2+. *Environmental Science and Technology*, *57*(32), 11958–11966. https://doi.org/10.1021/acs.est.3c01838

Röhnelt, A. M., Martin, P. R., Athmer, M., Bieger, S., Buchner, D., Karst, U., Huhn, C., Schmidt, T. C., & Haderlein, S. B. (2025). Glyphosate is a transformation product of a widely used aminopolyphosphonate complexing agent. *Nature Communications* , *16*(1), 1–11. https://doi.org/10.1038/s41467-025-57473-7

Roseberg, H., & La Nauze, J. M. (1967). The metabolism of phosphanates by microorganisms. The transport of aminoethylphosphonic acid in Basillus cereus. *BBA - General Subjects*, *141*(1), 79–90. https://doi.org/10.1016/0304-4165(67)90247-4

Rossi, F., Carles, L., Donnadieu, F., Batisson, I., & Artigas, J. (2021). Glyphosate-degrading behavior of five bacterial strains isolated from stream biofilms. *Journal of Hazardous Materials*, *420*(July), 126651. https://doi.org/10.1016/j.jhazmat.2021.126651

Rott, E., Steinmetz, H., & Metzger, J. W. (2018). Organophosphonates: A review on environmental relevance, biodegradability and removal in wastewater treatment plants. *Science of the Total Environment*, *615*, 1176–1191. https://doi.org/10.1016/j.scitotenv.2017.09.223

Ruffolo, F., Dinhof, T., Murray, L., Zangelmi, E., Chin, J. P., Pallitsch, K., & Peracchi, A. (2023). Phosphonates. *Molecules*. 2023 Sep 29;28(19):6863. doi: 10.3390/molecules28196863.

Santos-Beneit, F. (2015). The Pho regulon: A huge regulatory network in bacteria. *Frontiers in Microbiology*, *6*(APR), 1–13. https://doi.org/10.3389/fmicb.2015.00402

Schowanek, D., & Verstraete, W. (1990). Phosphonate utilization by bacterial cultures and enrichments from environmental samples. *Applied and Environmental Microbiology*, *56*(4), 895–903. https://doi.org/10.1128/aem.56.4.895-903.1990

Schwientek, M., Rügner, H., Haderlein, S. B., Schulz, W., Wimmer, B., Engelbart, L., Bieger, S., & Huhn, C. (2024). Glyphosate contamination in European rivers not from herbicide application? *Water Research*, *263*, 122140. https://doi.org/https://doi.org/10.1016/j.watres.2024.122140

Seweryn, P., Van, L. B., Kjeldgaard, M., Russo, C. J., Passmore, L. A., Hove-

Jensen, B., Jochimsen, B., & Brodersen, D. E. (2015). Structural insights into the bacterial carbon-phosphorus lyase machinery. *Nature*, *525*(7567), 68–72. https://doi.org/10.1038/nature14683

Shushkova, T. V., Ermakova, I. T., Sviridov, A. V., & Leontievsky, A. A. (2012). Biodegradation of glyphosate by soil bacteria: Optimization of cultivation and the method for active biomass storage. *Microbiology*, *81*(1), 44–50. https://doi.org/10.1134/S0026261712010134

Shushkova, T. V., Vinokurova, N. G., Baskunov, B. P., Zelenkova, N. F., Sviridov, A. V., Ermakova, I. T., & Leontievsky, A. A. (2016). Glyphosate acetylation as a specific trait of Achromobacter sp. Kg 16 physiology. *Applied Microbiology and Biotechnology*, *100*(2), 847–855. https://doi.org/10.1007/s00253-015-7084-1

Silva, V., Montanarella, L., Jones, A., Fernández-Ugalde, O., Mol, H. G. J., Ritsema, C. J., & Geissen, V. (2018). Distribution of glyphosate and aminomethylphosphonic acid (AMPA) in agricultural topsoils of the European Union. *Science of the Total Environment*, *621*, 1352–1359. https://doi.org/10.1016/j.scitotenv.2017.10.093

Skark, C., Zullei-Seibert, N., Schöttler, U., & Schlett, C. (1998). The occurrence of glyphosate in surface water. *International Journal of Environmental Analytical Chemistry*, *70*(1–4), 93–104. https://doi.org/10.1080/03067319808032607

Skeff, W., Recknagel, C., Düwel, Y., & Schulz-Bull, D. E. (2018). Adsorption behaviors of glyphosate, glufosinate, aminomethylphosphonic acid, and 2-aminoethylphosphonic acid on three typical Baltic Sea sediments. *Marine Chemistry*, *198*(November 2017), 1–9. https://doi.org/10.1016/j.marchem.2017.11.008

Stosiek, N., & Klimek-ochab, M. (2020). *Carbon-Phosphorus Lyase — the State of the Art*. Apr;190(4):1525-1552. doi: 10.1007/s12010-019-03161-4

Studnik, H., Liebsch, S., Forlani, G., Wieczorek, D., Kafarski, P., & Lipok, J. (2015). Amino polyphosphonates - chemical features and practical uses, environmental durability and biodegradation. *New Biotechnology*, *32*(1), 1–6. https://doi.org/10.1016/j.nbt.2014.06.007

Sviridov, A. V., Shushkova, T. V., Epiktetov, D. O., Tarlachkov, S. V., Ermakova, I. T., & Leontievsky, A. A. (2021). Biodegradation of Organophosphorus Pollutants by Soil Bacteria: Biochemical Aspects and Unsolved Problems. *Applied Biochemistry and Microbiology*, *57*(7), 836–844. https://doi.org/10.1134/S0003683821070085

Sviridov, A. V., Shushkova, T. V., Ermakova, I. T., Ivanova, E. V., Epiktetov, D. O., & Leontievsky, A. A. (2015). Microbial degradation of glyphosate herbicides (review). *Applied Biochemistry and Microbiology*, *51*(2), 188–195. https://doi.org/10.1134/S0003683815020209

Sviridov, Alexey V., Shushkova, T. V., Zelenkova, N. F., Vinokurova, N. G., Morgunov, I. G., Ermakova, I. T., & Leontievsky, A. A. (2012). Distribution of glyphosate and methylphosphonate catabolism systems in

soil bacteria Ochrobactrum anthropi and Achromobacter sp. *Applied Microbiology and Biotechnology*, *93*(2), 787–796. https://doi.org/10.1007/s00253-011-3485-y

Tarlachkov, S. V., Epiktetov, D. O., Sviridov, A. V., Shushkova, T. V., Ermakova, I. T., & Leontievsky, A. A. (2020). Draft Genome Sequence of Glyphosate-Degrading Achromobacter insolitus Strain Kg 19 (VKM B-3295), Isolated from Agricultural Soil. *Microbiology Resource Announcements*, *9*(17), 19–20. https://doi.org/10.1128/mra.00284-20

Venditti, S., Kiesch, A., & Hansen, J. (2023). Fate of glyphosate and its metabolite AminoMethylPhosponic acid (AMPA) from point source through wastewater sludge and advanced treatment. *Chemosphere*, *340*(July), 139843. https://doi.org/10.1016/j.chemosphere.2023.139843

Villarreal-Chiu, J. F., Quinn, J. P., & McGrath, J. W. (2012). The genes and enzymes of phosphonate metabolism by bacteria, and their distribution in the marine environment. *Frontiers in Microbiology*, *3*(JAN), 1–13. https://doi.org/10.3389/fmicb.2012.00019

Wackett, L. P., Wanner, B. L., Venditti, C. P., & Walsh, C. T. (1987). Involvement of the phosphate regulon and the psiD locus in carbon-phosphorus lyase activity of Escherichia coli K-12. *Journal of Bacteriology*, *169*(4), 1753–1756. https://doi.org/10.1128/jb.169.4.1753-1756.1987

Wang, S., Seiwert, B., Kästner, M., Miltner, A., Schäffer, A., Reemtsma, T., Yang, Q., & Nowak, K. M. (2016). (Bio)degradation of glyphosate in water-sediment microcosms - A stable isotope co-labeling approach. *Water Research*, *99*, 91–100. https://doi.org/10.1016/j.watres.2016.04.041

Wicke, D., Schulz, L. M., Lentes, S., Scholz, P., Poehlein, A., Gibhardt, J., Daniel, R., Ischebeck, T., & Commichau, F. M. (2019). Identification of the first glyphosate transporter by genomic adaptation. *Environmental Microbiology*, *21*(4), 1287–1305. https://doi.org/10.1111/1462-2920.14534

Wimmer, B., Neidhardt, H., Schwientek, M., Haderlein, S. B., & Huhn, C. (2022). Phosphate addition enhances alkaline extraction of glyphosate from highly sorptive soils and aquatic sediments. *Pest Management Science*, *78*(6), 2550–2559. https://doi.org/10.1002/ps.6883

Zhang, Y., Pham, T. M., Kayrouz, C., & Ju, K. S. (2022). Biosynthesis of Argolaphos Illuminates the Unusual Biochemical Origins of Aminomethylphosphonate and Nε-Hydroxyarginine Containing Natural Products. *Journal of the American Chemical Society*, *144*(22), 9634–9644. https://doi.org/10.1021/jacs.2c00627

Chapter 3

3 Biotransformation of Glyphosate and AMPA Sorbed to Goethite

Kleanthi Kourtaki[1], Philipp R. Martin[1‖], Katharine J. Thompson[2], Stefan B. Haderlein[1]

[1]Department of Geosciences, Eberhard Karls University Tübingen, Germany
[2]Institute of Sanitary Engineering, Water Quality and Solid Waste Management (ISWA), University of Stuttgart, Germany
‖Present Address: Division for Environmental Geosciences, Centre for Microbiology and Environmental Systems Science, University of Vienna, Austria

Author	Author position	Scientific ideas	Data generation*	Analysis & interpretation	Paper writing
K. Kourtaki	1	60	65	60	70
P. Martin	2	10	0	10	10
K. Thompson	3	10	0	15	10
S. Haderlein	4	20	0	15	10

Title of the paper:
Biotransformation of glyphosate and AMPA sorbed to goethite

Status in the publication process:
Manuscript in preparation

*Experiments were conducted with the help of Larissa Werle, Tamara Pruneddu (see acknowledgements)

Chapter 3

3.1 Abstract

Glyphosate and its primary metabolite, aminomethylphosphonic acid (AMPA), are widely detected in soils, and their transformation is driven primarily by biotransformation. Their bioavailability and mobility in the environment, however, are strongly affected by interactions with mineral surfaces, such as the widespread iron (oxyhydr)oxide goethite. However, how sorption influences the biotransformation of glyphosate and AMPA is still rarely studied and understood. In this study, we investigated the sorption behavior and microbial transformation of glyphosate and AMPA in the presence of goethite. Batch experiments were conducted to quantify sorption isotherms, assess competitive sorption between the two compounds, and evaluate their microbial degradation in mineral suspensions. Both glyphosate and AMPA showed strong sorption on goethite, with Langmuir-type monolayer adsorption and high affinity, particularly for glyphosate. Competitive sorption experiments of glyphosate and AMPA revealed that glyphosate preferentially binds to goethite, likely due to its more negative net charge and additional functional groups. Transformation experiments with *Achromobacter insolitus* strain Kg 19 in mineral suspensions revealed that sorption on goethite did not retard the biotransformation of either glyphosate or AMPA. Both compounds were rapidly transformed, with similar rates compared to goethite-free setups. These results challenge previous assumptions about the persistence of AMPA and demonstrate that ad- and desorption to mineral surfaces like goethite did not limit the bacterial transformation of organophosphonates under the experimental conditions applied. This study contributes to a more accurate understanding of organophosphonate sorption-biotransformation dynamics in soils with high iron oxide content and has important implications for predicting their residence times in these compartments.

3.2 Introduction

Glyphosate (N-phosphonomethylglycine) is the most widely used herbicide globally, with annual application rates projected to reach up to 920 thousand tons by 2025 (Maggi et al., 2020). Its herbicidal effect is based on the inhibition of the enzyme 5-enolpyruvylshikimate-3-phosphate synthase (EPSPS), which disrupts the synthesis of essential aromatic amino acids such as tryptophan and tyrosine, primarily in plants (Giesy et al., 2000). Glyphosate gained popularity upon its market introduction due to its high efficacy against perennial weeds and its perceived safety for humans. Its widespread use was further expanded with the development of genetically modified glyphosate-tolerant crops, which enabled efficient weed control without damaging the crop. However, its extensive use, frequent detection in soil and water, and classification as "probably carcinogenic to humans" by the International Agency for Research on Cancer (IARC) have raised concerns about its potential impacts on both human health and the

environment (IARC, 2015). These concerns have prompted increasing research into glyphosate's environmental behavior and impacts, a trend that has recently intensified following evidence linking glyphosate contamination in European surface waters to emissions of aminopolyphosphonate chelating agents (Schwientek et al., 2024). Notably, glyphosate has been shown to form abiotically as a transformation product of diethylenetriamine penta(methylenephosphonate) (DTPMP) in both natural and wastewater systems, demonstrating an additional source of glyphosate beyond agricultural or urban herbicide use (Röhnelt et al., 2025; Engelbart and Bieger, 2025).

Although glyphosate is generally considered to have limited mobility in soils due to its strong sorption to soil matrices, it is frequently detected in European ground- and surface water (Sanchis et al., 2012; Wimmer et al., 2022; Schwientek et al., 2024). This suggests that glyphosate can still be transported, either in its dissolved form or bound to soil components (Gimsing et al., 2004; Coupe et al., 2012; Aparicio et al., 2013). Direct spraying on areas neighboring surface waters, deposition of wastewater discharge, and wind erosion are also common routes by which glyphosate can be transported (Borggaard & Gimsing, 2008). Once present in the environment, glyphosate can also undergo biodegradation, primarily through microbial use as a phosphorus (P) source (Balthazor & Hallas, 1986). Two main microbial degradation pathways have been identified, involving either cleavage of the carbon–phosphorus (C–P) bond or the carbon–nitrogen (C–N) bond. These lead to the formation of sarcosine and phosphate, or aminomethylphosphonic acid (AMPA) and glyoxylate, respectively (Hove-Jensen et al., 2014). Microorganisms can subsequently use these transformation products as sources of carbon, nitrogen, or phosphorus to meet their metabolic needs (Borggaard & Gimsing, 2008). Among microorganisms, bacteria are the main drivers of glyphosate degradation, with most active bacterial strains transforming glyphosate primarily to access P under P-limited conditions, by converting it to phosphate or AMPA. However, when P is readily available–particularly in the form of orthophosphate or organo-phosphates–glyphosate biodegradation is often suppressed (Pipke et al., 1987). Recently, it was shown that coexisting aminomonophosphonates such as AMPA or 2-aminoethylphosphonate (2-AEP) can prevent glyphosate biotransformation, as glyphosate becomes a less preferred P-substrate (Kourtaki et al., 2025). As a result, when environmental P-levels exceed microbial demand, glyphosate may persist longer in the environment due to reduced biodegradation (Pessagno et al., 2005).

In addition to the presence of coexisting P-sources, sorption processes likely influence the biodegradation rates of glyphosate and its metabolite AMPA. This may contribute to the wide range of reported half-lives of glyphosate: from 7 to 142 days in the labile (more bioavailable) phase, and from 76 to 240 days in the non-labile (sorbed) phase; AMPA generally shows even greater persistence than glyphosate (Annett et al., 2014; Bento et al., 2016; Carretta et al., 2021). A key factor governing the environmental fate of glyphosate is soil composition, particularly its mineral content, which affects both sorption and degradation processes. Various naturally occurring soil minerals—particularly those containing

transition metals with multiple valence states—can adsorb or chemically transform organic contaminants such as glyphosate. For instance, dissolved manganese (Mn^{2+}) and manganese oxides like birnessite (MnO_2) have been shown to significantly influence the environmental fate of glyphosate and AMPA, either by forming them from DTPMP or degrading them into orthophosphate (Barrett & McBride, 2005; Paudel et al., 2015; Li et al., 2016; Röhnelt et al., 2025). Glyphosate has a strong affinity for iron and aluminum oxides, hydroxides, and oxyhydroxides—such as hematite (Fe_2O_3), gibbsite ($Al(OH)_3$), and goethite (α-FeOOH) (Borggaard & Gimsing, 2008). While strong sorption reduces its mobility and lowers the risk of groundwater contamination (Sprankle et al., 1975; Pessagno et al., 2005), it also leads to accumulation in the soil matrix, thereby prolonging its environmental residence time (Wauchope et al., 2002). For glyphosate and AMPA, various sorption mechanisms have been proposed, largely governed by the mineral composition of the soil (Piccolo et al., 1994). These mechanisms include electrostatic (outer-sphere) interactions as well as ligand exchange (inner-sphere complexation) with metal ions such as Fe^{3+} and Al^{3+}. Inner-sphere complex formation typically involves the phosphonate group of glyphosate or AMPA, which can directly coordinate to reactive surfaces of Fe_2O_x and Al_2O_x–similar to the behavior of simpler analogs like methylphosphonate (Sheals et al., 2002; Barja & Dos Santos Afonso, 2005). Comparable sorption patterns have also been observed for polyphosphonates, despite their higher negative charge from multiple phosphonic acid groups (Barja & Dos Santos Afonso, 2005). Further studies have explored the detailed mechanisms of glyphosate and AMPA sorption onto Fe_2O_x and Al_2O_x surfaces (Rampazzo et al., 2013; Báez et al., 2015; Cicilinski et al., 2025), demonstrating that ad- and desorption dynamics are highly dependent on environmental conditions such as pH, competing ions, and mineral surface characteristics. For example, phosphate ions, which have a stronger affinity for mineral binding sites, can displace glyphosate from surfaces, leading to its remobilization and increased leaching potential (Gimsing et al., 2004; Wimmer et al., 2022). pH is also a critical factor, as it affects the protonation state of glyphosate and AMPA, as well as the surface charge and reactivity of soil minerals (Wauchope et al., 2002).

To accurately assess the environmental fate of glyphosate and AMPA, it is essential to consider sorption and biodegradation processes in parallel. As discussed above, glyphosate strongly interacts with soil minerals–especially Fe_2O_x and Al_2O_x–through mechanisms such as inner-sphere complexation. Most studies demonstrating high microbial degradation potential for glyphosate and AMPA have been conducted in liquid cultures under controlled laboratory conditions (Ermakova et al., 2017; Masotti et al., 2021; Riedel et al., 2024). While such studies provide important mechanistic insights, they often fail to capture the complexity of natural environments. In soils, microorganisms are embedded in heterogeneous matrices where factors like limited nutrient availability, microbial competition, and especially sorption can strongly influence degradation rates. Despite the recognized importance of both sorption and microbial transformation

in governing glyphosate's fate, few studies have addressed how these processes interact. Given glyphosate's high sorption affinity for mineral surfaces, microbial degradation may contribute little to its overall attenuation–particularly under conditions where strong sorption limits its bioavailability. However, sorption is not inherently detrimental to microbial activity. For instance, Schnürer et al. (2006) found that adding goethite to humus soil reduced glyphosate's toxicity to microbes, thereby mitigating its negative effect on microbial respiration.

Building on these insights, here we investigate the interplay between sorption and biotransformation by examining the microbial degradation potential of glyphosate and AMPA in the presence of a suspended mineral sorbent. Goethite was selected as a model mineral due to its widespread occurrence in soils and sediments and high affinity to the target compounds. A series of sorption experiments was conducted with and without bacterial cells in bacterial and mineral suspensions to (i) quantify glyphosate's and AMPA's sorption affinity for goethite and (ii) assess whether sorption limits its bioavailability as a P-source for microbial metabolism. In other words, we aimed to determine whether and how goethite impedes the uptake and subsequent degradation of glyphosate and AMPA by bacteria.

3.3 Materials and Methods

Chemicals and materials
All chemicals were purchased from Merck (Darmstadt, Germany) in the highest available purity if not described differently. Glyphosate (>98%) and AMPA (>99%) were from Sigma Aldrich (Steinheim, Germany). MOPS buffer (99.5%) was bought from Carl Roth (Karlsruhe, Germany) and sodium acetate (>99.5%) from Chemsolute (Renningen, Germany). For eluent preparation, sodium hydroxide (NaOH, 49-51%) was used (Supelco, Merck, Darmstadt, Germany). For the sorption experiments, a commercially available goethite (α–FeOOH, Bayferrox 920 Z, Lanxess GmbH, Cologne, Germany) was used. Ultrapure water (>18MΩ cm-1) was used for all experiments obtained by a Barnstead GenPure system (Thermo Fischer Scientific, Germany).

Design of batch adsorption studies
Goethite suspensions (22 or 28 g/L) were prepared in growth medium buffered with 50 mM MOPS at a pH of 7±0.1. The ionic strength was calculated to be approximately 0.1 M. The BET surface area of goethite was calculated to be 9.98 m^2/g by nitrogen sorption-desorption isotherms after overnight degassing under vacuum at 120 °C (analyzed using Micromeritics' Gemini VII Version 5.01). Its point of zero charge (pH_{pzc}) was determined on a Zetasizer Nano ZSP (Malvern Pananalytical, Malvern, United Kingdom) at 20 °C. For analysis, mineral suspensions were prepared in 15 mM NaCl + 5 mM MES buffer, and the pH was adjusted by 0.1 or 1 M NaOH. The pH_{pzc} was determined by performing linear

regression of the plotted zeta potential as a function of the adjusted pH (see SI, Fig. B1). The pH_{pzc} of goethite was determined to be equal to 7.0 ±0.1. Adsorption experiments were performed in 50 mL polypropylene centrifugation tubes (Fisher Scientific, Waltham, MA, USA). To achieve equilibrium conditions, the tubes were shaken overhead for 24 hours, which was shown in preliminary tests to be sufficient to achieve equilibrium. Batch adsorption experiments were conducted in triplicate. This concentration range was selected as it is consistent with the concentration range used during the biotransformation experiments. After adsorption was completed, 4 mL of the sample was withdrawn and transferred to a 5 mL centrifugation tube (Eppendorf, Hamburg, Germany) for centrifugation (10 minutes at 12,000 rcf). Next, the supernatant was filtered through a 0.2 µm syringe filter (surfactant-free cellulose acetate, Sartorius, Göttingen, Germany). The sorbed fractions of glyphosate or AMPA on the goethite were desorbed using 4 mL of 0.1 M $NaOH/Na_2HPO_4$ for 10 min, placed on the overhead shaker. The samples were subsequently centrifuged and filtered as described previously. All filtered samples from the aqueous and sorbed phases were then stored at -20 °C in the dark till concentration analysis, if not analyzed directly.

Design of batch transformation experiments

Goethite suspensions (28 g/L, corresponding to 279.44 m^2/L) were prepared in sterile 100 mL glass serum bottles sterilized at 180 °C for 4.5 hours. The suspensions were prepared in growth medium containing either glyphosate or AMPA as P-sources–at concentrations of 0.5 mM for single P-source experiments, or 0.25 mM for each experiment with both P-sources. Goethite suspensions were equilibrated overnight with glyphosate and/or AMPA before the bottles were inoculated with living cells. 100 µL of a freshly prepared preculture was used for the inoculations and the start of the experiment. Experiments were performed with the bacterial strain *Achromobacter insolitus* strain Kg 19 (hereafter referred to as *A*. Kg 19) and *Ochrobactrum pituitosum* strain GPr1-13 (*O*. GPr1-13) (as previously described by Kourtaki et al., 2025). Each experiment consisted of three living replicates with living cells and goethite suspensions, three abiotic controls with goethite without cells to assess the dynamics of glyphosate and AMPA with goethite surface over the course of the experiment, as well as three cultures without goethite and the respective abiotic controls to assess the activity of the cells and potential contaminations in the bottles, respectively. All experiments were conducted at pH 6.8. Bacterial growth in the goethite-free setups was monitored via optical density measurements at a wavelength of 560 nm for strain *A*. Kg 19 and 600 nm for strain *O*. GPr1-13 with a UV5Bio spectrophotometer (Mettler Toledo, Germany) (Sviridov et al., 2021). To quantify the total bacterial cell population over selected experiments, quantitative real-time PCR (qPCR) (Bio-Rad Laboratories, Inc. Hercules, CA, USA) targeting 16S rRNA-gene abundances of *A*. Kg 19 was carried out as described elsewhere (Lueder et al., 2022). The measured gene copy numbers serve as a proxy to monitor the growth trend of A. Kg 19 throughout the experiment. Genomic DNA was extracted from living

replicates using DNeasy® UltraClean® Microbial Kit (Qiagen GmbH, Hilden, Germany) following the manufacturer's instructions.

Quantification of glyphosate and AMPA
Glyphosate and AMPA concentrations were quantified with a 930 Compact Flex ion chromatograph equipped with an amperometric detector operated in integrated pulsed amperometric detection (iPAD) mode (Metrohm, Herisau, Switzerland) as previously described by Kourtaki et al. (2025). Before the analysis, all samples were diluted with ultrapure water and quantified with external standards in a concentration range of 0 to 20 µM.

Scanning Electron Microscopy (SEM)
Scanning electron microscopy was employed to examine cell–mineral interactions at various time points during the experiment. Sample preparation followed the protocol described by Dreher et al. (2025).

3.4 Results and Discussion

Glyphosate and AMPA sorption on goethite
Batch adsorption–transformation experiments were conducted at pH 7 using glyphosate and AMPA, with the chemical structures shown in Table 3.1. A schematic illustration of bidentate complex formation between glyphosate or AMPA and a goethite surface at pH 7 is presented in Figure 3.1. Adsorption of glyphosate and AMPA on goethite was measured for 10 different total concentrations (0.1, 0.2, 0.3, 0.4, 0.5, 0.6, 0.7, 0.8, 0.9, and 1 mM). Adsorption isotherms for glyphosate and AMPA on goethite–both individually and in combination–are shown in Figure 3.2. The experimental data were fitted using the Langmuir model, and the resulting coefficients are summarized in Table 3.2. The model provided a reasonable fit to the data, with a normalized root mean square error (NRMSE) of 0.08 (NRMSE<0.2, indicating strong agreement between predictions and observations). These results are consistent with monolayer adsorption onto a surface possessing homogeneously distributed binding sites. Quantitatively, both compounds displayed substantial Langmuir adsorption affinities (K_l), reflecting strong sorption to the goethite surface. In single adsorbate system with goethite suspensions (22 g/L, corresponding to 219.56 m^2/L), glyphosate exhibited a K_L of 163 L/mmol, whereas AMPA showed a K_L of 18 L/mmol. They showed similar sorption capacities of 16 µmol/g and 19 µmol/g for glyphosate and AMPA, respectively, suggesting that under comparable pH conditions, both compounds occupy a similar number of surface sites. In double adsorbate systems with glyphosate and AMPA, the K_l decreased to 70 L/mmol for glyphosate and increased to 47 L/mmol for AMPA, indicating potential

competitive interactions and partial site sharing between the two adsorbates (see SI for detailed sorption isotherm modeling), while their sorption capacities were split, indicating competitive sorption (10 µmol/g and 7 µmol/g for glyphosate and AMPA, respectively). These results demonstrate that glyphosate and AMPA compete for common sorption sites on the goethite surface in an additive manner. These values differ from those reported in earlier studies. For instance, Barja and Dos Santos Afonso (2005) observed higher K_L values for AMPA than for glyphosate, and typical K_L values for glyphosate on goethite were around 30 L/mmol. These discrepancies may reflect not only differences in goethite surface reactivity or competitive adsorption dynamics, but also the composition of the experimental conditions. Earlier adsorption studies were generally conducted in simple electrolyte solutions such as NaCl, whereas in our case, sorption was carried out in the presence of a complex bacterial growth medium containing organic nutrients, multiple ions, as well as buffering agents that can also influence surface chemistry.

Glyphosate exhibited a stronger overall sorption tendency onto goethite compared to AMPA, likely due to electrostatic interactions with the mineral surface. At pH 6.8, glyphosate carries a net charge of –2, while AMPA has a charge of –1. This difference is attributed to glyphosate's additional carboxylic acid group, which may enhance its sorption affinity (Cicilinski et al., 2025). As a result, glyphosate interacts more strongly with the positively charged goethite surface. Sorption of both compounds onto goethite is known to be pH-dependent (Sidoli et al., 2016; Cicilinski et al., 2025). As pH increases, both the organophosphonates and the mineral surface gradually deprotonate. The point of zero charge (pH_{pzc}) of goethite is approximately 7, meaning the net surface charge is positive below this pH. Maximum adsorption typically occurs at low equilibrium concentrations and at pH values above the pKa of the organophosphonates, where favorable electrostatic interactions can develop (De Gerónimo & Aparicio, 2022). However, at pH values above the pH_{pzc}, the goethite surface becomes negatively charged, reducing its affinity for the anionic forms of glyphosate and AMPA. At pH 6.8, goethite still carries a weak positive surface charge, while glyphosate and AMPA predominantly exist as zwitterions, promoting strong sorption (Sidoli et al., 2016). Several studies have examined the adsorption mechanisms of glyphosate and AMPA on goethite as a function of pH. In agreement with the present findings, Barja and Dos Santos Afonso (2005) reported similar adsorption behavior for glyphosate and AMPA on goethite, identifying two dominant surface complexes involving the phosphonate group. In contrast, compounds such as sarcosine, which lack the phosphonate group, do not form complexes with goethite. Other studies (e.g., Orcelli et al., 2018) have further confirmed that the amine and carboxyl groups do not significantly contribute to glyphosate binding on goethite. In agricultural soils, with pH ranging from 4 to 8, sorption has been well correlated with iron and aluminium oxide content (Morillo et al., 2000; Carretta et al., 2021).

In summary, our findings confirm that both glyphosate and AMPA sorb effectively onto the goethite suspensions used, with glyphosate generally exhibiting stronger sorption—likely due to its more negative net charge. However, under environmentally relevant conditions, particularly at pH ~6.8 (as used in this study), both compounds displayed comparable adsorption behavior. This interaction plays a crucial role in controlling their partitioning between solid and aqueous phases, potentially influencing their mobility and bioavailability. As such, sorption to goethite may significantly affect the environmental fate and biotransformation of glyphosate and AMPA, especially at interfaces where soil, water, and microbial communities intersect.

Table 3.1 Summary of key physicochemical properties of glyphosate (pKa values from Sprankle et al., 1975; Sidoli et al., 2016) and AMPA (pKa values from Popov et al., 2001).

	Glyphosate	AMPA
pK_a	0.8 2.6 5.6 10.6	<2 5.41 10.04
Structure at pH 6.8	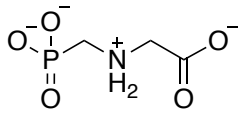	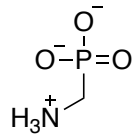
Molar mass [g/mol]	169.07	111.04

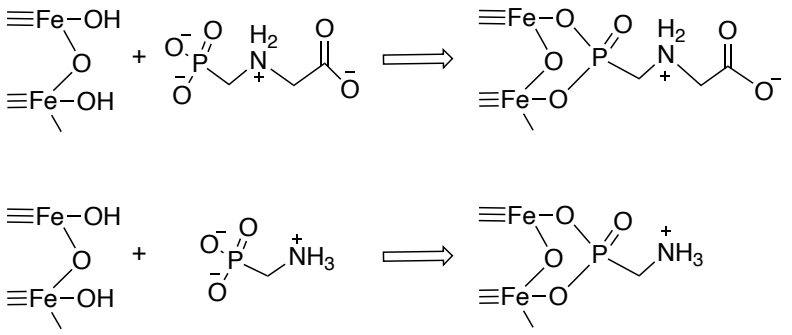

Figure 3.1 Schematic illustration of bidentate complex formation between glyphosate or AMPA and a goethite surface at pH=6.8.

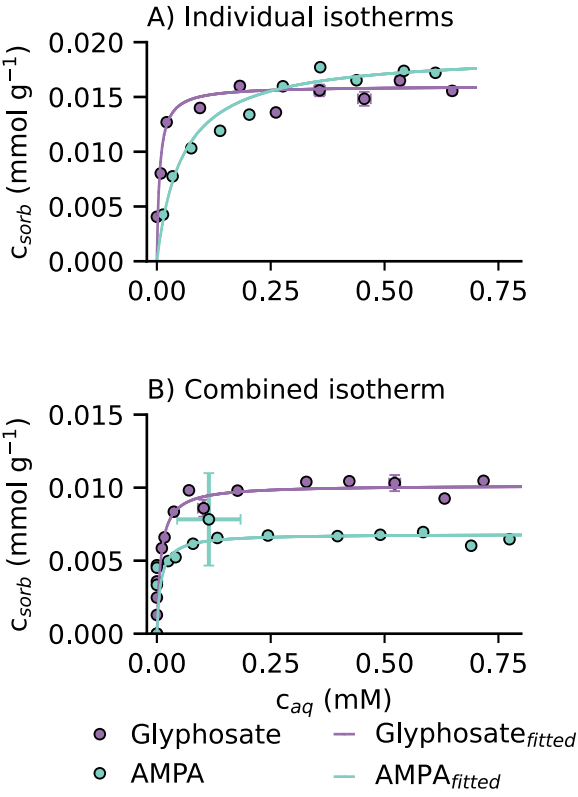

Figure 3.2 Adsorption isotherms of glyphosate (purple symbols) and AMPA (green symbols) concentrations in the presence of goethite (22 g/L) in the growth media matrix (I≃0.1 M, at room temperature (21 ± 1 °C)). Isotherms, fitted with the Langmuir model, are shown for compounds added either individually (A) or simultaneously (B) over a concentration range of 0.1 to 1 mM. The x-axis indicates the aqueous concentration remaining in solution after adsorption; the y-axis shows the corresponding sorbed fraction. Error bars represent the standard deviation of triplicate setups (if not visible, error bars are smaller than the data points).

Table 3.2 Langmuir fitting parameters ($C_{sorb,max}$ and K_L) for sorption isotherms of glyphosate and AMPA on 22 g/L goethite at pH 7 (I=0.1 M, T=21 ± 1 °C)

	Langmuir parameters	Glyphosate	AMPA
Individual isotherms	$C_{sorb,max}$ (mmol/g)	0.016	0.019
	K_L (L/mmol)	163	18
	NRMSE	0.08	0.08
Combined isotherm	K_L (L/mmol)	70	47
	$C_{sorb,max}$ (mmol/g)	0.017	
	NRMSE	0.08	

Glyphosate and AMPA biotransformation in the presence of goethite

Strain *A.* Kg 19 was cultivated using either glyphosate or AMPA as the sole P-source in experimental setups with or without goethite. The corresponding results are shown in Figure 3.3. In the goethite-containing setups, the mineral suspensions were pre-equilibrated with glyphosate or AMPA for 24h, resulting in a distribution of the compounds between the sorbed and aqueous phases. At day 0, when bacterial inoculation occurred, more than 70% of the total added glyphosate and AMPA was adsorbed on goethite, while approximately 30% remained dissolved. These percentages are consistent with the non-inoculated abiotic controls, which showed similar distribution of the target compounds between the two phases and no change in glyphosate or AMPA concentrations over time, implying no abiotic chemical degradation related to the goethite mineral (see SI, Fig. B2).
Following inoculation, degradation of both glyphosate and AMPA proceeded rapidly, with near-complete depletion from both the aqueous and sorbed phases within five days. A decrease in the concentration of both compounds began after day 1 and occurred in parallel from both phases. Once the aqueous fraction was depleted, the rate of uptake from the sorbed phase increased. Since decreases were observed in both aqueous and sorbed glyphosate or AMPA without a corresponding increase in the aqueous fractions, the data indicate either direct transformation from the sorbed phase or transformation rates in the aqueous phase exceeding desorption and detection. When comparing inoculated setups with and without goethite (open vs. filled purple and green squares), degradation trends for glyphosate and AMPA were nearly identical. In goethite-amended systems, transformation proceeded at 0.120 ± 0.011 and 0.136 ± 0.004 mM/day for glyphosate and AMPA, respectively, while in goethite-free controls, rates were 0.135 ± 0.002 and 0.122 ± 0.003 mM/day (transformation rates were determined by performing a linear regression between day 0 and 3). These results suggest that no substantial differences were observed, indicating that *A.* Kg 19 utilized glyphosate and AMPA equally well regardless of goethite's presence.

Ochrobactrum pituitosum strain GPr1-13 (*O*. GPr1-13) was also cultivated with glyphosate as the sole P-source in the presence and absence of goethite suspensions. Glyphosate degradation proceeded without retardation by goethite, showing trends comparable to those observed for *A*. Kg 19. (see SI, Fig. B3). These findings align with those of Schnürer et al. (2006), who investigated the biodegradation of glyphosate adsorbed onto goethite under various conditions. They concluded that sorption to goethite did not hinder microbial degradation. Using ATR-FTIR spectroscopy to study surface complexes, the authors observed decarboxylation of glyphosate in samples containing microbially active soil–providing evidence of microbial activity. In contrast, this behavior was absent in sterile samples, reinforcing the role of microorganisms in the degradation process. These results demonstrate the strain's ability to degrade both glyphosate and AMPA from both the aqueous and sorbed phases. qPCR-based quantification of gene copy numbers (used here as a proxy for cell numbers) showed that all setups started with similar cell abundances of approximately 5.9 x 10^6 ±8.9 x 10^5 copies/mL. Notably, in the goethite-setups, the estimated cell numbers reached by the end of the experiment were consistently higher than in the goethite-free controls —by approximately a factor of 2 for AMPA and by a factor of 1.3 for glyphosate (Fig. 3.3A and B, open vs. filled light green squares). This pattern was observed regardless of whether glyphosate or AMPA served as the P-source. Consistent with these observations, Scanning Electron Microscopy (SEM) images taken on days 0, 3, 4, and 7 of the experiment revealed a progressive increase in the number of microbial cells attached to mineral surfaces (see Fig. 3.4), indicating potential microbe–mineral interactions. Cells are usually negatively charged and thus can bind easily to iron minerals such as goethite. As the cells utilize the glyphosate or AMPA, additional binding sites on the mineral surface may become available for further cell attachment, reinforcing these interactions. While SEM effectively illustrates microbial attachment to goethite over time, it cannot distinguish whether degradation occurs through direct access to mineral-bound compounds or through prior desorption into the aqueous phase. Additionally, it remains unclear whether microbial contact with the mineral surface facilitates substrate uptake or whether the surface simply serves as a site for attachment or protection. Due to analytical limitations, no physical or chemical changes to the particle surfaces were monitored that might have supported identification of direct microbe–mineral interactions. As a result, additional complementary analyses are needed to clarify whether microbial uptake occurs directly from the mineral surface. Without this information, no definitive conclusions can be drawn about the relative roles of desorption and biodegradation–specifically, whether degradation was primarily driven by chemical equilibrium shifts leading to desorption or by direct microbial access to sorbed compounds.

Overall, these findings indicate that the presence of goethite did not limit the degradation of either glyphosate or AMPA. Although a large fraction of glyphosate and AMPA was initially sorbed on goethite, degradation still proceeded efficiently till target compounds were depleted from both phases.

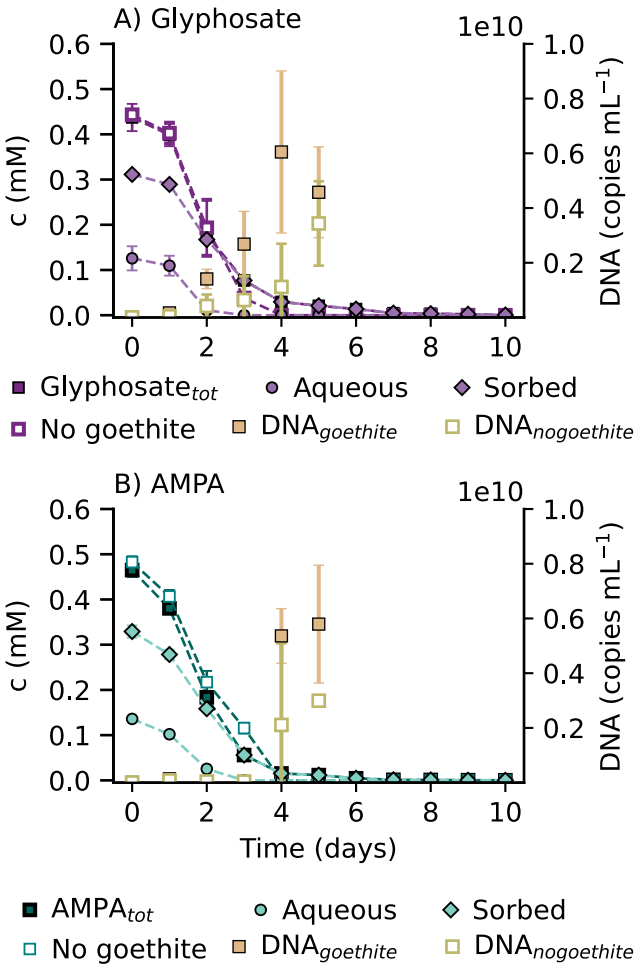

Figure 3.3 A) Glyphosate (purple symbols) and B) AMPA (green symbols) concentration when individually added in inoculated cultures with *A*. Kg 19 in the presence and absence of goethite (28 g/L) at a concentration of 0.25 mM each. Circles represent the aqueous concentrations, diamonds represent the sorbed concentrations, and squares represent the sum of the aqueous and sorbed fractions. Open squares indicate glyphosate (purple symbols) and AMPA (green symbols)

concentrations in non-inoculated abiotic controls without goethite. Open squares indicate glyphosate (purple symbols) and AMPA (green symbols) concentrations in inoculated cultures without goethite. Filled and open light green squares indicate DNA copies in goethite and goethite-free setups, respectively, inoculated with strain *A*. Kg 19 in the presence of 0.5 mM A) glyphosate (purple symbols) and B) AMPA (green symbols). Error bars represent the standard deviation of triplicate setups (if not visible, error bars are smaller than the data points).

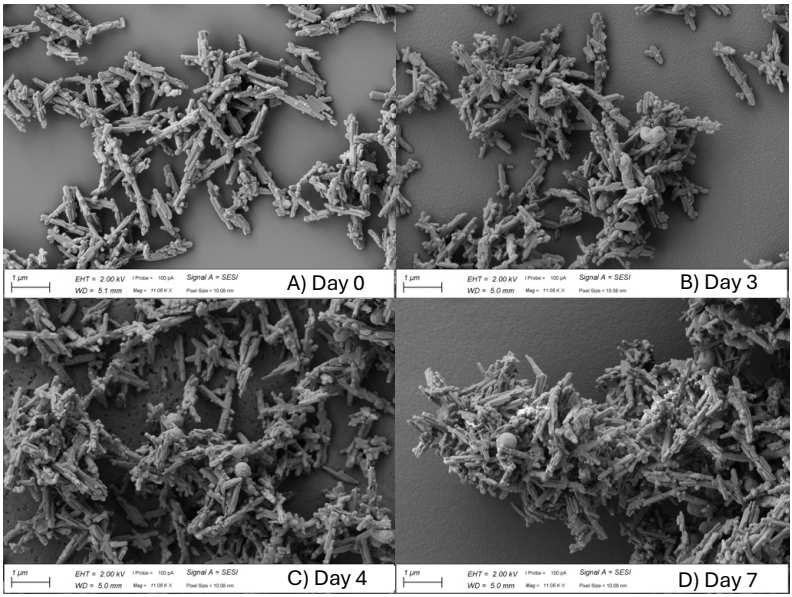

Figure 3.4 Scanning Electron Microscopy (SEM) images of *A*. Kg 19 in setups containing goethite at different time points: A) day of inoculation, B) after 3 days of cultivation, C) after 4 days of cultivation, and D) after 7 days of cultivation.

Competitive glyphosate and AMPA biotransformation in the presence of goethite
Next, we investigated the interplay of the competitive sorption and biotransformation of AMPA and glyphosate in the presence of goethite mineral. Strain *A*. Kg 19 was cultivated with both glyphosate and AMPA in the presence of 28 g/L goethite mineral, and the results are shown in Figure 3.5. Before inoculation, glyphosate and AMPA were pre-equilibrated with goethite for 24h,

leading to their distribution between the aqueous and sorbed phases. Besides the parallel provision of glyphosate and AMPA as P-sources, competitive sorption and desorption processes also took place on the sorption sites of goethite, influencing the partitioning of both compounds. Consistent with previous isotherm studies, glyphosate exhibited a stronger affinity for goethite, with more than 80% present in the sorbed phase and less than 20% remaining in solution, whereas AMPA was 62% sorbed, and 38% remained dissolved. After cell inoculation, AMPA was rapidly transformed, first disappearing from the aqueous phase, followed by the complete degradation of both phases by day 4. Glyphosate transformation began on day 1 and occurred concurrently with AMPA, resulting in complete depletion by day 6. These results confirm that AMPA serves as a preferred P-source over glyphosate, but both can be transformed simultaneously when AMPA is not in excess. Contrary to previous assumptions that AMPA degrades more slowly, this study found no delay in AMPA biodegradation compared to glyphosate, suggesting that acetylation prior to P-acquisition via C–P bond cleavage may not be necessary, as also discussed by Hove-Jensen et al. (2014). Control experiments without goethite showed similar trends, indicating that goethite does not retard the transformation of either compound, with both being depleted by day 7 in all setups. Abiotic controls showed a decrease in glyphosate and AMPA concentrations after day 5, which was attributed to contamination rather than chemical degradation, as evidenced by increased turbidity (see SI, Fig. B3). However, this contamination did not impact the main experiment, since both glyphosate and AMPA were almost completely depleted by that time.

In conclusion, these findings demonstrate that both glyphosate and AMPA are efficiently degraded by strain *A*. Kg 19 in the presence of goethite when provided simultaneously as P-sources. Overall, these results point to a potential for biodegradation even in mineral-rich environments where strong sorption could otherwise be expected to limit bioavailability. However, it is important to acknowledge that the experimental conditions employed here involved well-dispersed goethite suspensions composed of small particles, which maximize surface area and likely facilitate microbial access to sorbed compounds. By contrast, in natural soils and sediments, iron oxides typically occur as aggregates or are embedded within complex mineral matrices. Under such conditions, diffusion of sorbed substrates from within aggregates to the surrounding solution may become a rate-limiting step, potentially slowing down biodegradation kinetics. Moreover, natural environments add further complexity through heterogeneous mineralogy, competing ions, and the presence of organic matter, all of which may influence the balance between sorption, desorption, and microbial transformation. Thus, while the findings demonstrate the capacity of microorganisms to transform sorbed glyphosate and AMPA, extrapolation to field conditions requires consideration of these additional transport and accessibility constraints. Nevertheless, these insights deepen our understanding of organophosphonate transformation in goethite suspensions and underscore the

potential for effective bioremediation of glyphosate and AMPA in soils containing iron oxides such as goethite.

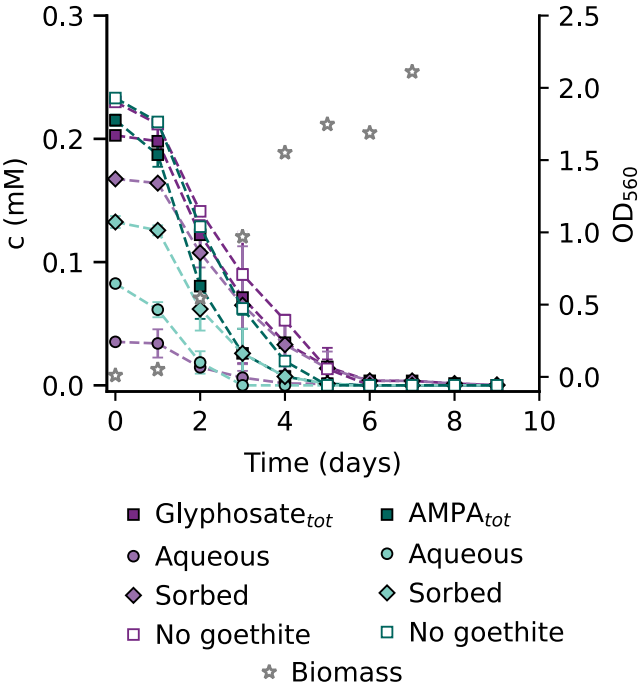

Figure 3.5 Glyphosate (purple symbols) and AMPA (green symbols) concentration when simultaneously added in inoculated cultures with *A*. Kg 19 in the presence and absence of goethite (28 g/L) at a concentration of 0.25 mM each. Circles (connected by lines represent the aqueous concentrations, triangles (connected by lines) represent the sorbed concentrations, and squares (connected by lines) represent the sum of the aqueous and sorbed fractions. Open squares indicate glyphosate (purple symbols) and AMPA (green symbols) concentrations in inoculated cultures without goethite. Open gray stars indicate optical density goethite-free setups inoculated with strain *A*. Kg 19 in the presence of 0.25 mM glyphosate (purple symbols) and AMPA (green symbols). Error bars represent the standard deviation of triplicate setups (if not visible, error bars are smaller than the data points).

3.5 Conclusion

Investigating the interplay between sorption and biotransformation of organic compounds in the presence of minerals is crucial for understanding the fate of ionic contaminants such as glyphosate and AMPA in natural environments. Although the biotransformation of glyphosate and AMPA has been widely studied, investigations under environmentally relevant conditions—particularly those that account for the role of mineral sorption—remain scarce. Minerals such as goethite not only serve as sorption sites, concentrating organic molecules and influencing their bioavailability, but also participate in dynamic, competitive processes of adsorption and desorption that directly impact microbial access to these compounds.

This study studied the interplay between sorption and microbial degradation in the presence of goethite, a widely abundant iron hydroxide mineral in soils. Our results demonstrated that while goethite significantly affects the distribution of glyphosate and AMPA between sorbed and aqueous phases, it does not inhibit their microbial transformation. Both compounds were effectively biodegraded–individually and in parallel–even when strongly sorbed on goethite, indicating that mineral-bound fractions remain bioavailable for microbial utilization. Despite glyphosate's higher sorption affinity, its degradation was not delayed compared to the less strongly sorbed AMPA. On the contrary, AMPA was depleted more rapidly, confirming its preferential use as a P-source. The findings challenge the assumption that mineral sorption necessarily hinders biodegradation, showing that microbial activity can effectively access and degrade sorbed substrates. They underscore the resilience of microbial P-acquisition and carry important implications for bioremediation, nutrient cycling, and risk assessment of organophosphonate contaminants in mineral-rich environments. However, these results cannot be directly extrapolated to field conditions, as factors such as mineral heterogeneity and soil structure were not captured in the experimental design. In natural systems, iron oxides often form larger aggregates within complex soil matrices, where diffusion barriers may restrict access to sorbed compounds and slow biodegradation. To better reflect environmental complexity, future studies should also consider other mineral phases (e.g., clays, aluminum oxides), which differ in surface properties and sorption capacities. Furthermore, exploring mixed microbial communities and field-derived consortia could provide insights into competitive degradation dynamics and microbial adaptation under more complex environmental conditions, as they capture competitive interactions and adaptive responses under natural conditions. Time-resolved analysis of sorption–desorption kinetics during biodegradation, coupled with spectroscopy (e.g., X-ray Photoelectron Spectroscopy (XPS), Attenuated Reflectance-Fourier Transform Infrared Spectroscopy (ATR-FTIR), or stable isotope analysis with labeled substrate), would help identify the specific mechanisms and pathways responsible for accessing sorbed organophosphonates. Lastly, long-term microcosm or field-scale

experiments could reveal how seasonal changes, redox fluctuations, or organic matter inputs further modulate these processes in situ.

3.6 References

Annett, R., Habibi, H. R., & Hontela, A. (2014). Impact of glyphosate and glyphosate-based herbicides on the freshwater environment. *Journal of Applied Toxicology*, *34*(5), 458–479. https://doi.org/10.1002/jat.2997

Aparicio, V. C., De Gerónimo, E., Marino, D., Primost, J., Carriquiriborde, P., & Costa, J. L. (2013). Environmental fate of glyphosate and aminomethylphosphonic acid in surface waters and soil of agricultural basins. *Chemosphere*, *93*(9), 1866–1873. https://doi.org/10.1016/j.chemosphere.2013.06.041

Báez, M. E., Espinoza, J., Silva, R., & Fuentes, E. (2015). Sorption-desorption behavior of pesticides and their degradation products in volcanic and nonvolcanic soils: interpretation of interactions through two-way principal component analysis. *Environmental Science and Pollution Research*, *22*(11), 8576–8585. https://doi.org/10.1007/s11356-014-4036-8

Balthazor, T. M., & Hallas, L. E. (1986). Glyphosate-degrading microorganisms from industrial activated sludge. *Applied and Environmental Microbiology*, *51*(2), 432–434. https://doi.org/10.1128/aem.51.2.432-434.1986

Barja, B. C., & Dos Santos Afonso, M. (2005). Aminomethylphosphonic acid and glyphosate adsorption onto goethite: A comparative study. *Environmental Science and Technology*, *39*(2), 585–592. https://doi.org/10.1021/es035055q

Barrett, K. A., & McBride, M. B. (2005). Oxidative degradation of glyphosate and aminomethylphosphonate by manganese oxide. *Environmental Science and Technology*, *39*(23), 9223–9228. https://doi.org/10.1021/es051342d

Bento, C. P. M., Yang, X., Gort, G., Xue, S., van Dam, R., Zomer, P., Mol, H. G. J., Ritsema, C. J., & Geissen, V. (2016). Persistence of glyphosate and aminomethylphosphonic acid in loess soil under different combinations of temperature, soil moisture and light/darkness. *Science of the Total Environment*, *572*, 301–311. https://doi.org/10.1016/j.scitotenv.2016.07.215

Borggaard, O. K., & Gimsing, A. L. (2008). Fate of glyphosate in soil and the possibility of leaching to ground and surface waters: A review. *Pest Management Science*, *64*(4), 441–456. https://doi.org/10.1002/ps.1512

Carretta, L., Cardinali, A., Onofri, A., Masin, R., & Zanin, G. (2021). Dynamics of Glyphosate and Aminomethylphosphonic Acid in Soil Under Conventional and Conservation Tillage. *International Journal of Environmental Research*, *15*(6), 1037–1055. https://doi.org/10.1007/s41742-021-00369-3

Cicilinski, A. D., Melo, V. F., & Peralta-Zamora, P. (2025). Glyphosate and AMPA sorption onto synthetic iron (oxyhydr)oxides: A comparative study. *Journal of Molecular Liquids*, *426*(November 2024), 127303. https://doi.org/10.1016/j.molliq.2025.127303

Coupe, R. H., Kalkhoff, S. J., Capel, P. D., & Gregoire, C. (2012). Fate and transport of glyphosate and aminomethylphosphonic acid in surface waters of agricultural basins. *Pest Management Science*, *68*(1), 16–30. https://doi.org/10.1002/ps.2212

De Gerónimo, E., & Aparicio, V. C. (2022). Changes in soil pH and addition of inorganic phosphate affect glyphosate adsorption in agricultural soil. *European Journal of Soil Science*, *73*(1), 1–16. https://doi.org/10.1111/ejss.13188

Dreher, C. L., Schad, M., Duda, J.-P., Fischer, S., Shuster, J., Li, Y., Konhauser, K. O., & Kappler, A. (2025). Impact of silica on the identity of minerals formed in Archean oceans during Fe cycling by cyanobacteria and iron(III)-reducing bacteria. *Geochimica et Cosmochimica Acta*, *404*(March), 202–222. https://doi.org/10.1016/j.gca.2025.07.023

Engelbart, L., Bieger, S., Thompson, K., Fischer, L., Bader, T., Kramer, M., Haderlein, S. B., Röhnelt, A. M., & Huhn, C. (2025). In-situ formation of glyphosate and AMPA in activated sludge from phosphonates used as antiscalants and bleach stabilizers in households and industry. *Water Research*, *280*. https://doi.org/10.1016/j.watres.2025.123464

Ermakova, I. T., Shushkova, T. V., Sviridov, A. V., Zelenkova, N. F., Vinokurova, N. G., Baskunov, B. P., & Leontievsky, A. A. (2017). Organophosphonates utilization by soil strains of Ochrobactrum anthropi and Achromobacter sp. *Archives of Microbiology*, *199*(5), 665–675. https://doi.org/10.1007/s00203-017-1343-8

Giesy, J. P., Dobson, S., & Solomon, K. R. (2000). Ecotoxicological risk assessment for Roundup® herbicide. *Reviews of Environmental Contamination and Toxicology*, *167*, 35–120. https://doi.org/10.1007/978-1-4612-1156-3_2

Gimsing, A. L., Borggaard, O. K., & Bang, M. (2004). Influence of soil composition on adsorption of glyphosate and phosphate by contrasting Danish surface soils. *European Journal of Soil Science*, *55*(1), 183–191. https://doi.org/10.1046/j.1365-2389.2003.00585.x

Hove-Jensen, B., Zechel, D. L., & Jochimsen, B. (2014). Utilization of Glyphosate as Phosphate Source: Biochemistry and Genetics of Bacterial Carbon-Phosphorus Lyase. *Microbiology and Molecular Biology Reviews*, *78*(1), 176–197. https://doi.org/10.1128/mmbr.00040-13

International Agency for Research on Cancer. IARC Monographs Volume 112: Evaluation of Five Organophosphate Insecticides and Herbicides. 2015. Available online: www.iarc.fr/en/media-centre/ iarcnews/pdf/MonographVolume112.pdf

Kourtaki, K., Buchner, D., Martin, P. R., Thompson, K., & Haderlein, S. B. (2025).

Influence of organophosphonates as alternative P-sources on bacterial transformation of glyphosate. *Environmental Pollution*, 125872. https://doi.org/https://doi.org/10.1016/j.envpol.2025.125872

Li, H., Joshi, S. R., & Jaisi, D. P. (2016). Degradation and Isotope Source Tracking of Glyphosate and Aminomethylphosphonic Acid. *Journal of Agricultural and Food Chemistry*, 64(3), 529–538. https://doi.org/10.1021/acs.jafc.5b04838

Lueder, U., Maisch, M., Jørgensen, B. B., Druschel, G., Schmidt, C., & Kappler, A. (2022). Growth of microaerophilic Fe(II)-oxidizing bacteria using Fe(II) produced by Fe(III) photoreduction. *Geobiology*, *20*(3), 421–434. https://doi.org/10.1111/gbi.12485

Maggi, F., la Cecilia, D., Tang, F. H. M., & McBratney, A. (2020). The global environmental hazard of glyphosate use. *Science of the Total Environment*, *717*, 137167. https://doi.org/10.1016/j.scitotenv.2020.137167

Masotti, F., Garavaglia, B. S., Piazza, A., Burdisso, P., Altabe, S., Gottig, N., & Ottado, J. (2021). Bacterial isolates from Argentine Pampas and their ability to degrade glyphosate. *Science of the Total Environment*, *774*, 145761. https://doi.org/10.1016/j.scitotenv.2021.145761

Morillo, E., Undabeytia, T., Maqueda, C., & Ramos, A. (2000). Glyphosate adsorption on soils of different characteristics. Influence of copper addition. *Chemosphere*, *40*(1), 103–107. https://doi.org/10.1016/S0045-6535(99)00255-6

Orcelli, T., di Mauro, E., Urbano, A., Valezi, D. F., da Costa, A. C. S., Zaia, C. T. B. V., & Zaia, D. A. M. (2018). Study of Interaction Between Glyphosate and Goethite Using Several Methodologies: an Environmental Perspective. *Water, Air, and Soil Pollution*, *229*(5). https://doi.org/10.1007/s11270-018-3806-1

Paudel, P., Negusse, A., & Jaisi, D. P. (2015). Birnessite-Catalyzed Degradation of Glyphosate: A Mechanistic Study Aided by Kinetics Batch Studies and NMR Spectroscopy. *Soil Science Society of America Journal*, *79*(3), 815–825. https://doi.org/10.2136/sssaj2014.10.0394

Pessagno, R. C. ;, Dos, S., & Afonso, M. (2005). N-(Phosphonomethyl)Glycine Interactions With Soils. *The Journal of the Argentine Chemical Society*, *93*(6), 97–106.

Piccolo, A., Celano, G., Arienzo, M., & Mirabella, A. (1994). Adsorption and desorption of glyphosate in some European soils. *Journal of Environmental Science and Health Part B-Pesticides Food Contaminants and Agricultural Wastes*, *29*(6), 1105–1115. https://doi.org/10.1080/03601239409372918

Pipke, R., Schulz, A., & Amrhein, N. (1987). Uptake of Glyphosate by an Arthrobacter sp. *Applied and Environmental Microbiology*, *53*(5), 974–978.

Popov, K., Rönkkömäki, H., & Lajunen, L. H. J. (2001). Critical evaluation of stability constants of phosphonic acids (IUPAC Technical Report). *Pure Appl. Chem.*, *73*(10), 1641–1677.

Rampazzo, N., Todorovic, G. R., Mentler, A., & Blum, W. E. H. (2013).

Adsorption of glyphosate and aminomethylphosphonic acid in soils. *International Agrophysics*, *27*(2), 203–209. https://doi.org/10.2478/v10247-012-0086-7

Riedel, R., Commichau, F. M., Benndorf, D., Hertel, R., Holzer, K., Hoelzle, L. E., Mardoukhi, M. S. Y., Noack, L. E., & Martienssen, M. (2024). Biodegradation of selected aminophosphonates by the bacterial isolate Ochrobactrum sp. BTU1. *Microbiological Research*, *280*, 127600. https://doi.org/10.1016/j.micres.2024.127600

Röhnelt, A. M., Martin, P. R., Athmer, M., Bieger, S., Buchner, D., Karst, U., Huhn, C., Schmidt, T. C., & Haderlein, S. B. (2025). Glyphosate is a transformation product of a widely used aminopolyphosphonate complexing agent. *Nature Communications* , *16*(1), 1–11. https://doi.org/10.1038/s41467-025-57473-7

Sanchís, J., Kantiani, L., Llorca, M., Rubio, F., Ginebreda, A., Fraile, J., Garrido, T., & Farré, M. (2012). Determination of glyphosate in groundwater samples using an ultrasensitive immunoassay and confirmation by on-line solid-phase extraction followed by liquid chromatography coupled to tandem mass spectrometry. *Analytical and Bioanalytical Chemistry*, 402(7), 2335–2345. https://doi.org/10.1007/s00216-011-5541-y

Schnürer, Y., Persson, P., Nilsson, M., Nordgren, A., & Giesler, R. (2006). Effects of surface sorption on microbial degradation of glyphosate. *Environmental Science and Technology*, *40*(13), 4145–4150. https://doi.org/10.1021/es0523744

Schwientek, M., Rügner, H., Haderlein, S., Schulz, W., Wimmer, B., Engelbart, L., Bieger, S., & Huhn, C. (2024). Glyphosate contamination in European rivers not from herbicide application? *Water Research*, *263*(May), 1–18. https://doi.org/10.1016/j.watres.2024.122140

Sheals, J., Sjöberg, S., & Persson, P. (2002). Adsorption of glyphosate on goethite: Molecular characterization of surface complexes. *Environmental Science and Technology*, *36*(14), 3090–3095. https://doi.org/10.1021/es010295w

Sidoli, P., Baran, N., & Angulo-Jaramillo, R. (2016). Glyphosate and AMPA adsorption in soils: laboratory experiments and pedotransfer rules. *Environ. Sci. Pol. Res.*, *23*(6), 5733–5742. https://doi.org/10.1007/s11356-015-5796-5

Sprankle, P., Meggitt, W. F., & Penner, D. (1975). *Adsorption, Mobility, and Microbial Degradation of Glyphosate in the Soil*. 23(3), 224–228. 229–34. JSTOR, http://www.jstor.org/stable/4042279.

Sviridov, A. V., Shushkova, T. V., Epiktetov, D. O., Tarlachkov, S. V., Ermakova, I. T., & Leontievsky, A. A. (2021). Biodegradation of Organophosphorus Pollutants by Soil Bacteria: Biochemical Aspects and Unsolved Problems. *Applied Biochemistry and Microbiology*, *57*(7), 836–844. https://doi.org/10.1134/S0003683821070085

Wauchope, R. D., Yeh, S., Linders, J. B. H. J., Kloskowski, R., Tanaka, K., Rubin, B., Katayama, A., Kördel, W., Gerstl, Z., Lane, M., & Unsworth, J. B.

(2002). Pesticide soil sorption parameters: Theory, measurement, uses, limitations and reliability. *Pest Management Science*, *58*(5), 419–445. https://doi.org/10.1002/ps.489

Wimmer, B., Neidhardt, H., Schwientek, M., Haderlein, S. B., & Huhn, C. (2022). Phosphate addition enhances alkaline extraction of glyphosate from highly sorptive soils and aquatic sediments. *Pest Management Science*, *78*(6), 2550–2559. https://doi.org/10.1002/ps.6883

Chapter 4

4 The overlooked Role of Manganese in Biodegradation Studies of Higher Aminopolyphosphonates

Kleanthi Kourtaki[1], Philipp R. Martin[1,2], Stefan B. Haderlein[1,*]

[1]Department of Geosciences, Eberhard Karls Universität Tübingen, Tübingen, Germany

[2]Division for Environmental Geosciences, Centre for Microbiology and Environmental Systems Science, University of Vienna, Austria

Author	Author position	Scientific ideas	Data generation*	Analysis & interpretation	Paper writing
K. Kourtaki	1	70	85	70	70
P. Martin	2	15	0	15	15
S. Haderlein	3	15	0	15	15

Title of the paper:
The overlooked Role of Manganese in Biodegradation Studies of Higher Aminopolyphosphonates

Status in the publication process:
Manuscript published in Environmental Science and Technology Research

*Experiments were conducted with the help of Larissa Werle and Jana Geiselhardt (see acknowledgements)

or any corrections. The Version of Record is available online at: https://doi.org/10.1007/s11356-025-37105-9

Kourtaki, K., Martin, P.R. & Haderlein, S.B. The overlooked role of manganese in biodegradation studies of higher aminopolyphosphonates. Environ Sci Pollut Res (2025). https://doi.org/10.1007/s11356-025-37105-9

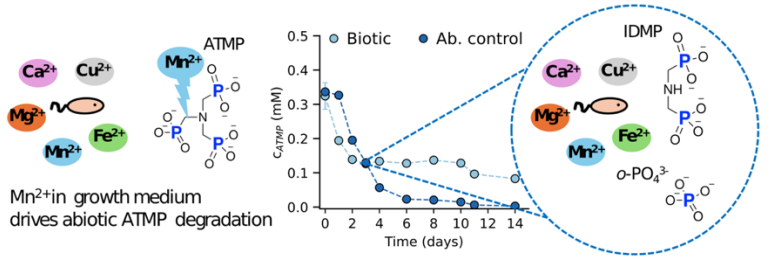

Scheme 4. 1. Graphical abstract summarizing the main findings and methodological approach of chapter 4.

- **Keywords:** Synthetic phosphonates; Complexing agents; IDMP; P-cycling; APP degradation; *Achromobacter*

Highlights:

- Standard media for studying the aerobic biodegradation of phosphonates are unsuitable for higher aminopolyphosphonates (APPs) such as aminotrimethylphosphonate (ATMP) and ethylenediamine tetra(methylene phosphonate) (EDTMP).
- Dissolved Mn(II), typically present in trace mineral solutions used in microbial growth media, catalyses the abiotic oxidation of higher APPs by molecular oxygen.

- Even trace concentrations of dissolved Mn(II) (< 10 µM) led to the transformation of 0.5 mM ATMP into iminodimethylenephosphonate (IDMP) and *o*-PO_4.
- Bacterial degradation of ATMP or EDTMP by *A*. Kg 19 could not be assessed due to rapid abiotic degradation in the medium.
- The addition of EDTA as a metal complexing agent slowed but did not prevent the abiotic degradation of ATMP in the growth medium.

4.1 Abstract

Higher aminopolyphosphonates (APPs, with three or more C–P bonds) are common complexing agents, but their environmental fate and degradation/transformation pathways remain poorly understood. While abiotic degradation of higher APPs has been reported, recent studies have also proposed the potential for enzymatic breakdown based on laboratory model systems. However, herein we show rapid transformation of two representative higher APPs–aminotris(methylenephosphonate) (ATMP, with three C–P bonds) and ethylenediaminetetramethylenephosphonate (EDTMP, with four C–P bonds) – in bacterial growth media both in the presence and the absence of *Achromobacter insolitus* strain Kg 19. The abiotic transformation was driven by trace levels of dissolved Mn(II) – typically present in mineral solutions used in growth media. Mn(II) catalyzed the abiotic oxidation of ATMP by molecular oxygen, yielding iminodimethylenephosphonate (IDMP) and orthophosphate (*o*-PO_4) as transformation products, via a known mechanism previously described in simpler matrices. The addition of ethylenediaminetetraacetic acid (EDTA) as metal complexing agent retarded but did not prevent the abiotic transformation. Bacterial growth under phosphorous (P)-limiting conditions in the presence of ATMP and EDTMP was thus supported by the formation of P-containing transformation products of the concurrent abiotic degradation rather than biotransformation of ATMP and EDTMP. These findings reveal a critical limitation in prior biodegradation studies of higher APPs, which likely overestimated biotransformation by overlooking Mn(II)–mediated abiotic degradation. Future research must redesign biodegradation approaches and disentangle biotic and abiotic mechanisms to accurately evaluate the actual biodegradability of higher APPs.

Chapter 4

4.2 Introduction

Higher aminopolyphosphonates (APPs) are synthetic organophosphorus compounds featured with the presence of one or more amine (-NH_2) and three or more phosphonic acid groups attached to carbon atoms (–P(=O)$(OH)_2$) (Studnik et al., 2015). Their market introduction was driven by a need for more effective and environmentally acceptable chelating agents as alternatives to traditional polyphosphates and polycarboxylates like ethylenediaminetetraacetate (EDTA) (Knepper, 2003; Jaworska et al., 2002). APPs are particularly effective in hard waters. The fact that they are effective at concentrations one or more magnitudes lower than polyphosphates, further contributes to their widespread use and commercial importance (Studnik et al., 2015). Their strong metal-chelating properties and ability to inhibit scale formation have made them popular in industrial and household applications such as water treatment, detergents, and metal cleaning (Knepper, 2003).
APPs primarily enter the environment through wastewater discharge or point sources like cooling system effluents (Fischer 1993; Jaworska et al., 2002). Although generally regarded as non-toxic to aquatic biota such as invertebrates and fish (Knepper, 2003; HERA, 2004), they can have indirect effects by binding essential trace metals, reducing their bioavailability, and indirectly compromising growth by altering nutrient dynamics (Schowanek et al., 1996). As a result, their release into aquatic environments can disrupt ecosystems, affecting microbial competition for these essential minerals. Recently, it was shown that glyphosate is a transformation product (TP) of diethylenetriamine penta(methylene phosphonate) (DTPMP) during manganese-catalyzed oxidation, as well as during incubation in sewage sludge (Röhnelt et al., 2025b, Engelbart & Bieger et al., 2025).

Various abiotic degradation processes, such as photolysis, ozonation, or Mn(II)-driven oxidation by molecular oxygen, have been reported to efficiently break them down (Greenlee et al., 2014; Lesueur et al., 2005; Kuhn et al., 2018; Martin et al, 2022; Marks et al., 2023; Röhnelt et al., 2023). APPs were previously considered largely resistant to degradation due to their strong C–P bond (Ternan et al., 1998). To date, sorption to sewage sludge is regarded as the primary cause for their partial retention in wastewater treatment plants (WWTPs) (Fischer, 1993; Nowack, 1998; Nowack, 2002; Knepper, 2003). Biodegradation in WWTPs was initially considered negligible due to the high availability of inorganic phosphorus (P) which inhibits the induction of enzymes like C–P lyases – key enzymes for breaking down synthetic APPs under P-limiting conditions (McGrath et al., 1997; Kononova & Nesmeyanova, 2002; Santos-Beneit, 2015; Stosiek & Klimek-ochab, 2020). These observations are in line with the outcomes of standard OECD biodegradability tests, which have consistently shown low or negligible levels of biodegradation for compounds such as aminotris(methylenephosphonate (ATMP) (HERA, 2004). The poor performance of APPs in these tests is not necessarily due

to inherent environmental persistence but rather reflects test conditions that fail to promote the activity of specialized phosphonate-degrading microorganisms. In particular, the presence of excess phosphate buffers in test media inhibits the microbial pathways responsible for APP breakdown, mirroring the limitations observed under WWTP conditions (Strotmann et al., 2023).

Nevertheless, recent studies proposed biodegradation of higher APPs. Cyanobacterial strains such as *Spirulina platensis*, *Arthrospira fusiformis*, and *Anabaena variabilis* were shown to sustain growth by metabolizing hexamethylenediamine-N,N,N′,N′-tetrakis(methylphosphonate) or DTPMP (Forlani et al., 2011). Bacterial strains have also been isolated with demonstrated APP-degrading abilities. *Ochrobactrum* sp. strain BTU1 (abbreviated as BTU1), for instance, was recently enriched from a DTPMP solution and degradation tests with EDTMP showed 80% decrease in ethylenediaminetetramethylenephosphonate (EDTMP) concentration (c_0=0.23 mM), alongside biomass production. In subsequent tests, a decrease in ATMP concentration was also shown when provided as P-source to *O*. strain BTU1 and when sewage sludge was used as inoculum (Riedel et al., 2023). In an earlier study, Schowanek and Verstraete (1990) showed that EDTMP was degraded by activated sludge cultures, achieving up to 85% removal. Further screening identified enrichment cultures capable of utilizing higher APPs as sole C, N, or P sources, however, analytical limitations restricted this study to phosphate (PO_4^{3-}) quantification rather than direct measurement of parent compounds (McGrath et al., 1997). PO_4^{3-} has often been used as proxy for APP transformation (Schowanek and Verstraete, 1990; Riedel et al., 2024). Recent evidence, however, suggests that this approach may overestimate actual degradation, as PO_4^{3-} quantification can be skewed by matrix interferences in samples containing high levels of higher APPs (Guo et al., 2025). Thus, relying solely on PO_4^{3-} release is insufficient for accurately assessing higher APP transformation.

Our study critically evaluates earlier studies on higher-APP biodegradability by investigating the transformation of ATMP and EDTMP – by *Achromobacter insolitus* strain Kg 19 under P-limiting conditions using commonly applied culture media. We critically evaluate the influence of media composition – particularly the presence of trace metals – on the degradation behavior of these analytes. ATMP and EDTMP were chosen due to their widespread use in cleaning products across Europe (HERA, 2004; Jaworska et al., 2002) and their detection in WWTP effluents (Rott et al., 2018). Experiments were conducted in C- and N-rich media supplemented with bivalent cations, following standard protocols for assessing phosphonate biodegradability. By examining both microbial and media-related factors on higher-APP transformation, this work aims to advance our understanding of the fate of higher APPs and inform future risk assessments and treatment strategies.

4.3 Materials and Methods

Chemicals and materials

EDTMP (>96.0 %) has been purchased in solid form from Zschimmer and Schwarz (Lahnstein, Germany. ATMP (>97.0%) and IDMP (≥97%) have been purchased as solids from Sigma Aldrich (Steinheim, Germany). MOPS buffer (99.5%) was bought from Carl Roth (Karlsruhe, Germany) and sodium acetate (>99.5%) from Chemsolute (Renningen, Germany). The cation-exchange resin (DOWEX 50 W X 8, 100-200 mesh, H^+-form) was purchased from Roth (Karlsruhe, Germany). For eluent preparation sodium hydroxide (NaOH, 49-51%) was used (Supelco, Merck, Darmstadt, Germany). Additional chemicals used for the experiments were purchased from Merck in their highest purity (Darmstadt, Germany). Ultrapure water (ρ >18MΩ cm) was used for all experiments obtained by a Barnstead GenPure system (Thermo Fischer Scientific, Germany).

Setup of biodegradation batch experiments

Biotransformation experiments were conducted in 100 mL glass serum bottles, continuously shaken at 150 rpm on a rotary shaker at room temperature (21 ± 1 °C) under ambient light conditions, as previously described by Kourtaki et al. (2025). The bacterial strain *Achromobacter insolitus* strain Kg 19 (hereafter referred to as *A*. Kg 19), originally isolated from the Krasnodar region in Russia (45°03'10.8"N, 38°52'22.8"E), was obtained as freeze-dried culture from the Russian Centre of Microorganisms (VKM) (VKM B-3295) (Tarlachkov et al., 2020). *A*. Kg 19 was cultivated in $Medium_1$, buffered at pH 7.0 ± 0.1 with 50 mM MOPS. The medium included 10 g/L Na-glutamate, 2 g/L NH_4Cl as N-source, 0.5 g/L K_2SO_4, 0.2 g/L $MgSO_4$ x 7 H_2O, 1 mL/L of a 7-Vitamin solution, and a trace element solution (TES) with: 20 mg/L $ZnSO_4$ x $7H_2O$, 10 mg/L $CaCl_2$ x 6 H_2O, 2.5 mg/L $FeSO_4$ x 7 H_20, 2 mg/L $CuSO_4$ x 5 H_2O, 1 mg/L $MnSO_4$ x H_2O, 0.3 mg/L Na_2MoO_4, 0.06 mg/L H_3BO_3, and 0.05 mg/L $NiCl_2$ x $6H_2O$. Details on the preparation of bacterial cultures are provided in the Supporting Information (SI).

Each experiment consisted of three biotic replicates and three abiotic controls to assess potential interactions with the APPs and the medium.

Setup of abiotic transformation batch experiments

The effect of different medium components on ATMP was tested by preparing 0.5 mM of ATMP in seven solutions as outlined in Table 4. 1) 50 mM MOPS, 2) 50 mM MOPS with 1 mL/L of the 7-Vitamin solution, 3) 50 mM MOPS with TES 4) same as (3) with 100 µM Na_2-EDTA x $2H_2O$, 5) sterile $medium_1$ (as described in Materials and Methods) 6) same as (5) with 100 µM Na_2-EDTA x $2H_2O$, and 7)

sterile medium$_2$ used for cultivation of *Ochrobactrum pituitosum* strain GPr1-13 (abbreviated as *O*. GPr1-13) in previous research. Medium$_2$ consisted of 10 g/L Na-glutamate, 5 g/L NH_4Cl as N-source, 0.5 g/L K_2SO_4, 0.16 g/L $MgSO_4$ x $7H_2O$, 0.08 g/L $CaCl_2$ x $6H_2O$, 1 mL/L of a 7-Vitamin solution and was buffered at pH 7.0 ± 0.1 with 50 mM MOPS. The effect of Mn(II) was tested by examining three different concentrations (2.5, 6, and 10 µM) using $MnSO_4$ x $7H_20$ prepared in ultrapure water. The experiments were conducted in sterile 50 mL centrifugation tubes (polypropylene, Fisher Scientific, Waltham, MA, USA) placed in a rotary shaker running at 25 rpm.

Table 4.1 Experimental setup testing the effect of seven different medium components, each with an initial ATMP concentration of 0.5 mM.

Setups	MOPS	Vitamins	TES	EDTA	Medium$_1$	Medium$_2$
1	✓					
2	✓	✓				
3	✓		✓			
4	✓		✓	✓		
5	✓	✓	✓		✓	
6	✓	✓	✓	✓	✓	
7	✓	✓				✓

All transformation experiments were conducted in triplicates at room temperature (21 ± 1 °C). ATMP and EDTMP stock solutions (c=25 mM) were prepared in ultrapure water, adjusted at pH=7.0 ±0.1 using 1 M NaOH, and filtered-sterilized through 0.2 µm syringe filters ((surfactant-free) cellulose acetate, Sartorius, Göttingen, Germany).

Sampling of transformation batch experiments

For each sampling point, 1 mL of sample aliquot was withdrawn under sterile conditions and added to a 2 mL centrifugation tube containing 50 mg ± 2 mg of cation exchange resin to quench any potential interaction between APPs and

cations present in the solutions tested. The vials were placed for 1 hour on an overhead shaker. Afterward, the resin-free supernatant containing the APPs in their free (uncomplexed) form was stored at -20 °C in the dark till concentration analysis, if not analyzed directly. The treatment and storage procedure had no adverse effect with respect to the stability of the APPs. Samples containing cells were first centrifuged (10 minutes at 12,000 rcf) and the biomass-free supernatant was subsequently treated with the cation exchange resin.

ATMP, EDTMP, and IDMP quantification

Quantification of ATMP, EDTMP, and IDMP was conducted by ion chromatography (Metrohm, Herisau, Switzerland) coupled to integrated amperometric detection (Wall- Jet Cell, Metrohm) (Röhnelt et al., 2025). Samples treated with cation-exchange were diluted 1:25 with ultrapure water for analysis. Calibration was carried out using external standards ranging from 0.01 to 20 µM, and normalization was performed based on repeated injections of control standards.

Orthophosphate (o-PO_4) quantification

Orthophosphate (*o*-PO_4) formation as a transformation product of APP degradation was monitored photometrically at 710 nm with a UV5Bio spectrophotometer (Mettler Toledo, Germany) using the molybdenum-blue method adapted from Murphy and Riley (1962) after a 10x dilution of the samples in a 1 cm PP cuvette.

4.4 Results and Discussion

ATMP and EDTMP transformation in inoculated and sterile growth medium

To investigate the biotransformation potential of higher APPs, ATMP and EDTMP were provided to strain *A*. Kg 19 as sole P-sources. The change in APP concentration, as well as the growth indicated by an increase in optical densities in biotic and abiotic setups, are shown in Figure 4.1. Over time, a significant decrease in the ATMP and EDTMP concentrations was observed in biotic setups, accompanied by cell growth. The transformation of ATMP and EDTMP reached 74% and 22%, respectively, and plateaued after 4 to 6 days. A significant decrease in both APP concentrations, however, was also observed in cell-free abiotic controls (dark-blue data in Figure 4.1), which led to depletion of ATMP and EDTMP by day 6 and 18, respectively. Schowanek and Verstraete (1990) also reported abiotic degradation in the growth medium while investigating APP biodegradation. However, in their study, the biologically mediated degradation was up to two orders of magnitude faster than the abiotic process, and thus, the

latter was not considered to significantly contribute to the total degradation of APPs. In contrast, the data shown in Figure 4.1 demonstrate rapid abiotic breakdown of ATMP and EDTMP in the media matrix, occurring concurrently with potential biotransformation that cannot be neglected. The cultivation medium used here has been frequently applied in previous studies to assess the biodegradability of aminomono- and diphosphonates such as glyphosate, aminomethylphosphonic acid (AMPA), IDMP, and 1-hydroxyethane-1,1-diphosphonate (HEDP) without significant reactivity in cell-free controls (Kourtaki et al., 2025). Yet, for higher APPs, the abiotic degradation shown in cell-free controls challenges the distinction between concurrent biotic and abiotic degradation of ATMP or EDTMP, hindering the assessment of strain *A*. Kg 19's potential ability to use the tested APPs as sole P-sources.

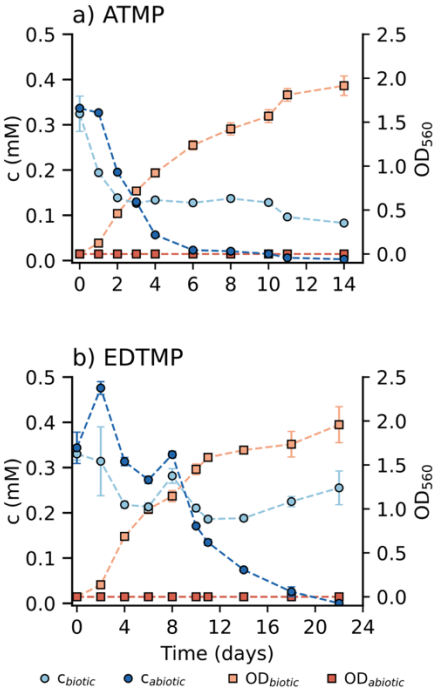

Figure 4.1 Changes in APP concentration and optical density of *A*. Kg 19 over time when (a) ATMP and (b) EDTMP were provided at 0.5 mM as sole P-sources

to study the biotransformation potential of ATMP and EDTMP by strain *A*. Kg 19. Light-blue circles (connected by lines) represent the change in APP concentration in inoculated biotic setups, while dark-blue circles indicate APP concentrations in cell-free abiotic controls. Light-orange squares represent the optical density of *A*. Kg 19 growing cells with APP, and dark-orange squares show the optical density in abiotic setups. Error bars represent the standard deviation of triplicate cultures (if not visible, error bars are smaller than the symbols).

Effect of trace Mn(II) concentrations on ATMP

To further explore the abiotic degradation of higher APPs in sterile medium, follow-up experiments focused on ATMP, which exhibited greater susceptibility to degradation. Standard approaches to APP biodegradation are typically conducted using nutrient-rich growth media designed to support microbial activity. Riedel et al. (2023) proposed a standardized degradation test for assessing the biodegradability of higher APP and highly recommended the inclusion of a TES. These solutions typically contain metals such as Zn, Ca, Fe, Cu, Mn, and Ni, with dissolved Mn(II) added at concentrations between 2.5 and 10 µM (Ermakova & Shushkova, Leont'evskii 2008; Riedel et al., 2023; Riedel et al., 2024; Kourtaki et al., 2025). Notably, Mn(II) has been shown to catalyse abiotic oxidation of higher APPs by molecular oxygen in tap water and buffered distilled water (Nowack & Stone, 2000).

In this study, we aimed to evaluate the role of dissolved Mn(II) present in the trace element solution with respect to abiotic ATMP degradation observed in the sterile growth medium. To this end, 0.5 mM ATMP in 50 mM MOPS buffer at pH 7.0 was supplemented with three different Mn(II) concentrations (2.5, 6, and 10 µM). The results of these experiments are shown in Figure 4.2. A rapid decrease in ATMP concentration was observed across all tested Mn(II) concentrations. The ATMP degradation rate linearly correlated with Mn(II) concentration, with rates of 0.096 ±0.003, 0.142 ±0.010, and 0.210 ±0.006 mM day^{-1} for Mn(II) levels of 2.5, 6, and 10 µM, respectively ($R^2 = 0.995$, see SI, Figure C2). ATMP degradation was accompanied by the formation of IDMP and *o*-PO_4 as transformation products, confirming the occurrence of abiotic ATMP breakdown in the presence of trace Mn(II). While *o*-PO_4 formation was stoichiometric with the decrease of ATMP in all setups (Fig. 4.2c), IDMP was produced in sub-stoichiometric amounts (Fig. 4.2b). This suggests the involvement of alternative or multi-step degradation pathways that may yield additional, unidentified P-containing byproducts. This interpretation is supported by Marks et al. (2024), who investigated the photolytic degradation of ATMP and identified several P-containing transformation products beyond IDMP, including AMPA, hydroxymethylphosphonic acid (HMP), formylphosphonic acid, methylphosphonic acid, and phosphonic acid using high-resolution mass spectrometry. Interestingly, AMPA was not detected as a transformation product of IDMP in our experiments. Overall, these results clearly demonstrate that trace-concentrations of Mn(II) in bacterial growth

media significantly compromise ATMP stability. This abiotic process, first described by Nowack & Stone (2000), involves a three-step oxidation mechanism: (1) the formation of an Mn(II)-ATMP complex, (2) oxygen-driven oxidation of Mn(II) to Mn(III) within the Mn(III)ATMP complex, and (3) intramolecular electron transfer leading to bond cleavage in ATMP and regeneration of Mn(II). Martin et al. (2022) further elucidated this process using stable carbon isotope analysis, identifying two parallel degradation pathways.

In summary, these results show that Mn(II), even at low micromolar concentrations – commonly used in biodegradation studies of higher APPs – can transform 0.5 mM ATMP into *o*-PO_4, IDMP, and likely other P-containing degradation products. This has significant implications for biodegradation research, as the formation of such metabolites can confound the interpretation of microbial activity and lead to overestimation of true biodegradability.

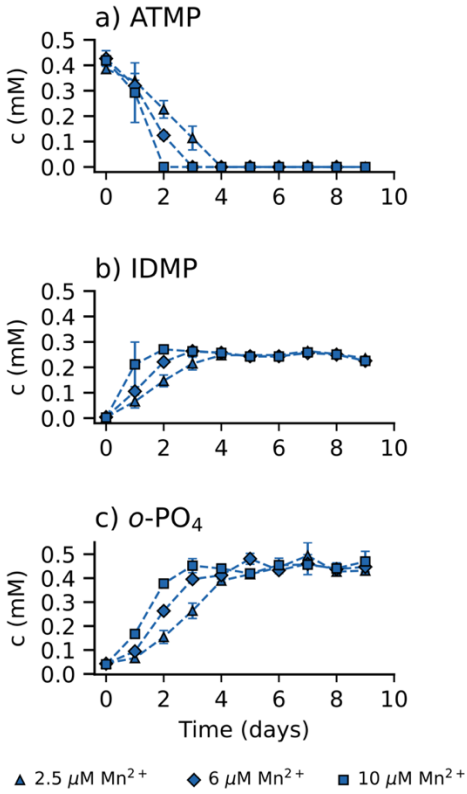

Figure 4.2 Investigation of ATMP (a), IDMP (b) and *o*-PO4 (c) concentrations vs time in the presence of various concentrations of Mn^{2+} in 50 mM MOPS buffer (pH 7.0). Triangles (connected by lines) indicate setups with 2.5 µM Mn^{2+} in 50 mM MOPS, diamonds (connected by lines) indicate setups with 6 µM Mn^{2+} in 50 mM MOPS, and squares (connected by lines) indicate setups with 10 µM Mn^{2+} in 50 mM MOPS. Error bars represent the standard deviation of triplicate setups (if not visible, error bars are smaller than the symbols).

Effect of bacterial growth media composition on ATMP stability

To shed further light on the abiotic breakdown of ATMP in sterile growth medium, further experiments were conducted in seven different matrices (c(ATMP)=0.5 mM, pH=7.0)), as summarized in Table 4.1. The concentrations of ATMP, IDMP,

and *o*-PO_4 in these setups are shown in Figure 4.3. Consistent with previous results (Fig. 4.1), ATMP degraded rapidly in the medium used for cultivating *A*. Kg 19 ($Medium_1$) (see Fig. 4.3a), with a corresponding release of IDMP and *o*-PO_4 (Figs. 4.3a-c). Contrarily, ATMP remained stable in $Medium_2$ over 9 days, with no release of IDMP or *o*-PO_4 observed. Both media contained the same amounts of organic carbon and buffer but differed in the concentration of the nitrogen source ($c_{NH4Cl, Medium2}$= 2.5 x $c_{NH4Cl, Medium1}$~ 93.5 mM) and the amount of Ca(II) ($c_{Ca2+, Medium2}$= 8 x $c_{Ca2+, Medium1}$ ~365 µM). Most notably, $Medium_2$ was not supplemented with a TES and consequently was manganese-free. The TES (Zn, Ca, Fe, Cu, Mn, and Ni) was identified as the driving factor for ATMP degradation in an experiment with TES-spiked MOPS. ATMP was completely degraded within 2 days (rate: 0.161 mM day^{-1}), producing stoichiometric amounts of *o*-PO_4 (0.47 mM) and sub-stoichiometric amounts of IDMP (0.26 mM). While the fastest degradation occurred in MOPS with the TES, ATMP also degraded in $Medium_1$, albeit at a slower rate of 0.093 mM day^{-1}. This reduced rate may be due to the presence of competing cations such as Mg(II) (~0.8 mM), which can competitively form complexes with ATMP, and potentially modulate the reaction kinetics. Nowack and Stone (2002) demonstrated that certain bivalent cations found in trace element solutions—such as Ca(II) and Zn(II)—do not promote ATMP degradation, but rather slow down the reaction by complex formation. This aligns with our observations: ATMP degraded more rapidly in MOPS with Mn(II) alone than in media also containing Cu(II) or Mg(II) (see Figs. 4.2 and 4.3). Interestingly, ATMP degradation also occurred in $Medium_1$ amended with EDTA, a common metal chelator used in biodegradation studies (Forlani et al., 2011; Riedel et al., 2023, 2024). For 15 days, over 50% of ATMP was degraded, producing 0.19 mM IDMP and 0.14 mM *o*-PO_4. Visual MINTEQ calculations showed that at the EDTA concentrations used, most metals-including Mn(II) were complexed (percentages equaled to 98.8%, 16.5%, 73.6%, 100%, 99.3%, and 0.2% for Fe(II), Ca(II), Cu(II), Zn(II), Mn(II), and Mg(II), respectively) (complex formation constants are summarized in the SI, in Table C3). Despite this, metal-mediated ATMP degradation persisted, suggesting that even EDTA-complexed Mn(II) remains catalytically active. This was further confirmed in a simplified system containing only MOPS, trace elements, ATMP, and EDTA, where 63% degradation occurred by day 15. Thus, although EDTA significantly slowed the reaction, it did not fully inhibit it. Complementary tests with MOPS buffer, with or without a vitamin solution, showed no adverse effect on ATMP – no IDMP or *o*-PO_4 was released over the 9 days, indicating no hydrolysis.
Overall, in accordance with literature knowledge, our results clearly identify Mn(II) as the main driver of abiotic ATMP degradation in aqueous systems containing trace elements. Degradation was consistently accompanied by the release of IDMP and *o*-PO_4, confirming abiotic transformation under the tested conditions. Importantly, *o*-PO_4 is the most accessible P-source for microbes and can suppress the expression of phosphonate uptake and degradation genes at concentrations above 4 µM (Tetsch & Jung, 2009; Stosiek & Klimek-Ochab,

2020). In mixed systems, these breakdown products themselves can serve as P-sources for microbial growth. Microorganisms are likely to first consume available *o*-PO_4 and smaller transformation products like IDMP before turning to the parent compound, such as ATMP.

These findings imply that previous studies on biodegradation of higher-APP in growth media containing EDTA and TES may have overlooked abiotic PO_4^{3-} release driven by Mn(II)-driven oxidation. As a result, microbial growth observed in biodegradation experiments may reflect utilization of these more bioavailable metabolites rather than the parent compound. This undermines the use of growth as a proxy for biodegradation and may lead to significant overestimation of microbial degradation potential of higher APPs. Overall, these findings emphasize the need for careful distinction between biotic and abiotic processes when assessing the environmental fate of higher APPs.

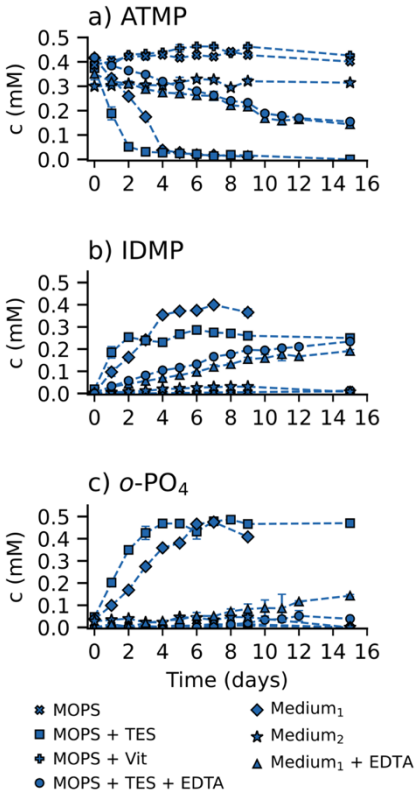

Figure 4.3 Investigation of ATMP (a), IDMP (b), and o-PO4 (c) concentrations vs time under various experimental conditions. Crosses (connected by lines) indicate setups with 50 mM MOPS, squares (connected by lines) indicate setups with 50 mM MOPS and TES, plus signs (connected by lines) indicate setups with 50 mM MOPS and vitamin solution, diamonds (connected by lines) describe the medim1 used for strain A. Kg 19, stars (connected by lines) describe the $Medium_2$ for strain O. GPr1-13, triangles (connected by lines) describe the setups with Medium1 with 100 µm EDTA, and circles (connected by lines) demonstrate setups with 50 mM MOPS, trace element solution and 100 µm EDTA. Error bars represent the standard deviation of triplicate setups (if not visible, error bars are smaller than the symbols).

4.5 Conclusions and implications

This work demonstrates that common microbial growth media are inadequate for assessing the aerobic biodegradation of higher APPs such as ATMP and EDTMP due to the prevalence of the abiotic Mn(II)-catalyzed degradation. Trace concentration levels of dissolved Mn(II), commonly present in mineral media, were shown to rapidly transform ATMP, forming IDMP and *o*-PO_4, even in the presence of the metal-chelating agent EDTA. Consequently, this abiotic process significantly interfered with the accurate assessment of ATMP and EDTMP biodegradability by *Achromobacter insolitus* strain Kg 19, as the parent compounds were rapidly transformed into other more bioavailable P-containing transformation products. The bacterial growth observed was likely supported by the utilization of such transformation products as P-source rather than by the direct biotransformation of ATMP or EDTMP. This suggests that microbial activity reported in previous studies may also have been sustained by such abiotic degradation intermediates, leading to a potential overestimation of the actual biodegradability of higher APPs. The release of *o*-PO_4 further complicates the interpretation of APP biodegradability by suppressing microbial APP utilization pathways, as observed previously in strain *A*. Kg 19.

While the degradation of higher APPs in the presence of oxygen and trace Mn(II) is a known environmental process, the role of Mn(II) has been largely overlooked in biodegradation studies of higher APPs. Thus, the findings presented here reveal a critical gap in current biodegradation testing approaches that fail to distinguish between microbially mediated degradation and metal-catalyzed abiotic reactions. Future research should focus on developing biodegradation approaches that will minimize abiotic interference while ensuring that media compositions support the full degradative potential of the test organisms. This includes the use of Mn(II)-free cultivation media (for microbes tolerant to Mn-deficient conditions) or media with bioavailable Mn-complexes, as well as the implementation of rigorous controls to clearly differentiate between biotic and abiotic transformation pathways. High-resolution mass spectrometry should also be employed to fully characterize degradation pathways and identify P-containing transformation products. This is particularly relevant for intermediates such as AMPA, which are environmentally persistent and ecologically concerning. Other products—such as methylphosphonic acid, phosphonic acid, and formylphosphonic acid—may also be formed during the degradation of higher APPs. These compounds can contribute to the overall P-load in the environment and may persist in soil and aquatic systems, influencing nutrient cycles and microbial communities. Such methodological improvements are essential for accurately assessing the biodegradability of higher APPs – as non-degradable compounds can build up in ecosystems and pose long-term risks to both environmental and human health.

4.6 References

Engelbart, L., Bieger, S., Thompson, K., Fischer, L., Bader, T., Kramer, M., Haderlein, S. B., Röhnelt, A. M., & Huhn, C. (2025). In-situ formation of glyphosate and AMPA in activated sludge from phosphonates used as antiscalants and bleach stabilizers in households and industry. *Water Research*, *280*. https://doi.org/10.1016/j.watres.2025.123464

Ermakova, I. T., Shushkova, T. V., & Leont'evskii, A. A. (2008). Microbial degradation of organophosphonates by soil bacteria. *Microbiology*, *77*(5), 615–620. https://doi.org/10.1134/S0026261708050160

Fischer, K. (1993). Distribution and elimination of HEDP in aquatic test systems. *Water Research*, *27*(3), 485–493. https://doi.org/10.1016/0043-1354(93)90049-N

Forlani, G., Prearo, V., Wieczorek, D., Kafarski, P., & Lipok, J. (2011). Phosphonate degradation by Spirulina strains: Cyanobacterial biofilters for the removal of anticorrosive polyphosphonates from wastewater. *Enzyme and Microbial Technology*, 48(3), 299–305. https://doi.org/10.1016/j.enzmictec.2010.12.005

Greenlee, L. F., Freeman, B. D., & Lawler, D. F. (2014). Ozonation of phosphonate antiscalants used for reverse osmosis desalination: Parameter effects on the extent of oxidation. *Chemical Engineering Journal*, *244*, 505–513. https://doi.org/10.1016/j.cej.2014.02.002

Guo, R., Röhnelt, A. M., Martin, P. R., & Haderlein, S. B. (2025). Limitations of the molybdenum blue method for phosphate quantification in the presence of organophosphonates. *Analytical and Bioanalytical Chemistry*, 0123456789. https://doi.org/10.1007/s00216-025-05850-y

HERA. (2004). Human & Environmental Risk Assessment on ingredients of European household cleaning products Phosphonates. *Assessment*, 1–114.

Jaworska, J., Van Genderen-Takken, H., Hanstveit, A., Van de Plassche, E., &

Feijtel, T. (2002). Environmental risk assessment of phosphonates, used in domestic laundry and cleaning agents in the Netherlands. *Chemosphere*, *47*(6), 655–665. https://doi.org/10.1016/S0045-6535(01)00328-9

Knepper, T. P. (2003). Synthetic chelating agents and compounds exhibiting complexing properties in the aquatic environment. *TrAC - Trends in Analytical Chemistry*, *22*(10), 708–724. https://doi.org/10.1016/S0165-9936(03)01008-2

Kononova, S. V, & Nesmeyanova, M. A. (2002). *Phosphonates and their degradation by microorganisms*. *Biochemistry (Moscow)*, 67(2), 184–195. https://doi.org/10.1023/A:1014409929875.

Kourtaki, K., Buchner, D., Martin, P. R., Thompson, K., & Haderlein, S. B. (2025). Influence of organophosphonates as alternative P-sources on bacterial transformation of glyphosate. *Environmental Pollution*, 125872. https://doi.org/https://doi.org/10.1016/j.envpol.2025.125872

Kuhn, R., Jensch, R., Bryant, I. M., Fischer, T., Liebsch, S., & Martienssen, M. (2018). The influence of selected bivalent metal ions on the photolysis of diethylenetriamine penta(methylenephosphonic acid). *Chemosphere*, *210*, 726–733. https://doi.org/10.1016/j.chemosphere.2018.07.033

Lesueur, C., Pfeffer, M., & Fuerhacker, M. (2005). Photodegradation of phosphonates in water. *Chemosphere*, *59*(5), 685–691. https://doi.org/10.1016/j.chemosphere.2004.10.049

Marks, R. G. H., Drees, F., Rockel, S., Kerpen, K., Jochmann, M. A., & Schmidt, T. C. (2023). Mechanistic investigation of phosphonate photolysis in aqueous solution by simultaneous LC-IRMS and HRMS analysis. *Journal of Photochemistry and Photobiology A: Chemistry*, *439*(September 2022), 114582. https://doi.org/10.1016/j.jphotochem.2023.114582

Marks, R. G. H., Rockel, S. P., Kerpen, K., Somnitz, H., Martin, P. R., Jochmann, M. A., & Schmidt, T. C. (2024). Effects of pH-dependent speciation on the photolytic degradation mechanism of phosphonates. *Journal of Photochemistry and Photobiology A: Chemistry*, *448*, 115327.

https://doi.org/10.1016/j.jphotochem.2023.115327

Martin, P. R., Buchner, D., Jochmann, M. A., Elsner, M., & Haderlein, S. B. (2022). Two Pathways Compete in the Mn(II)-Catalyzed Oxidation of Aminotrismethylene Phosphonate (ATMP). *Environmental Science and Technology*, *56*(7), 4091–4100. https://doi.org/10.1021/acs.est.1c06407

McGrath, J. W., Ternan, N. G., & Quinn, J. P. (1997). Utilization of organophosphonates by environmental microorganisms. *Letters in Applied Microbiology*, *24*(1), 69–73. https://doi.org/10.1046/j.1472-765X.1997.00350.x

Murphy J., R. J. P. (1962). A modified single solution method for the determination of phosphate in natural waters. *Analytica Chimica Acta*, 8(1), 11–16. https://doi.org/10.18393/ejss.477560

Nowack, B. (1998). The behavior of phosphonates in wastewater treatment plants of Switzerland. *Water Research*, *32*(4), 1271–1279. https://doi.org/10.1016/S0043-1354(97)00338-2

Nowack, B. (2002). Aminopolyphosphonate removal during wastewater treatment. *Water Research*, *36*(18), 4636–4642. https://doi.org/10.1016/S0043-1354(02)00196-3

Nowack, B., & Stone, A. T. (2000). Degradation of nitrilotris(methylenephosphonic acid) and related (amino)phosphonate chelating agents in the presence of manganese and molecular oxygen. *Environmental Science & Technology*, 34(22), 4759–4765. https://doi.org/10.1021/es0000908

Riedel, R., Krahl, K., Buder, K., Böllmann, J., Braun, B., & Martienssen, M. (2023). Novel standard biodegradation test for synthetic phosphonates. *Journal of Microbiological Methods*, *212*(June). https://doi.org/10.1016/j.mimet.2023.106793

Riedel, R., Meißner, K., Kaschubowski, A., Benndorf, D., Martienssen, M., & Braun, B. (2024). Laundry Isolate Delftia sp. UBM14 Capable of Biodegrading Industrially Relevant Aminophosphonates. *Microorganisms*,

12(8), 1–20. https://doi.org/10.3390/microorganisms12081664

Röhnelt, A. M., Martin, P. R., Buchner, D., & Haderlein, S. B. (2023). Transformation of Iminodi(methylene phosphonate) on Manganese Dioxides - Passivation of the Mineral Surface by (Formed) Mn2+. *Environmental Science and Technology*, *57*(32), 11958–11966. https://doi.org/10.1021/acs.est.3c01838

Röhnelt, A. M., Martin, P. R., Marks, R. G. H., Buchner, D., Weiss, J., Schmidt, T. C., & Haderlein, S. B. (2025). Green quantification of amino(poly)phosphonates using ion chromatography coupled to integrated pulsed amperometric detection. *Analytical and Bioanalytical Chemistry*, *417*(8), 1581–1594. https://doi.org/10.1007/s00216-025-05747-w

Röhnelt, A. M., Martin, Athmer M., Bieger S., Buchner, D., Carst U., Huhn C., Schmidt, T. C., & Haderlein, S. B. (2025). Glyphosate is a transformation product of a widely used complexing agent. *Nature Communications*, *16*(1), 2438. doi: 10.1038/s41467-025-57473-7

Rott, E., Steinmetz, H., & Metzger, J. W. (2018). Organophosphonates: A review on environmental relevance, biodegradability and removal in wastewater treatment plants. *Science of the Total Environment*, 615, 1176–1191. https://doi.org/10.1016/j.scitotenv.2017.09.223

Santos-Beneit, F. (2015). The Pho regulon: A huge regulatory network in bacteria. *Frontiers in Microbiology*, *6*(402), 1–13. https://doi.org/10.3389/fmicb.2015.00402

Schowanek, D., & Verstraete, W. (1990). Phosphonate utilization by bacterial cultures and enrichments from environmental samples. *Applied and Environmental Microbiology*, *56*(4), 895–903. https://doi.org/10.1128/aem.56.4.895-903.1990

Schowanek, D., McAvoy, D., Versteeg, D., & Hanstveit, A. (1996). Effects of nutrient trace metal speciation on algal growth in the presence of the chelator [S,S]-EDDS. *Aquatic Toxicology*, *36*(3–4), 253–275. https://doi.org/10.1016/S0166-445X(96)00807-7

Stosiek, N., & Klimek-ochab, M. (2020). Carbon-Phosphorus Lyase — the State of the Art. *Applied Biochemistry and Biotechnology*, 190(4), 1525–1552. https://doi.org/10.1007/s12010-019-03161-4.

Strotmann, U., Thouand, G., Pagga, U., Gartiser, S., & Heipieper, H. J. (2023). Toward the future of OECD/ISO biodegradability testing-new approaches and developments. *Applied Microbiology and Biotechnology*, *107*, 2073–2095. https://doi.org/10.1007/s00253-023-12406-6

Studnik, H., Liebsch, S., Forlani, G., Wieczorek, D., Kafarski, P., & Lipok, J. (2015). Amino polyphosphonates - chemical features and practical uses, environmental durability and biodegradation. *New Biotechnology*, *32*(1), 1–6. https://doi.org/10.1016/j.nbt.2014.06.007

Tarlachkov, S. V., Epiktetov, D. O., Sviridov, A. V., Shushkova, T. V., Ermakova, I. T., & Leontievsky, A. A. (2020). Draft Genome Sequence of Glyphosate-Degrading Achromobacter insolitus Strain Kg 19 (VKM B-3295), Isolated from Agricultural Soil. *Microbiology Resource Announcements*, *9*(17). https://doi.org/10.1128/mra.00284-20

Ternan, N. G., Mc Grath, J. W., Mc Mullan, G., & Quinn, J. P. (1998). Review: Organophosphonates: Occurrence, synthesis and biodegradation by microorganisms. *World Journal of Microbiology and Biotechnology*, *14*(5), 635–647. https://doi.org/10.1023/A:1008848401799

Tetsch, L., & Jung, K. (2009). The regulatory interplay between membrane-integrated sensors and transport proteins in bacteria. *Molecular Microbiology*, *73*(6), 982–991. https://doi.org/10.1111/j.1365-2958.2009.06847.x

Chapter 5

5 Sample cleanup prior to carbon CSIA of glyphosate and AMPA from biotransformation experiments- advances and challenges

Kleanthi Kourtaki[1], Philipp R. Martin[1,2], Daniel Buchner[1], Stefan B. Haderlein[1,*]

[1]Department of Geosciences, Eberhard Karls Universität Tübingen, Tübingen, Germany

[2]Division for Environmental Geosciences, Centre for Microbiology and Environmental Systems Science, University of Vienna, Austria

Author	Author position	Scientific ideas	Data generation*	Analysis & interpretation	Paper writing
K. Kourtaki	1	40	65	60	70
P. Martin	2	35	10	20	20
D. Buchner	3	15	0	10	0
S. Haderlein	4	10	0	10	10

Title of the paper:
Sample cleanup prior to carbon CSIA of glyphosate and AMPA from biotransformation experiments-advances and challenges

Status in the publication process:
Manuscript in preparation

*Experiments were conducted with the help of Teresa Weis-Reyes, Tamara Pruneddu (see acknowledgements

Chapter 5

5.1 Abstract

Carbon compound-specific carbon isotope analysis (carbon-CSIA) by liquid chromatography–isotope ratio mass spectrometry (LC-IRMS) is a promising tool for studying the transformation of polar organic compounds, such as organophosphonates (OPs), including the world's most applied herbicide, glyphosate. While the biodegradation of glyphosate and its main metabolite, aminomethylphosphonate (AMPA), has been widely investigated under controlled laboratory conditions, associated kinetic (carbon) isotope effects remain poorly understood, despite their potential to reveal enzymatic mechanisms, identify rate-limiting steps, and distinguish transformation pathways. This is largely due to analytical challenges, including high carbon content in microbial media and the limited sensitivity of CSIA, which necessitate effective cleanup strategies. This study evaluated two approaches to reduce the carbon content associated with glutamic acid (glutamate), a common carbon source in glyphosate and AMPA bacterial transformation experiments. First, ion exchange with a strong cation exchange resin at acidic pH was tested to selectively retain positively charged glutamate, while glyphosate and AMPA occurred as zwitterions in solution. This method achieved 95% glyphosate recovery and 75% glutamate removal in solid-phase extraction (SPE) batch treatments, but residual carbon levels remained too high. Column-SPE experiments improved glutamate removal (>95%) but significantly reduced recoveries of glyphosate and AMPA, rendering the method unsuitable for CSIA. Next, aluminum oxide was tested as a positively charged mineral (point of zero charge ~ 9) to promote electrostatic interaction as well as glyphosate and AMPA sorption via their phosphonic acid groups. This method resulted in over 99% glutamate removal, while glyphosate and AMPA recoveries exceeded 80% in both standards and transformation samples. Preliminary CSIA showed no significant isotope effects from the cleanup process or early-stage transformation. However, at later time points, poor chromatographic separation—likely due to co-eluting metabolites or glutamate residues—limited further isotope analysis. These findings underscore the need for further refinement of cleanup and enrichment methods to enable accurate and reliable carbon-CSIA of OP biotransformation.

5.2 Introduction

Organophosphonates (OPs), including glyphosate—the world's most applied herbicide—and its primary degradation product aminomethylphosphonic acid (AMPA), have become ubiquitous contaminants in aquatic and terrestrial environments (Schwientek et al., 2024; Wimmer et al., 2022). Their extensive application in agriculture and industry has raised concerns about their persistence, mobility, and potential ecological impacts. Understanding the environmental fate of OPs is crucial, as their transformation products can be as persistent or even more

mobile than the parent compounds, posing risks to water quality and ecosystem health (Bento et al., 2016). Traditional studies on the biodegradation of glyphosate and AMPA have focused on identifying transformation pathways and quantifying degradation rates using concentration-based measurements. However, characterizing degradation processes in the environment is challenging. Non-reactive processes, such as sorption, diffusion, or dilution, also influence the aqueous concentrations of glyphosate and AMPA, but they do not lead to permanent dissipation of these compounds. Thus, these approaches often fall short in distinguishing between physical removal and true chemical or biological transformation.

In this context, compound-specific carbon isotope analysis (carbon-CSIA) by liquid chromatography coupled to isotope ratio mass spectrometry (LC-IRMS) emerges as a powerful analytical technique for investigating the environmental fate and transformation of organic contaminants (Elsner & Imfeld, 2016; Hofstetter et al., 2024). The contribution of carbon-CSIA in environmental research has been well recognized over the last few decades, providing important information on the source allocation and degradation mechanisms. It offers unique insights into the mechanisms and extent of in-situ degradation processes without relying on concentration monitoring campaigns that are often inconclusive due to the complexity of environmental processes. By tracking subtle changes in the stable carbon isotope ratios ($^{13}C/^{12}C$) of target compounds, carbon-CSIA enables the identification and estimation of the degree of (bio-)degradation occurring in complex environmental matrices.

Carbon-CSIA methods for polar compounds like glyphosate and AMPA are established (Kujawinski et al., 2013; Li et al., 2016; Limon et al., 2020). However, applying this technique to study biotransformation processes remains in early development, primarily due to methodological challenges. A key challenge is the technique's inherently low sensitivity, which, combined with the typically low concentrations of these analytes in environmental samples, makes it difficult to obtain reliable CSIA measurements. Overall, chromatographic performance in LC-IRMS is often poor, with analyte peaks appearing broad. Options for improvement are very limited, since the systems must be operated under isocratic conditions and only carbon-free solvents, compatible with oxidation, can be used. Laboratory-based degradation studies pose additional challenges due to the high carbon content of cultivation media, which increases the carbon background, elevates CO_2 levels, and impairs chromatographic resolution. In biodegradability experiments, to support microbial growth, the cultivation media are supplemented with high levels of carbon substrates, following the Redfield ratio (C:N:P = 106:16:1, Redfield, 1958). Glutamic acid (glutamate), a highly bioavailable amino acid, is commonly used as the primary C-source, typically at concentrations exceeding several grams per liter (e.g., >290 mM-C), while P-substrates such as glyphosate or AMPA are typically added in much lower concentrations, ranging from 0.5 to 1 mM. To maintain stable pH conditions, organic buffers such as MOPS are often

added at high concentrations (approximately 20-50 mM), introducing additional CO_2 signals during LC-IRMS analysis.

The development of selective cleanup and enrichment methods to improve sample purity and expand the applicability of CSIA for polar contaminants has been a major focus of research in recent years (Bakkour et al., 2018; Torrentó et al., 2019; Glöckler et al., 2023; Bakkour et al., 2024). For example, Limon et al. (2020) enhanced the sensitivity of carbon isotope analysis for glyphosate and AMPA by applying freeze-drying as a concentration step, achieving up to a 500-fold increase in analyte concentration. While glyphosate showed no isotopic shifts across the tested concentration range (10 μg L^{-1} to 25 mg L^{-1}), AMPA exhibited isotopic fractionation at lower concentrations (10 μg L^{-1}), underscoring the importance of method-specific validation. However, freeze-drying has limitations, particularly when applied to samples from biodegradation studies conducted in complex media. Even when no isotope effects are caused by the treatment itself, the evaporation process can concentrate not only the target analyte but also matrix components. This co-concentration can intensify matrix effects and reduce the reliability of CSIA measurements. Despite these limitations, freeze-drying has been successfully applied in some cases. For instance, Ehrl et al. (2018) used the method to study glyphosate biodegradation by *Ochrobactrum* sp. FrEM, observing a significant normal carbon isotope effect (glyphosate enrichment factor of –4.5 ± 0.5‰ (95% CI)). Nonetheless, more selective cleanup strategies are needed to effectively isolate polar contaminants from complex matrices and minimize matrix-related interferences in CSIA.

Various cleanup strategies have been explored for CSIA of polar compounds, including molecularly imprinted polymers (MIPs), preparatory high-performance liquid chromatography (HPLC), liquid-liquid extraction, solid-phase extraction (SPE) with various sorbents, and derivatization techniques. Among these, SPE-based methods (batch or column strategies) are the most widely used. The effectiveness of SPE largely depends on the selection of an appropriate sorbent, chosen based on specific interaction mechanisms—such as ion exchange, van der Waals forces, π–π interactions, hydrogen bonding, or polarity-based interactions—between the sorbent and the target analyte. Bakkour et al. (2024) have comprehensively outlined the limitations on the sensitivity of various sample preparation techniques that have so far hindered the application of carbon-CSIA to environmental micropollutants.

In this study, we aimed to develop a purification method tailored for samples derived from microbial degradation experiments, where high levels of organic carbon, introduced through carbon sources and buffering agents, complicate carbon-CSIA of glyphosate and AMPA. Effective purification requires careful consideration of analyte speciation and the chemical environment, especially pH, as these govern molecular charge states and interactions with sorbents. Glyphosate, AMPA, and glutamate are all polar molecules possessing amine and carboxylic acid groups, and there is no pH range in which glutamate carries an opposite charge to glyphosate or AMPA. Their similar charge behavior and functional groups make

selective separation challenging, highlighting the need for strategies that exploit subtle differences in interactions with solid phases. While techniques such as MIPs or preparatory HPLC offer selectivity, they tend to be more complex and less commonly used. Liquid-liquid extraction and derivatization can enhance detection sensitivity but add steps and risks of fractionation or losses, complicating CSIA applications. Therefore, solid-phase extraction (SPE) methods stand out as the most suitable. Therefore, we tested two SPE-based approaches: The first approach aimed to remove glutamate by exploiting its positive charge at low pH, using a strong cation exchange resin to retain it while allowing glyphosate and AMPA, predominantly present as zwitterions, not to interact. The second strategy used aluminum oxide as a sorbent, taking advantage of its surface charge and affinity for phosphonic acid groups to selectively bind glyphosate and AMPA. Both methods were systematically assessed for their ability to recover the target compounds and reduce glutamate content. Finally, we evaluated whether the purified samples were suitable for carbon isotope analysis and whether isotope fractionation associated with glyphosate and AMPA degradation could be observed in biodegradation experiments using *Achromobacter insolitus* strain Kg 19.

5.3 Materials and Methods

Chemicals and reagents

Glyphosate (>98%) and AMPA (99%) were purchased from Sigma Aldrich (Steinheim, Germany). MOPS buffer (99.5%) was bought from Carl Roth (Karlsruhe, Germany) and sodium acetate (>99.5%) from Chemsolute (Renningen, Germany). The eluent for concentration and carbon isotope analysis was prepared from sulfuric acid (95–97%, EMSURE®, Merck Millipore, Darmstadt, Germany). $Na_2S_2O_8$ (≥98%, Sigma-Aldrich, Steinheim, Germany) and H_3PO_4 (85%, EMSURE®, Merck Millipore, Darmstadt, Germany) were used as reactants for LC-IRMS analysis. Additional chemicals used for the experiments were purchased from Merck in their highest purity (Darmstadt, Germany). Ultrapure water was used for all experiments obtained by a Barnstead GenPure system (Thermo Fischer Scientific, Germany).

Batch biotransformation experiments

Biotransformation experiments were conducted in 100 mL glass serum bottles continuously shaken on a rotary shaker at 150 rpm with the bacterial strain *Achromobacter insolitus* strain Kg 19 (hereafter referred to as *A*. Kg 19) (as previously described by Kourtaki et al., 2025). Glyphosate or AMPA was used as P-sources at concentrations equal to 1 mM. The growth medium used for the cultivation of *A*. Kg 19 was buffered at pH 7.0 ± 0.1 with 50 mM MOPS in

experiments where glyphosate was used as a P-source, while when AMPA was provided, the medium was unbuffered. During the experiment, the pH was maintained between 6.8 and 7.5 by the addition of 20% sterile H_2SO_4 in all cases. Other medium components included 10 g/L Na-glutamate, 2 g/L NH_4Cl as N-source, 0.5 g/L K_2SO_4, 0.2 g/L $MgSO_4$ x 7 H_2O, 1 mL/L of a 7-Vitamin solution, and a trace element solution with: 20 mg/L $ZnSO_4$ x $7H_2O$, 10 mg/L $CaCl_2$ x 6 H_2O, 2.5 mg/L $FeSO_4$ x 7 H_20, 2 mg/L $CuSO_4$ x 5 H_2O, 1 mg/L $MnSO_4$ x H_2O, 0.3 mg/L Na_2MoO_4, 0.06 mg/L H_3BO_3, and 0.05 mg/L $NiCl_2$ x $6H_2O$. For each sampling point, 1 mL of sample was withdrawn under sterile conditions with a transfer pipette and transferred to a 1 cm PP cuvette for monitoring growth via optical density measurement with a UV5Bio spectrophotometer (Mettler Toledo, Germany). An additional 5 mL of sample was withdrawn and transferred to a 5 mL centrifugation tube (Eppendorf, Hamburg, Germany) for centrifugation (10 minutes at 12,000 rcf). The biomass-free supernatant was separated from the cell pellet and stored in 2 mL centrifugation tubes at -20 °C in the dark till concentration analysis, if not analyzed directly. The storage procedure had no adverse effect with respect to the stability of the OPs.

Each experiment consisted of three biotic replicates and three abiotic controls to assess potential interactions with the APPs and the medium.

Solid-Phase Extraction (SPE) batch setup for glyphosate samples cleanup using cation exchange resin

Batch experiments were conducted to assess the removal of glutamate from glyphosate-containing standards using strong cation exchange resin (DOWEX® 50 WX8, 100–200 mesh, converted to Na^+ form; Carl Roth, Karlsruhe, Germany). Standards with glyphosate concentrations ranging from 0.05 mM to 1 mM were prepared in growth medium, acidified to pH 1.5 with phosphoric acid (H_3PO_4), and transferred to 5 mL Eppendorf tubes. For each sample, 4 mL was mixed with 500 mg of cation exchange resin and placed on an overhead shaker overnight at room temperature. After shaking, samples were centrifuged at 12,000 rcf for 10 minutes. The resulting particle-free supernatant was either analyzed immediately for glyphosate and glutamate content or stored at −20 °C until analysis. All experiments were performed in duplicate.

SPE-column setups for Glyphosate and AMPA sample cleanup using cation exchange resin

Solid-phase extraction (SPE) was employed to clean up glyphosate and AMPA standards, as well as samples from biotransformation experiments. Standards were prepared in growth medium at concentrations ranging from 0.1 mM to 1 mM. Before cleanup, all samples were acidified to pH 1.5 using H_3PO_4.

For the SPE procedure, 500 mg of DOWEX® 50 WX8 resin (100–200 mesh, Na^+ form; Carl Roth, Karlsruhe, Germany) was packed into self-built SPE columns.

Acidified samples were applied to the columns and percolated under pressure (870 mbar). The eluate was collected and either analyzed immediately for glyphosate and AMPA content or stored at −20 °C until analysis.
All samples were processed in duplicate.

SPE-batch setup for glyphosate and AMPA samples cleanup by adsorption onto alumina particles

High-purity alumina (pore diameter=9 nm, particle size 70% between 0.063-0.002 mm) (Al_2O_3, Merck, Darmstadt) was also tested to selectively retain glyphosate or AMPA. The optimal amount of Al_2O_3 for sample clean-up was determined by testing five quantities (50, 100, 250, 500, and 1000 mg). For each test, 3 mL of a 0.5 mM glyphosate stock solution, prepared in MS1 medium, was added to the Al_2O_3 in 5 mL Eppendorf tubes. The samples were vortexed and then placed on an overhead shaker for one hour to allow binding. To enhance the removal of loosely bound compounds, an additional washing step with 50 mM NaCl was performed for 15 minutes, which improved glutamate removal efficiency without affecting glyphosate recovery. Desorption was carried out by adding 100 mM NaOH and shaking for another hour. After centrifugation, the particle-free supernatant was either analyzed immediately for glyphosate and glutamate content or stored at −20 °C until analysis. All experiments were conducted in duplicate.
A mass of 50 mg Al_2O_3 was shown to perform the best, therefore the method was further employed to cleanup glyphosate and AMPA standards, as well as samples from biotransformation experiments.

SPE-column setups for Glyphosate and AMPA sample cleanup by adsorption onto alumina particles

Column-SPE was also assessed to clean up glyphosate standards, with varying amounts of sorbent used (50, 100, 250, 500, and 1000 mg Al_2O_3). The required amount of Al_2O_3 was packed into self-assembled columns and secured with a filter membrane. The columns were placed under vacuum (890 mbar), and samples were percolated. Each column was then washed with 3 mL of 50 mM NaCl to remove loosely bound impurities. Desorption of the analytes was carried out by conditioning the column with 3 mL of 100 mM NaOH. The resulting eluate was collected and either analyzed immediately for glyphosate and glutamate content or stored at −20 °C until analysis.

Compound-specific carbon isotope analysis

Stable carbon isotope analysis of glyphosate and AMPA samples, was performed using liquid chromatography coupled to isotope ratio mass-spectrometry (LC-IRMS). The procedure was adapted from the method described by Martin et al. (2020). Separation of glyphosate and AMPA from the growth media was achieved

using an UltiMate 3000 HPLC system (Thermo Fisher Scientific, Germering, Germany). Glyphosate was separated using an IC NI-424 anion chromatography column (100 mm × 4.6 mm, Shodex, Munich, Germany), while AMPA was separated using a Primesep 100 column (3.2 × 150 mm, Sielc, USA). The analysis was conducted at 40 °C with a 50 µL injection volume. The mobile phase consisted of 2.5 mM NaH_2PO_4 (EMSURE®, Merck Millipore, Darmstadt, Germany), adjusted to pH 3.1 for glyphosate and pH 1.9 for AMPA using H_3PO_4 (85%, EMSURE®, Merck Millipore), delivered at a flow rate of 500 µL min^{-1}. Carbon isotope ratio measurements were carried out on a Delta V Plus IRMS (Thermo Fisher Scientific, Bremen, Germany) hyphenated with the HPLC system via an LC Isolink interface. The eluent stream was post-column mixed with 1.5 M H_3PO_4 and 60 g L^{-1} sodium persulfate (both EMSURE®, Merck Millipore), at flow rates of 50 µL min^{-1} and 75 µL min^{-1}, respectively. The oxidation reactor was operated at a temperature of 99.9 °C. All samples were diluted with ultrapure water to a concentration of around 0.25 mM prior to analysis. The analytical uncertainty was ±0.5‰ (n = 2–3). For carbon isotope analysis, all solutions were degassed before use for 30 min within an ultrasonic bath under reduced pressure obtained by a water jet vacuum pump to remove dissolved CO_2. During the analysis, all solutions were purged with helium (grade 5.0, Westfalen AG, Münster, Germany) to minimize re-dissolution of atmospheric carbon dioxide. Samples contained in alkaline solution were first acidified at pH=3.1 with H_3PO_4 prior to their injection in the LC-IRMS.

Quantification of glyphosate, AMPA, and glutamate

The analytes were quantified with a 930 Compact Flex ion chromatograph equipped with an amperometric detector operated in integrated pulsed amperometric detection (iPAD) mode (Metrohm, Herisau, Switzerland) (as outlined by Röhnelt et al. (2025)). Separation of the analytes was realized on an anion-exchange column (Metrosep Carb 2, 100 x 4.0 mm, Metrohm). The analysis of glyphosate and AMPA included a flow gradient using 290 mM sodium acetate + 10 mM as eluent (as described by Kourtaki et al. (2025). Before the analysis, all samples were diluted with ultrapure water and quantified with external standards in a concentration range 0 to 20 µM.

Point of zero charge (pHpzc) determination

The pH_{pzc} of Al_2O_3 was measured using a Zetasizer Nano ZSP (Malvern Pananalytical, Malvern, United Kingdom) with folded capillary cells at 20 °C. For each measurement, 400 mg/L Al_2O_3 suspensions were prepared in 5 mM KCl and adjusted to different pH values using 0.1 M or 1 M NaOH and HCl. Zeta potential measurements were conducted in triplicate. The pH_{pzc} was determined by plotting the zeta potential as a function of pH and identifying the zero-crossing point through regression of the linear region. pH_{pzc} was found to be 9.0 ±0.1.

5.4 Results and Discussion

In laboratory biodegradation experiments, the high carbon content of cultivation media poses a major challenge for isotope analysis. Carbon-rich substrates such as glutamate are added in excess to support microbial growth, while organic buffers like MOPS are used to stabilize pH. Although necessary for cultivation, these components introduce intense CO_2 signals that interfere with chromatographic separation and isotope detection. Figure 5.1 illustrates chromatograms of a 0.25 mM glyphosate standard prepared in 0.1 mM glutamate solution and one diluted 1:2 in cultivation media. The comparison demonstrates that effective separation of glyphosate and glutamate is achievable at low glutamate concentrations. However, in the sample containing cultivation media, elevated CO_2 signals are observed that overlap with the CO_2 peak from glyphosate. This overlap compromises the precision and accuracy of $\delta^{13}C_{glyphosate}$ measurements, underscoring the significant impact of the media matrix. Similar matrix effects from carbon-rich growth media have also been reported in other microbial studies investigating the bacterial transformation of glyphosate, leading to co-eluting peaks, and raising the method detection limits (MDLs) (Mogusu E. Dissertation, 2015).

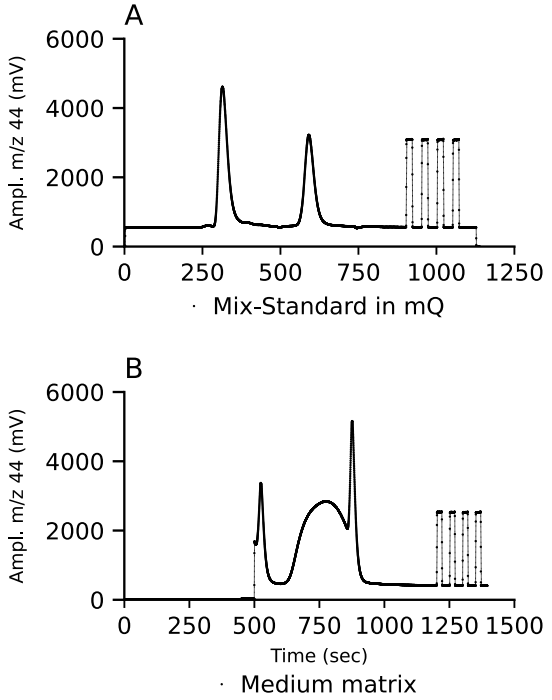

Figure 5.1 LC-IRMS chromatograms (amplitude, m/z 44 over time) of glyphosate standards under different matrix conditions. (A) Chromatogram of a 0.25 mM glyphosate standard prepared with 0.1 mM glutamate, showing the expected glyphosate and glutamate retention times approximately at 600 and 255 s, respectively, using a Shodex IC NI-424 column (4.6 × 100 mm) at pH 3.1. (B) Chromatogram of a 0.25 mM glyphosate standard prepared in cultivation medium diluted 1:2 with ultrapure water, illustrating the effects of matrix components on analyte separation and CO_2 signal response. During the first 500 seconds, no CO_2 signal was recorded because the IRMS split was turned off, and only the eluent was directed to the interface using an external pump. To minimize matrix interference, the sample flow during this initial period—when matrix components eluted—was diverted to waste. The four peaks at the end of both chromatograms correspond to the CO_2 monitoring gas.

Two different purification techniques were tested for mitigating glutamate matrix effects during isotope analysis, each based on a distinct interaction mechanism.

Among the carbon-rich components in the growth medium, glutamate and the buffer agent MOPS posed the greatest challenge for glyphosate and AMPA measurements, respectively. They were present at high concentrations and exhibited retention times similar to those of glyphosate and AMPA, compromising the separation during LC-IRMS analysis (for chromatograms see SI, Fig. D1 and D2). For glyphosate measurements, the matrix could be well separated chromatographically and did not interfere with the isotope analysis. In contrast, for AMPA measurements, MOPS could not be sufficiently separated and interfered with the chromatographic resolution. Therefore, MOPS was excluded from the growth medium in experiments involving AMPA, and the development of the cleanup method focused on glutamate removal.

The first purification method involved the use of a strong cation exchange resin to remove glutamate, exploiting electrostatic interactions to selectively retain positively charged molecules. The second method utilized aluminum oxide, which binds organophosphonate compounds like glyphosate and AMPA through ligand exchange and complex formation. Both methods were evaluated for their efficiency in reducing glutamate concentrations to mitigate matrix interference while preserving glyphosate and AMPA for subsequent CSIA analysis.

Validation of glyphosate and AMPA purification samples using strong cation exchange resin

Glutamate is an α-amino acid composed of an amine group, a carboxyl group, and a side chain containing two methylene groups that terminate in a second carboxylic acid group (see Table 5.1). Glyphosate and AMPA, in contrast, are organophosphonate compounds containing amine, phosphonic acid, and carboxylic acid functional groups. Biodegradation experiments are typically conducted at neutral pH, which represents optimal conditions for microbial activity. At this pH, glutamate, glyphosate, and AMPA primarily exist in deprotonated forms with respect to their carboxylic and/or phosphonic acid groups, while their amine groups remain protonated ($-NH_3^+$). Hence, all these compounds predominantly exist as zwitterions that carry both positive and negative charges. The zwitterionic nature complicates separation via electrostatic interactions with sorbents, as these molecules exhibit affinity for both positively and negatively charged moieties. Notably, no pH condition exists where glutamate and glyphosate/AMPA carry opposite charges (see SI, Fig. D3). To address this, sample treatment was attempted at pH 1.5, where the cationic species of glutamate is dominant (due to protonation of its carboxyl groups), while glyphosate and AMPA remain zwitterionic. This pH was chosen to promote selective interaction of glutamate with a cation exchange resin while minimizing retention of the target analytes.

Table 5.1 Summary of key physicochemical properties of glyphosate (pKa values from Sprankle et al., 1975; Sidoli et al., 2016), AMPA (pKa values from Popov et al., 2001), and glutamic acid (pKa values from Šarac & Hadži, 2021) relevant to sample preparation and separation strategies.

	Glyphosate	AMPA	Glutamic acid
pK_a	0.8 2.6 5.6 10.6	<2 5.41 10.04	2.21 4.26 9.78
Structure at pH 1.5	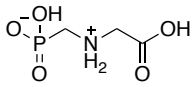	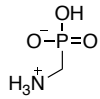	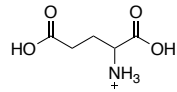
Structure at pH 7.0	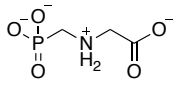		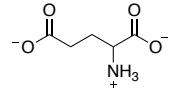
Molar mass [g/mol]	169.07	111.04	169.11

To evaluate the effectiveness of strong cation exchange treatment, glyphosate samples prepared in growth medium at concentrations ranging from 0.05 to 1 mM were purified under acidic conditions (pH=1.5). Figure 5.2 shows glyphosate recovery across this concentration range, along with the extent of glutamate removal following treatment. Results demonstrate consistent glyphosate recovery above 95% and glutamate removal of up to 75%, indicating selective retention of glutamate (positively charged) and minimal retention of glyphosate (zwitterionic) under the tested conditions. These findings support the applicability of strong cation exchange as a selective cleanup method for significantly reducing the glutamate content in samples and potentially mitigating matrix interferences in CSIA of glyphosate and/or AMPA biodegradation samples.

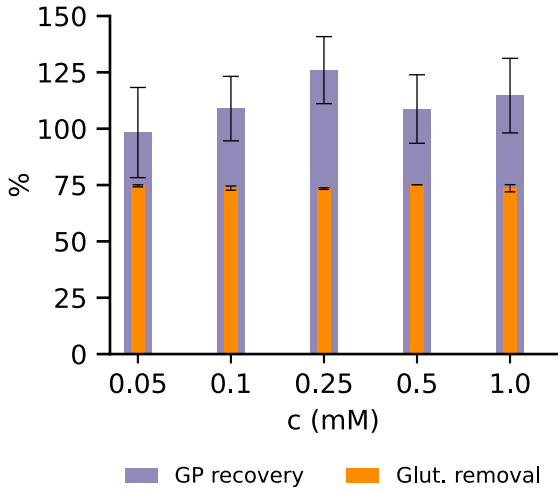

Figure 5.2 Recovery of glyphosate and removal of glutamate following treatment with strong cation exchange (batch) resin (DOWEX® 50 WX8) at pH 1.5. Purple bars indicate glyphosate recovery, calculated by comparing nominal concentrations with those measured after treatment. Orange bars represent glutamate removal efficiency, calculated as the percentage decrease between initial (nominal) and post-treatment concentrations. Error bars represent the deviation between duplicate samples.

Although approximately 75% of glutamate was removed in the initial SPE-batch experiments, the remaining concentration in the eluate was still about 15 mM (~2.5 g/L, ~900 mg C/L). This residual carbon content is 25 to 500 times higher than that of glyphosate under the tested conditions (0.03 to 0.6 mM). To increase interaction probability and efficient mass transfer between analyte and sorbent, in a following experiment, the resin was packed into SPE-columns, and the setup was evaluated. First, to optimize the sorbent mass in columns, a low glyphosate concentration was tested. To this end, glyphosate samples were prepared in a medium matrix containing 0.05 mM glyphosate (~1.8 mg C/L), using varying amounts of resin (500–1000 mg). Quantitative analysis showed that glutamate removal ranged from 87% to 98%, while glyphosate recoveries were between 82% and 95%, with the highest recovery observed using 500 mg of resin (see SI, Figure D4). These results suggest that while glyphosate recoveries during SPE were comparable to those obtained with batch setups, SPE treatment achieved more effective glutamate removal. Thus, column-SPE enabled enhanced selective removal of glutamate without compromising glyphosate recovery at low glyphosate concentration levels.

To further assess the performance of the method, varying glyphosate concentrations (0.1 to 1 mM) were processed in a medium matrix using 500 mg of resin in SPE-columns (see Fig. 5.3A). The effectiveness of the method was also evaluated for AMPA (see Fig. 5.3B). Under these conditions, glyphosate recoveries ranged from 69% to 77%, with glutamate removal percentages ranging from 77% to 90%. A similar trend was observed for AMPA, with recoveries between 68% and 74% and glutamate removal ranging from 67% to 90%. Notably, although glutamate removal remained high, the recoveries of glyphosate and AMPA dropped significantly compared to previous results. Whereas earlier recoveries consistently reached up to 95%, none of the current recoveries exceeded 80% within the tested concentration ranges.

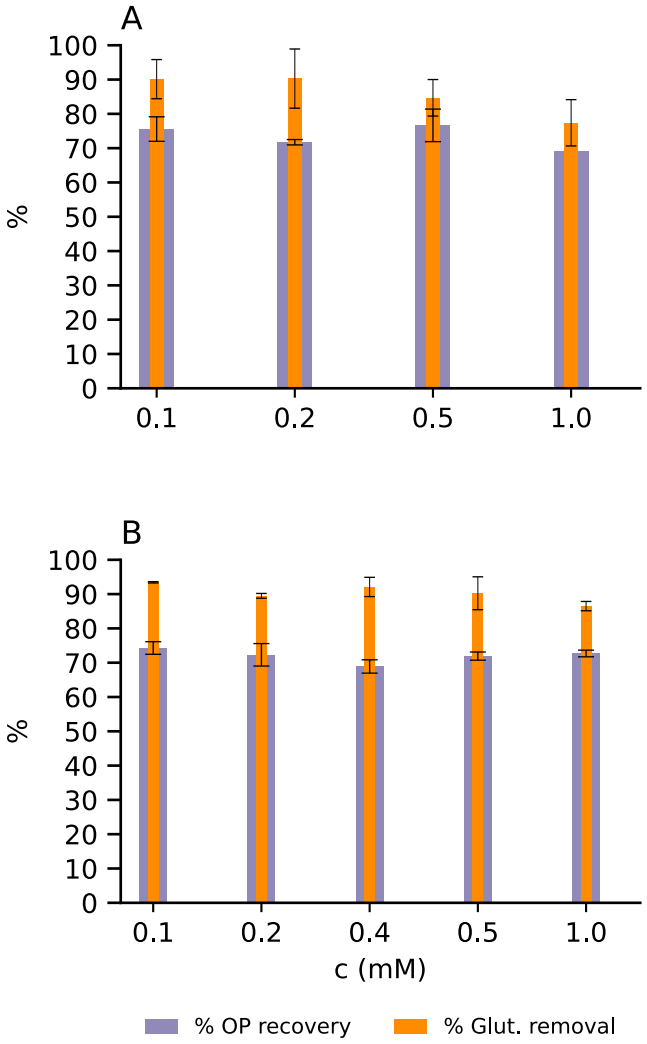

Figure 5.3 Recovery of organophosphonate (OP) (glyphosate or AMPA) and removal of glutamate following SPE treatment using 500 mg strong cation exchange resin (DOWEX® 50 WX8) at pH 1.5. (A) Glyphosate recovery (purple bars) and glutamate removal efficiency (orange bars). (B) AMPA recovery (blue

bars) and glutamate removal efficiency (orange bars). Recoveries were calculated by comparing nominal analyte concentrations to those measured after treatment. Glutamate removal efficiency represents the percentage decrease between initial and post-treatment glutamate concentrations. Error bars indicate deviations between duplicate samples.

Next, we assessed the validity of the method using real samples from a transformation experiment involving glyphosate or AMPA. In this experiment, glyphosate and AMPA were provided as the sole P-sources to strain *A*. Kg 19. During a 13-day glyphosate transformation experiment, approximately 52% of the glyphosate was transformed by strain *A*. Kg 19, resulting in a final glyphosate concentration of 0.4 mM. The concentration profiles are shown in Figure 5.4A (purple circles). In contrast, AMPA transformation occurred faster. By day 6, 67% of the provided AMPA was converted, with the remaining concentration around 0.2 mM. The corresponding concentration profiles before SPE-treatment are shown in Figure 4B (purple circles).

Samples from these experiments were then treated with SPE to remove glutamate. Glutamate removal ranged from 94% to 99% in glyphosate samples and consistently exceeded 99% in AMPA samples. However, analyte recoveries varied significantly. Glyphosate recovery ranged from 69% to 81%, whereas AMPA recovery was notably lower, not exceeding 55%. This suggests that although glutamate was effectively removed—especially in AMPA samples—the recovered concentrations of AMPA were much lower than expected based on results from medium-containing samples. Post-treatment concentrations are shown in Figures 5.4A and 5.4B (pink circles). One possible explanation for the reduced analyte recovery at later time points is the release of bacterial transformation products, which may interfere with the extraction process. However, this does not account for the low recovery observed even at the early stages of the experiment, suggesting that other factors may also be contributing to analyte loss.

In summary, while the column-SPE method was effective in reducing glutamate content in both glyphosate and AMPA transformation samples, significant losses of the target analytes were still observed. Therefore, a more selective method is needed to ensure organophosphonates are retained with high efficiency during sample processing and subsequent isotope analysis is not compromised.

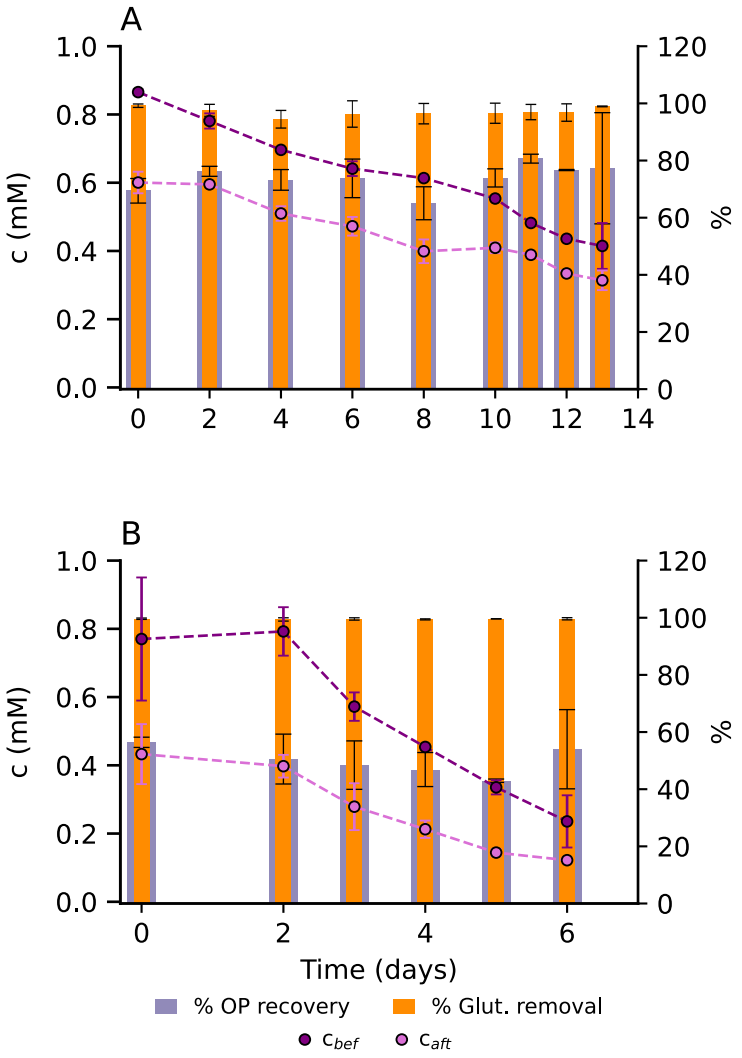

Figure 5.4 Transformation of organophosphonates (OP) A) glyphosate or B) AMPA by strain *A*. Kg 19 and recovery following SPE-column treatment using 500 mg strong cation exchange resin (DOWEX® 50 WX8) at pH 1.5. Circles indicate concentration profiles before (purple symbols) and after (pink symbols)

SPE treatment over the transformation experiment. Purple bars represent the percentage of OP recoveries, and orange bars show glutamate removal percentages. transformed at each time point. Recoveries were calculated by comparing nominal analyte concentrations to those measured after treatment. Glutamate removal efficiency represents the percentage decrease between initial and post-treatment glutamate concentrations. Error bars indicate deviations between duplicate samples.

Validation of glyphosate and AMPA purification samples via sorption to Al_2O_3

Next, we aimed to evaluate the efficiency of a different cleanup method that could potentially yield higher recoveries for glyphosate and AMPA, while also removing glutamate from the samples. For this purpose, we tested aluminum oxide (Al_2O_3) as a potential sorbent. Unlike cation exchange resin, which relies solely on ion exchange, Al_2O_3 offers additional interactions, including both electrostatic attraction and the formation of complexes between its surface and the target OPs, glyphosate, or AMPA. Glyphosate is known to bind strongly to aluminum oxide surfaces through several mechanisms (Vereecken, 2005; Purgel et al., 2009; Pereira et al., 2019). The adsorption process involves surface chemistry and molecular interactions such as ligand exchange, where the phosphonate group of glyphosate forms a stable inner-sphere complex by directly coordinating with aluminum atoms on the Al_2O_3 surface. This occurs as the phosphonate group replaces surface hydroxyl groups, while binding to the Al-sites. Electrostatic interactions also play a role, especially since the surface charge of Al_2O_3 and the ionization state of the analytes are both pH dependent. As shown in Table 5.1, glyphosate and AMPA can exist as zwitterionic or anionic species depending on the pH. Optimal adsorption takes place at pH values below the point of zero charge (pH_{pzc}) of Al_2O_3, which is equal to 9.0 (see SI, Fig. D5). Below this pH, the alumina surface is positively charged, which attracts the negatively charged phosphonate and carboxylate groups of glyphosate and AMPA, enhancing their retention. In contrast, glutamate does not contain a phosphonate group, so it is not expected to form similar complexes with Al_2O_3. Although glutamate also has negatively charged carboxylic acid groups at neutral pH, which could potentially interact with the alumina surface via electrostatic forces, these interactions are much weaker. Therefore, we attempted purification without acidifying the sample, relying on the selective retention of glyphosate and AMPA by Al_2O_3, while glutamate was largely excluded.

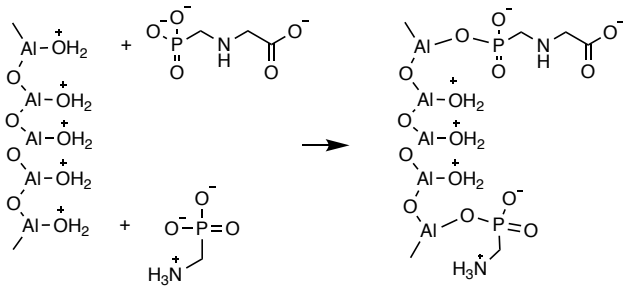

Figure 5.5 Schematic illustration of the adsorption mechanism of glyphosate and AMPA onto aluminum oxide (Al_2O_3) surfaces at pH = 7. The proposed mechanism involves the formation of stable inner-sphere complexes, where the phosphonic acid group of glyphosate, or AMPA, binds directly to positively charged surface aluminum (Al) sites, replacing surface hydroxyl groups on alumina. This interaction is facilitated by both ligand exchange and electrostatic attraction under near-neutral pH conditions.

To optimize the cleanup procedure, we first examined the effect of sorbent mass on glyphosate recovery from a medium matrix containing about 0.5 mM glyphosate. In this initial setup, 3 mL of the sample was treated using both batch and column methods, with sorbent amounts varying from 50 to 1000 mg. The desorption step was standardized for all samples, using 3 mL of 100 mM NaOH as the desorbing agent.

Figure 6 presents the concentrations of glyphosate before and after treatment, as well as the calculated recovery percentages and glutamate removal efficiencies for both batch and column treatments. The results from the batch experiments revealed that increasing the amount of Al_2O_3 sorbent led to a decrease in overall method efficiency. Specifically, with just 50 mg of sorbent, over 99% of glyphosate was recovered, and more than 95% of glutamate was removed. However, when the sorbent mass was increased to 100 mg, glyphosate recovery dropped sharply to below 13%, and glutamate removal efficiency fell to less than 70%. This decline in performance with higher sorbent masses can be attributed to the fixed volume of desorption agent: since only 3 mL of NaOH was used in all cases, larger amounts of Al_2O_3 likely required more desorption agent to effectively release the adsorbed glyphosate. In contrast, the column treatment showed consistently high glutamate removal efficiencies—always above 93%—regardless of the sorbent mass. Glyphosate recoveries after column treatment ranged from 26% to 84%, with the best results achieved using 250 or 500 mg of sorbent (approximately 84% glyphosate recovery and 93% glutamate removal). When 250 mg of Al_2O_3 was tested over a glyphosate concentration range of 0.1 to 1 mM, the method did not show improved performance, as glyphosate recoveries remained below 77% (see

SI, Fig. D6). Therefore, unlike previous results with cation exchangers, where column-SPE outperformed batch-SPE, these findings demonstrate that batch cleanup with Al_2O_3 is more effective for glyphosate samples than column-SPE under the tested conditions.

Although competitive anions such as sulfate present in the growth medium can reduce adsorption by occupying Al–OH sites due to electrostatic interaction, the method still performs well for glyphosate in the presence of the media matrix. Based on the excellent glyphosate recovery and glutamate removal observed with 50 mg of Al_2O_3 in batch treatment, this amount was selected for all subsequent experiments.

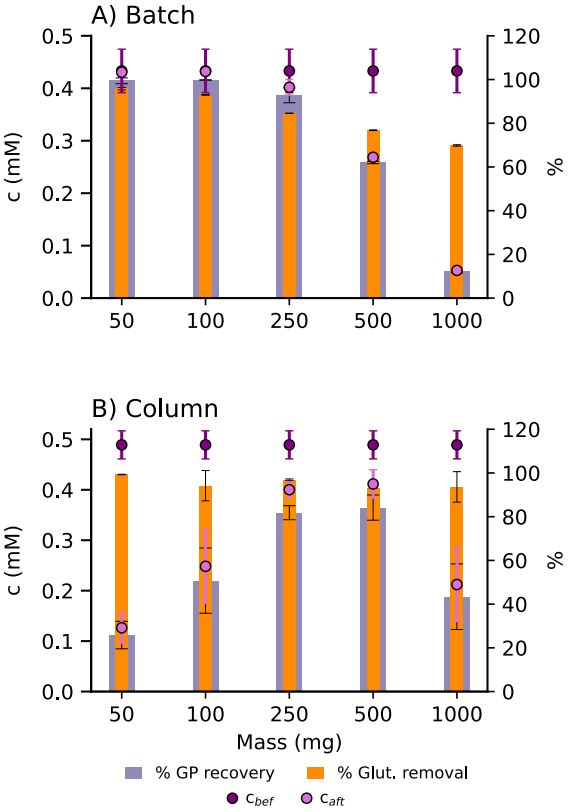

Figure 5.6 Effect of Al_2O_3 sorbent mass on glyphosate recovery and glutamate removal from a medium matrix containing glyphosate during A) Batch and B) SPE treatment. Circles indicate glyphosate concentrations before (purple symbols) and after (pink symbols) cleanup with varying amounts of Al_2O_3 (50–1000 mg). Purple bars represent glyphosate recovery percentages, while orange bars show glutamate removal efficiencies for each sorbent mass tested. Recoveries were calculated by comparing nominal glyphosate concentrations to those measured after cleanup. Glutamate removal efficiency represents the percentage decrease between initial and post-treatment glutamate concentrations. Error bars indicate deviations between duplicate samples.

Next, we aimed to evaluate the performance of the Al_2O_3 method for cleaning AMPA and glyphosate from used medium, simulating conditions representative of a real transformation experiment. To this end, we collected medium in which the transformation of 0.25 mM glyphosate had already occurred, ensuring that glyphosate was depleted and that the matrix closely reflected the composition expected in an actual experiment. The used medium was then spiked with 0.5 mM glyphosate or AMPA and subjected to cleanup, with the results shown in Figure 5.7. As observed previously, glutamate was efficiently removed—over 95%—and glyphosate and AMPA recoveries exceeded 76%. These results indicate that the method performs equally well for both compounds and that the presence of metabolites in the used medium did not significantly interfere with the method's performance compared to fresh medium.

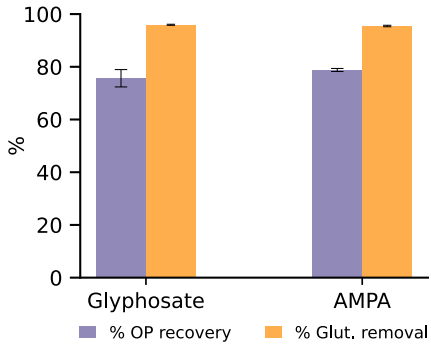

Figure 5.7 Recovery of the organophosphonates (OPs) glyphosate and AMPA from used medium using 50 mg of Al_2O_3 sorbent. Purple bars represent glyphosate and AMPA recovery percentages, while orange bars indicate glutamate removal efficiencies. Recoveries were calculated by comparing the nominal concentrations of glyphosate or AMPA to those measured after cleanup. Glutamate removal

efficiency reflects the percentage decrease between initial and post-treatment glutamate concentrations. Error bars show the variation between duplicate samples.

Next, the Al_2O_3 cleanup method was evaluated in a real transformation experiment involving the degradation of AMPA and glyphosate by strain *A*. Kg 19 (batch conditions, 50 mg Al_2O_3). The results, presented in Figures 8A and 8B, show that over the 27-day experimental period, both glyphosate and AMPA were continuously utilised by the strain, with transformation extents exceeding 92% by the end of the experiment.

Application of the cleanup method to samples from the glyphosate experiment resulted in recoveries consistently exceeding 77%, while glutamate removal efficiencies remained above 99% across all samples tested. Similarly, in the AMPA experiment, glutamate removal efficiencies exceeded 99% at all time points. However, AMPA recoveries varied more widely, ranging from 63% to 100%, indicating that the method was more effective for glyphosate than for AMPA. This difference is likely because AMPA lacks the carboxyl group present in glyphosate, relying solely on its phosphonate group for binding to Al_2O_3, which reduces its adsorption capacity.

Despite these differences in recovery, the cleaned samples were further analyzed to assess whether the recovered amounts of glyphosate and AMPA were sufficient for isotope analysis.

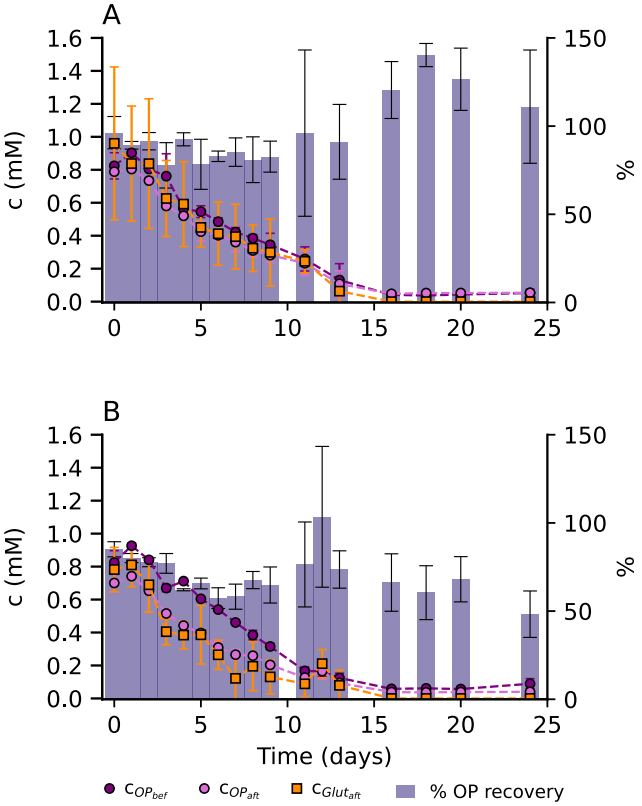

Figure 5.8 Transformation of organophosphonates (OP) A) glyphosate or B) AMPA by strain *A*. Kg 19 and recovery following treatment with 50 mg Al_2O_3. Circles (connected by lines) indicate concentration profiles prior to (purple symbols) and after (pink symbols) Al_2O_3-treatment over the transformation experiment. Orange squares (connected by lines) show the remaining glutamate concentration after Al_2O_3-treatment. Purple bars represent the percentage of OP recoveries. Recoveries were calculated by comparing nominal analyte concentrations to those measured after treatment. Glutamate removal efficiency represents the percentage decrease between initial and post-treatment glutamate concentrations. Error bars indicate deviations between duplicate samples.

Stable carbon isotope analysis of glyphosate and AMPA

To apply the developed Al_2O_3-cleanup method—based on the sorption of glyphosate and AMPA onto aluminum oxide surfaces—to real samples, isotope analysis was first established. As a key step, the limits of precise isotope analysis (LPIA) were determined for both glyphosate and AMPA (see Fig. 5.9). For glyphosate, a Shodex column (IC NI-424) provided the best chromatographic separation from other medium components, as indicated by distinct retention times (see SI, Fig. D1). In contrast, for AMPA, a Primesep 100 column was used, enabling effective separation as shown in SI, Figure D2.
The LPIAs were determined following the moving mean approach described by Jochmann et al. (2006). Standards of glyphosate and AMPA were analyzed in triplicate over a concentration range of 0.025–1 mM for glyphosate and 0.025–0.3 mM for AMPA. Isotopic signatures for glyphosate remained consistent (+-0.5‰) across the full concentration range tested, indicating no concentration-dependent effects. For AMPA, however, reliable and concentration-independent isotope values were only observed in the 0.1–0.3 mM range. At higher concentrations (0.3–1 mM), concentration-dependent effects on AMPA's isotopic signature were evident (see SI, Fig. D7). Although our LPIA values are higher than those reported by Kujawinski et al. (2013) (0.5 and 0.74 µg on column for glyphosate and AMPA, respectively), such differences can be attributed to variations in analytical methods and instrumentation.

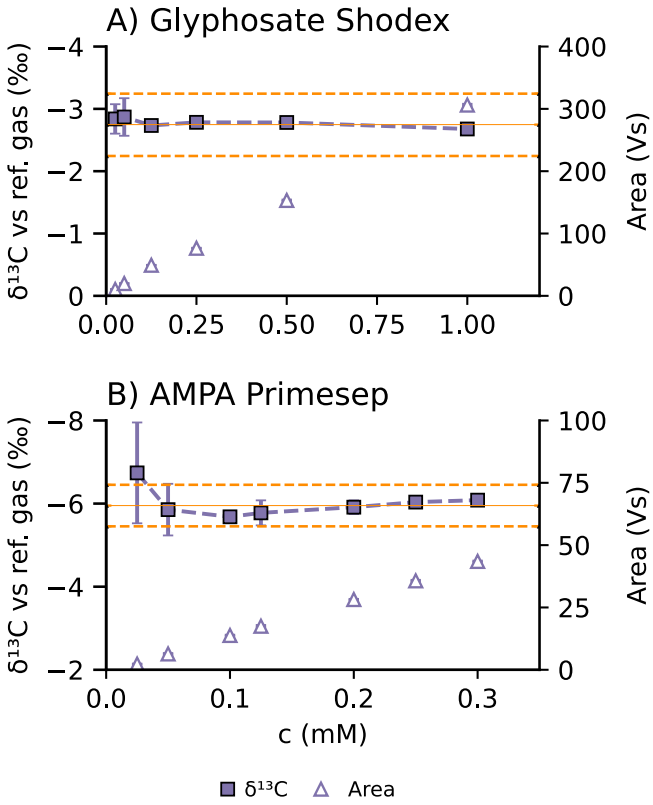

Figure 5.9 Linearity plots for (A) glyphosate (B) AMPA showing the dependency of the measured isotopic signature on the concentration of analyte. The solid line represents the mean isotopic signature of the four highest concentrations (0.025 to 1mM for glyphosate, 0.025 to 0.3 mM for AMPA) and the dashed lines marking the 0.5‰–range around this value, equal to the accepted error of the method. Standards were prepared in ultrapure water. Error bars correspond to the standard deviations of triplicate measurements.

The use of aluminum oxide (Al_2O_3) as a sorbent was evaluated for its effectiveness in selectively cleaning up samples with high glutamate content, which can cause matrix effects. This assessment was carried out using a sample from a glyphosate

transformation experiment. Specifically, a sample collected on day 1 from the experiment with strain *A*. Kg 19 was analyzed by LC-IRMS. Complete transformation curves for strain *A*. Kg 19, grown with either glyphosate or AMPA, are available in the SI, Figure D8.

After cleanup with Al_2O_3, the glyphosate concentration in the sample was 0.82 mM, and the sample was diluted fourfold (final concentration of 0.205 mM in microcosm 1, (MC1)) and acidified to pH≃3 before injection (concentrations before and after treatment are shown in Figure 5.8). As shown in Figure 5.10A, a clear glyphosate peak—comparable to the standard containing 0.25 mM glyphosate—was observed after Al_2O_3 treatment. The $\delta^{13}C$ values measured were −0.099 ± 0.080‰ for the sample and −0.114 ± 0.049‰ for the standard (n = 4), confirming the isotopic consistency of the analyte. Additionally, the difference in $\delta^{13}C$ values between the cleaned samples and the standard prepared in ultrapure water deviated by less than 0.5‰, implying that the method itself does not induce any isotope effects. In contrast, Figure 5.10B shows that, before cleanup, strong matrix effects prevented the detection of a distinct glyphosate peak.

These results demonstrate that Al_2O_3 treatment substantially reduced matrix effects, effectively removing glutamate and enabling reliable detection of glyphosate in the sample. Additionally, the difference in $\delta^{13}C$ values between the cleaned samples and the standard prepared in ultrapure water was less than 0.5‰. This indicates that the sorption and desorption of glyphosate on aluminum oxide do not introduce isotope effects that could alter the true carbon isotopic signatures of glyphosate or AMPA. These findings align with results from Röhnelt et al. (2023), who reported no isotope effects during the sorption and desorption of the aminodiphosphonate iminodi(methylene phosphonate) (IDMP) to and from manganese and aluminum oxide surfaces. Overall, the data presented here confirm the suitability of this cleanup method for effectively removing glutamate from glyphosate-containing samples, enabling accurate determination of carbon isotopic values.

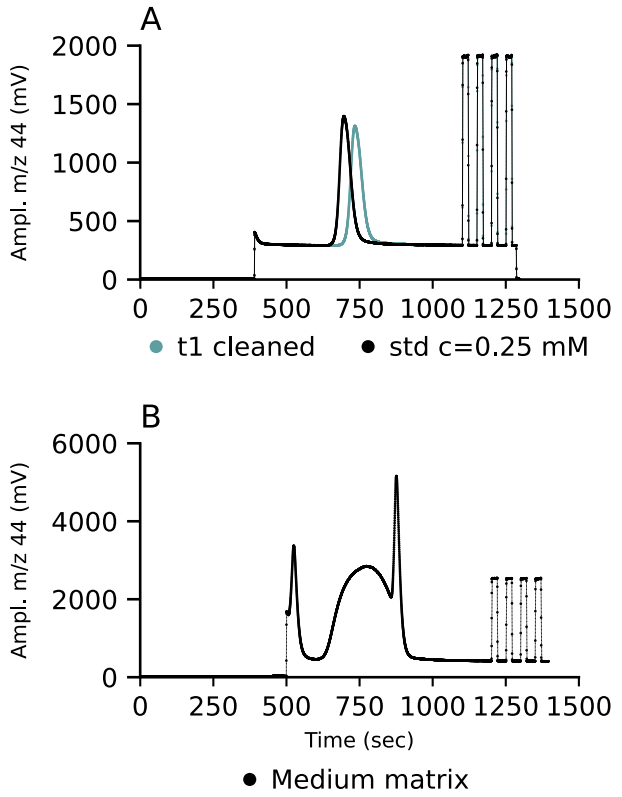

Figure 5.10 (A) Chromatogram of a glyphosate-containing sample (c_{final} = 0.205 mM) from day 1 of the transformation experiment with *A*. Kg 19 after Al_2O_3 cleanup, showing a distinct glyphosate peak comparable to a 0.25 mM glyphosate standard. (B) Chromatogram of the same sample before cleanup, illustrating the impact of matrix components—particularly glutamate—on analyte separation and suppression of the CO_2 signal. $\delta^{13}C$ (‰) values after acidification were −0.099 ± 0.080‰ for the sample (n=3) and −0.114 ± 0.049‰ for the standard (n = 4).

Analysis of the cleaned glyphosate samples (concentrations shown in Figure 5.8A) yielded chromatograms presented in Figure 5.11 for each microcosm for 11 days. All samples were diluted fourfold after Al_2O_3 cleanup and acidified with H_3PO_4 to pH~3. As shown in Figure 11, although minor shifts in glyphosate retention time were observed (780–901 s), clear glyphosate peaks were identified in most cases.

Importantly, no co-eluting peaks were detected that could interfere with glyphosate's $\delta^{13}C$ measurements especially as remaining glutamate levels were similar to glyphosate concentrations (for concentration profiles see Fig. 5.8A). Measured $\delta^{13}C$ values between day 0 and day 9 ranged from −0.6 to −0.3‰, indicating no significant carbon isotope fractionation during approximately 58% of glyphosate transformation. This contrasts with the substantial isotope fractionation reported by Ehrl et al. (2018), who observed an $\varepsilon^{13}C$ value of −4.5 ± 0.5‰ after 90% glyphosate transformation ($\Delta c<0.15$ mM). However, between day 9 and day 24, 94% of the added glyphosate was transformed. By this stage, residual glyphosate concentrations had dropped below 0.2 mM (see SI, Figure D8). After applying the required fourfold dilution, concentrations fell below the LPIA detection threshold for glyphosate (<0.05 mM), preventing reliable $\delta^{13}C$ analysis. Dilution was nevertheless essential. At day 11, analysis of undiluted samples (c=0.23 mM) yielded a $\delta^{13}C$ value of 5.78 ± 0.36‰, falsely indicating heavy isotope enrichment. However, this was due to co-elution: another peak overlapped with glyphosate, skewing the signal (see SI, Fig. D9). In contrast, diluted samples revealed more negative $\delta^{13}C$ values equal to −0.66 ± 0.71‰ (1:2 dilution) and −0.63 ± 0.12‰ (1:4 dilution), consistent with those obtained at early time points. Notably, no interfering peaks were observed at early time points. Since glutamate elutes before glyphosate in anion-exchange chromatography, the interfering peak observed at later stages was likely an unidentified bacterial transformation product.

Attempts to enrich glyphosate by desorbing it in half the volume used for sorption also led to co-enrichment of glutamate, making isotope analysis impossible at later time points when glyphosate transformation was extensive (see SI, Fig. D10). Overall, these results suggest that no significant isotope effects occurred during glyphosate biotransformation by strain *A*. Kg 19. However, it was not possible to assess $\delta^{13}C$ values at later time points—when more extensive transformation and potential isotope effects might occur—due to the low sensitivity of the analysis and the lack of an effective enrichment method.

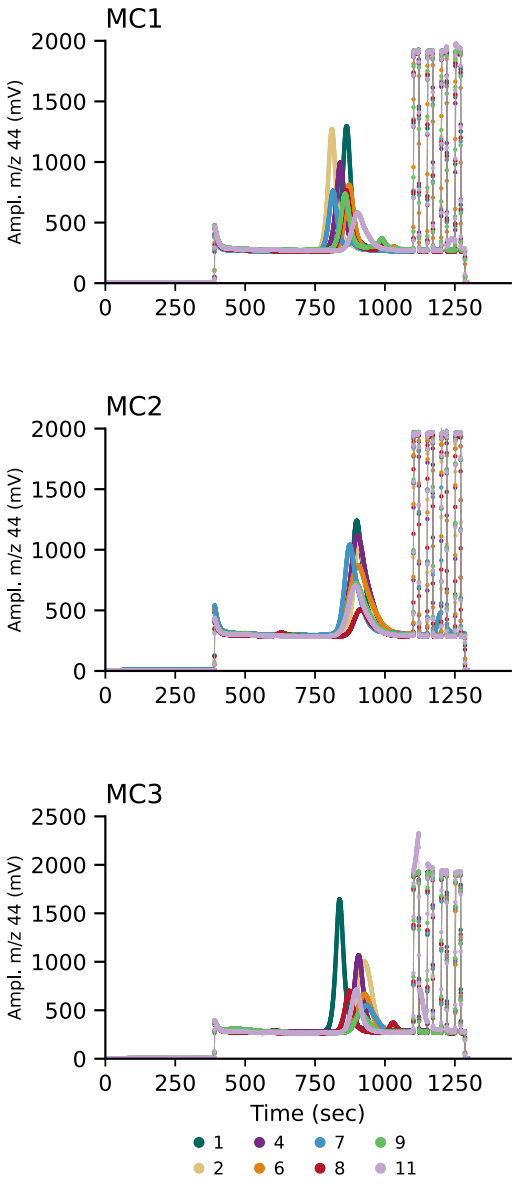
MC1
MC2
MC3
Ampl. m/z 44 (mV)
0
500
1000
1500
2000
2500
0
250
500
750
1000
1250
Time (sec)
1
2
4
6
7
8
9
11

Figure 5.11 LC-IRMS chromatograms (amplitude, m/z 44 over time) of glyphosate during 11-day transformation experiment by strain *A.* Kg 19 in microcosms MC1 (A), MC2 (B), and MC3 (C), shown across days 1 and 11. Chromatograms were acquired using a Shodex IC NI-424 column (4.6 × 100 mm) operated at pH 3.1. Glyphosate eluted between approximately 780 and 901 seconds. The four peaks at the end of each chromatogram correspond to the IRMS CO_2 reference gas used for signal calibration.

Chromatograms of the cleaned AMPA samples (concentrations shown in Figure 5.8B) were obtained for each microcosm across all time points (day 1 to day 6) as shown in Figure 5.12. To achieve baseline separation between AMPA (retention time ~350 s) and a nearby interfering peak (~450 s), the samples had to be diluted 5- to 8-fold: specifically, 5× for days 0 to 3, 8× for day 4, and 7× for days 5 and 6. Without this dilution, the peaks overlapped and could not be properly resolved.
Based on retention times from SI, Figure D2, glutamate elutes after AMPA when using the Primesep 100 column. As shown in Figure 5.8B, post-cleanup glutamate concentrations were similar to those of AMPA. This suggests that the recurring interfering peak observed after AMPA likely originated from residual glutamate that was not completely removed during sample cleanup. After cleanup, approximately 0.7 mM glutamate remained (~40 mg C/L), which is significantly higher than the carbon content originating from AMPA at the tested concentrations (e.g., <10 mg C/L, at day 0). Additionally, the necessary dilutions reduced AMPA concentrations below the lower performance isotope analysis (LPIA) threshold (0.1–0.3 mM) from day 3 onward. The $\delta^{13}C$ values measured between day 0 and day 3 ranged from -4.19 ± 0.39‰ to -3.93 ± 0.54‰, indicating no significant carbon isotope fractionation after 26% AMPA transformation occurring by day 3.
In summary, the applied cleanup protocol did not enable successful LC-IRMS analysis of AMPA. Interfering peaks close to the AMPA retention time prevented adequate baseline separation, and the necessary sample dilution lowered AMPA concentrations below the detection limit.

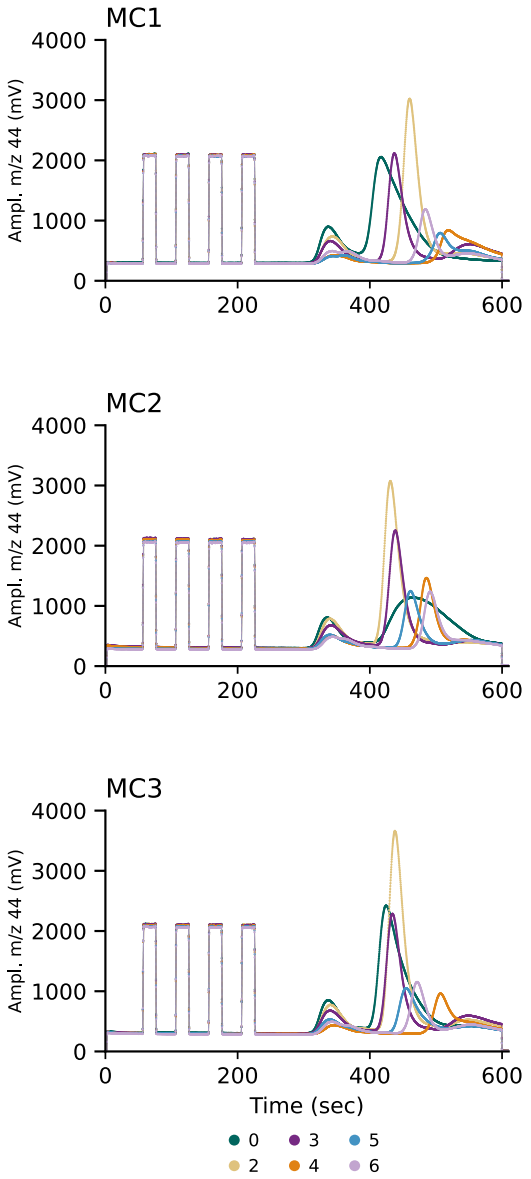
MC1
MC2
MC3
Ampl. m/z 44 (mV)
4000
3000
2000
1000
0
0
200
400
600
Time (sec)
0
2
3
4
5
6

Figure 5.12 LC-IRMS chromatograms (amplitude, m/z 44 over time) of AMPA during 6-day transformation experiment by strain *A*. Kg 19 in microcosms MC1 (A), MC2 (B), and MC3 (C), shown among days 0 and 6. Chromatograms were acquired using a Primesep 100 (P1QKO6HT) column (3.2 × 150 mm) operated at pH 1.9. AMPA and glutamate eluted at approximately 340 and 490 seconds, respectively. The four peaks at the beginning of each chromatogram correspond to the IRMS CO_2 reference gas used for signal calibration.

5.5 Implications

This study highlights key analytical advancements necessary for applying carbon-CSIA to the investigation of organophosphonate (OP) biotransformation. More specifically, it provides new insights into the applicability of two distinct cleanup methods aimed at reducing the carbon content from microbial growth media in experiments investigating the biotransformation of glyphosate and AMPA. By systematically evaluating and optimizing sample cleanup strategies, the research demonstrates that effective removal of interfering carbon sources, such as glutamate, is critical for accurate isotope analysis. The application of aluminum oxide as a sorbent achieved high glutamate removal and satisfactory OP recovery, representing a significant methodological improvement, which paves the way for tracking of carbon isotope effects associated with OP transformation. Additionally, the lack of significant isotope fractionation introduced by the cleanup process itself supports the method's compatibility with isotope-sensitive applications and strengthens confidence in the integrity of the analytical results. However, LC-IRMS analysis of cleaned samples revealed that while significant reductions in glutamate levels were achieved, the current approach still falls short of providing the selectivity and efficiency required to fully eliminate matrix effects that disturb accurate isotope signature determination. Specifically, persistent chromatographic challenges at later transformation stages were observed likely due to the presence of co-eluting metabolites and residual matrix components, underscoring the inherent complexity of working with real biotransformation samples.

Moreover, this work highlights a fundamental challenge: the low sensitivity of current LC-CSIA methods requires high analyte concentrations (≥1 mM) to enable time-resolved isotope analysis. While such concentrations may ensure signal detectability and allow for multiple sampling points, they may impair microbial activity, compromise biodegradation studies, and diverge from environmentally realistic scenarios. Therefore, future efforts must focus not only on refining cleanup procedures and improving chromatographic separation but also on enhancing method sensitivity to allow accurate CSIA at lower, more environmentally relevant concentrations. Ultimately, bridging these methodological and practical gaps will be essential to establishing CSIA as a viable tool for studying OP transformation under realistic conditions.

5.6 Outlook

Despite the challenges faced in this study, isotope analysis remains a valuable tool for investigating and characterizing degradation processes. To fully exploit the potential of CSIA in OP transformation studies, further optimization is required to improve chromatographic separation and mitigate interference from metabolites and residual media components at later stages of degradation. Integrating the aluminum oxide cleanup protocol with advanced separation strategies—such as multidimensional liquid chromatography (LC-LC) or even LC-LC-IRMS systems, as successfully demonstrated for other analytes like caffeine (Rockel et al., 2025)—could significantly improve the resolution of target compounds within complex bacterial growth media. Recent advances in high-resolution mass spectrometry, particularly Orbitrap isotope ratio mass spectrometry (Orbitrap-IRMS), can further aid in identifying and characterizing interfering components (Hofmann et al., 2020; Marks et al., 2022), guiding the development of more selective and efficient cleanup procedures. Exploring alternative carbon sources for microbial growth, such as glucose—which is structurally distinct from glyphosate—could also facilitate easier separation and minimize interference, addressing issues encountered with glutamate-based media. Moreover, the applicability of these improved methods should be tested across a wider range of OPs and in diverse, environmentally relevant matrices—such as soil, sediment, and natural waters—to ensure robustness and versatility. Addressing the challenge of working at lower, environmentally realistic concentrations will be essential for translating laboratory findings to real-world scenarios. This may involve developing more sensitive detection platforms or pre-concentration steps to allow accurate isotope analysis at trace levels without compromising microbial activity or environmental relevance.

Ultimately, these methodological advancements will not only enable more precise and reliable tracking of carbon isotope effects during OP biotransformation but also open new avenues for investigating the fate and transformation mechanisms of these persistent pollutants in complex environmental systems. Such insights are critical for improving risk assessment, guiding regulatory decisions, and informing the development of more effective management and remediation strategies for OP-contaminated environments.

5.7 References

Bakkour, R., Bolotin, J., Sellergren, B., & Hofstetter, T. B. (2018). Molecularly Imprinted Polymers for Compound-Specific Isotope Analysis of Polar Organic Micropollutants in Aquatic Environments. *Analytical Chemistry*, *90*(12), 7292–7301. https://doi.org/10.1021/acs.analchem.8b00493

Bakkour, R., Wabnitz, C., & Glöckler, D. (2024). Lack of selectivity in sample preparation – An achilles heel of compound-specific isotope analysis for environmental micropollutants. *TrAC - Trends in Analytical Chemistry*, *180*(March). https://doi.org/10.1016/j.trac.2024.117908

Bento, C. P. M., Yang, X., Gort, G., Xue, S., van Dam, R., Zomer, P., Mol, H. G. J., Ritsema, C. J., & Geissen, V. (2016). Persistence of glyphosate and aminomethylphosphonic acid in loess soil under different combinations of temperature, soil moisture and light/darkness. *Science of the Total Environment*, *572*, 301–311. https://doi.org/10.1016/j.scitotenv.2016.07.215

Ehrl, B. N., Mogusu, E. O., Kim, K., Hofstetter, H., Pedersen, J. A., & Elsner, M. (2018). High Permeation Rates in Liposome Systems Explain Rapid Glyphosate Biodegradation Associated with Strong Isotope Fractionation. *Environmental Science and Technology*, *52*(13), 7259–7268. https://doi.org/10.1021/acs.est.8b01004

Elsner, M., & Imfeld, G. (2016). Compound-specific isotope analysis (CSIA) of micropollutants in the environment - current developments and future challenges. *Current Opinion in Biotechnology*, *41*(Table 1), 60–72. https://doi.org/10.1016/j.copbio.2016.04.014

Glöckler, D., Wabnitz, C., Elsner, M., & Bakkour, R. (2023). Avoiding Interferences in Advance: Cyclodextrin Polymers to Enhance Selectivity in Extraction of Organic Micropollutants for Carbon Isotope Analysis. *Analytical Chemistry*, *95*(20), 7839–7848. https://doi.org/10.1021/acs.analchem.2c05465

Hofmann, A. E., Chimiak, L., Dallas, B., Griep-Raming, J., Juchelka, D., Makarov, A., Schwieters, J., & Eiler, J. M. (2020). Using Orbitrap mass spectrometry to assess the isotopic compositions of individual compounds in mixtures. *International Journal of Mass Spectrometry*, *457*, 116410. https://doi.org/10.1016/j.ijms.2020.116410

Hofstetter, T. B., Bakkour, R., Buchner, D., Eisenmann, H., Fischer, A., Gehre, M., Haderlein, S. B., Höhener, P., Hunkeler, D., Imfeld, G., Jochmann, M. A., Kümmel, S., Martin, P. R., Pati, S. G., Schmidt, T. C., Vogt, C., & Elsner, M. (2024). Perspectives of compound-specific isotope analysis of organic contaminants for assessing environmental fate and managing chemical pollution. *Nature Water*, *2*(1), 14–30. https://doi.org/10.1038/s44221-023-00176-4

Kourtaki, K., Buchner, D., Martin, P. R., Thompson, K., & Haderlein, S. B. (2025). Influence of organophosphonates as alternative P-sources on bacterial

transformation of glyphosate. *Environmental Pollution*, 125872. https://doi.org/https://doi.org/10.1016/j.envpol.2025.125872

Kujawinski, D. M., Wolbert, J. B., Zhang, L., Jochmann, M. A., Widory, D., Baran, N., & Schmidt, T. C. (2013). Carbon isotope ratio measurements of glyphosate and AMPA by liquid chromatography coupled to isotope ratio mass spectrometry. *Analytical and Bioanalytical Chemistry*, *405*(9), 2869–2878. https://doi.org/10.1007/s00216-012-6669-0

Li, H., Joshi, S. R., & Jaisi, D. P. (2016). Degradation and Isotope Source Tracking of Glyphosate and Aminomethylphosphonic Acid. *Journal of Agricultural and Food Chemistry*, *64*(3), 529–538. https://doi.org/10.1021/acs.jafc.5b04838

Limon, A. W., Moingt, M., & Widory, D. (2020). The carbon stable isotope compositions of glyphosate and aminomethylphosphonic acid (AMPA): Improved analytical sensitivity and first application to environmental water matrices. *Rapid Communications in Mass Spectrometry*, *35*(5), 1–10. https://doi.org/10.1002/rcm.9017

Marks, R. G. H., Jochmann, M. A., Brand, W. A., & Schmidt, T. C. (2022). How to Couple LC-IRMS with HRMS─A Proof-of-Concept Study. *Analytical Chemistry*, *94*(6), 2981–2987. https://doi.org/10.1021/acs.analchem.1c05226

Martin, P. R., Buchner, D., Jochmann, M. A., & Haderlein, S. B. (2020). Stable carbon isotope analysis of polyphosphonate complexing agents by anion chromatography coupled to isotope ratio mass spectrometry: method development and application. *Analytical and Bioanalytical Chemistry*, *412*(20), 4827–4835. https://doi.org/10.1007/s00216-019-02251-w

Mogusu, E. O. (2015). Compound Specific Isotopic Analysis To Investigate Sources and degradation of glyphosate. Dissertation.

Pereira, E. A. O., Melo, V. F., Abate, G., & Masini, J. C. (2019). Adsorption of glyphosate on Brazilian subtropical soils rich in iron and aluminum oxides. *Journal of Environmental Science and Health - Part B Pesticides, Food Contaminants, and Agricultural Wastes*, *54*(11), 906–914. https://doi.org/10.1080/03601234.2019.1644947

Popov, K., Rönkkömäki, H., & Lajunen, L. H. J. (2001). Critical evaluation of stability constants of phosphonic acids (IUPAC Technical Report). *Pure Appl. Chem.*, *73*(10), 1641–1677.

Purgel, M., Takács, Z., Jonsson, C. M., Nagy, L., Andersson, I., Bányai, I., Pápai, I., Persson, P., Sjöberg, S., & Tóth, I. (2009). Glyphosate complexation to aluminium(III). An equilibrium and structural study in solution using potentiometry, multinuclear NMR, ATR-FTIR, ESI-MS and DFT calculations. *Journal of Inorganic Biochemistry*, *103*(11), 1426–1438. https://doi.org/10.1016/j.jinorgbio.2009.06.011

Redfield, A. C. (1958). The biological control of chemical factors in the environment. *American Scientist, 46*(3), 205–221.

Rockel, S. P., Marks, R. G. H., Kerpen, K., Jochmann, M. A., & Schmidt, T. C.

(2025). Two-Dimensional Liquid Chromatography-Isotope Ratio Mass Spectrometry Opens New Possibilities in the Field of Compound-Specific Stable Isotope Analysis. *Analytical Chemistry*. https://doi.org/10.1021/acs.analchem.4c05956

Röhnelt, A. M., Martin, P. R., Buchner, D., & Haderlein, S. B. (2023). Transformation of Iminodi(methylene phosphonate) on Manganese Dioxides - Passivation of the Mineral Surface by (Formed) Mn2+. *Environmental Science and Technology*, *57*(32), 11958–11966. https://doi.org/10.1021/acs.est.3c01838

Röhnelt, A. M., Martin, P. R., Marks, R. G. H., Buchner, D., Weiss, J., Schmidt, T. C., & Haderlein, S. B. (2025). Green quantification of amino(poly)phosphonates using ion chromatography coupled to integrated pulsed amperometric detection. *Analytical and Bioanalytical Chemistry*, *417*(8), 1581–1594. https://doi.org/10.1007/s00216-025-05747-w

Šarac, B., & Hadži, S. (2021). Analysis of Protonation Equilibria of Amino Acids in Aqueous Solutions Using Microsoft Excel. *Journal of Chemical Education*, *98*(3), 1001–1007. https://doi.org/10.1021/acs.jchemed.0c01144

Schwientek, M., Rügner, H., Haderlein, S., Schulz, W., Wimmer, B., Engelbart, L., Bieger, S., & Huhn, C. (2024). Glyphosate contamination in European rivers not from herbicide application? *Research Square*, *263*(May), 1–18. https://doi.org/10.1016/j.watres.2024.122140

Sidoli, P., Baran, N., & Angulo-Jaramillo, R. (2016). Glyphosate and AMPA adsorption in soils: laboratory experiments and pedotransfer rules. *Environ. Sci. Pol. Res.*, *23*(6), 5733–5742. https://doi.org/10.1007/s11356-015-5796-5

Sprankle, P., Meggitt, W. F., & Penner, D. (1975). *Adsorption, Mobility, and Microbial Degradation of Glyphosate in the Soil*. *23*(3), 224–228. JSTOR, http://www.jstor.org/stable/4042279.

Torrentó, C., Bakkour, R., Glauser, G., Melsbach, A., Ponsin, V., Hofstetter, T. B., Elsner, M., & Hunkeler, D. (2019). Solid-phase extraction method for stable isotope analysis of pesticides from large volume environmental water samples. *The Analyst*, *144*(9), 2898–2908. https://doi.org/10.1039/c9an00160c

Vereecken, H. (2005). Mobility and leaching of glyphosate: A review. *Pest Management Science*, *61*(12), 1139–1151. https://doi.org/10.1002/ps.1122

Wimmer, B., Neidhardt, H., Schwientek, M., Haderlein, S. B., & Huhn, C. (2022). Phosphate addition enhances alkaline extraction of glyphosate from highly sorptive soils and aquatic sediments. *Pest Management Science*, *78*(6), 2550–2559. https://doi.org/10.1002/ps.6883

General Conclusion and Outlook

Conclusion

This dissertation advances understanding of the biodegradability of amino(poly)phosphonate (A(P)P) compounds, which is critical for assessing their environmental fate and persistence. The identification of key factors that shape the transformation potential of A(P)Ps aims to extend and refine existing knowledge in this field. More specifically:

- Chapter 2 examined how competing P-sources affect glyphosate biotransformation by two bacterial strains, using amino-mono- and diphosphonates alongside glyphosate as phosphorus (P) sources.
- Chapter 3 explored the impact of mineral sorption on biodegradation, using goethite as a model mineral phase, with a focus on glyphosate and AMPA—both commonly aminomonophosphonates detected in soils.
- Chapter 4 assessed the effect of common media matrix while investigating the biodegradability of APPs, using ATMP and EDTMP as model compounds due to their widespread use and frequent detection in wastewater treatment plant effluents.
- Chapter 5 applied cleanup techniques for enabling carbon compound-specific isotope analysis (CSIA) to investigate potential isotope fractionation effects during bacterial degradation of glyphosate and AMPA.

The main findings of each chapter are summarized as follows:

i) Chapter 2 demonstrated that both the presence and structure of coexisting P-sources can influence glyphosate's biodegradation potential. Glyphosate was preferred over the aminodiphosphonates IDMP and HEDP. However, when an aminomonophosphonate (AP) was provided alongside glyphosate as a P-source, glyphosate became the least preferred substrate. Its transformation occurred either after the second source was depleted (when supplied in excess) or simultaneously but at a slower rate (when glyphosate and a second AP were provided at equimolar concentrations). This pattern was consistent for AMPA, AEP, and PPA. Given the widespread presence of AMPA and other APs, these findings suggest that coexisting APs—serving as alternative P-sources for bacteria—can significantly reduce glyphosate's biodegradation, resulting in lower transformation rates than those reported in previous studies.

ii) Chapter 3 showed that the common ironoxyhydroxide goethite has a pronounced ability to adsorb both glyphosate and AMPA. When glyphosate and AMPA were present together, competitive sorption occurred, with glyphosate exhibiting a greater affinity for the goethite surface than AMPA. Biotransformation of glyphosate and AMPA in the presence of goethite revealed rapid depletion of both compounds from aqueous as well as sorbed phase when individually or in parallel supplied as P-sources. These findings strongly suggest that sorbed fractions of glyphosate and AMPA were highly bioavailable to the bacterial strain and that the sorption process did not limit their biodegradation.

iii) Chapter 4 examined the effect of common media matrix on higher APPs when studying their biotransformation potential by strain *A*. Kg 19. The results demonstrated that ATMP and EDTMP underwent rapid transformation in biotic as well as abiotic setups. Follow-up experiments with ATMP identified dissolved manganese (Mn(II)), present in the trace metal solution of the growth medium, as the key factor driving this abiotic breakdown. The detection of IDMP and orthophosphate (o-PO_4^{3-}) as transformation products confirmed the purely chemical degradation. These findings suggest that conventional methods for studying APP biodegradability may not be suitable for compounds like ATMP, due to overlapping abiotic and potential biotic processes. This represents a critical limitation of prior biodegradation studies, which likely overlooked the impact of Mn(II) and, as a result, overestimated the microbial contribution to APP degradation.

iv) Chapter 5 explored the development of a cleanup technique for studying isotope effects during bacterial transformation of glyphosate and AMPA. Because CSIA has limited sensitivity and growth media contribute a high carbon background, the work aimed at eliminating the glutamate content. A strong cation-exchange resin at acidic pH selectively removed glutamate while retaining glyphosate and AMPA in solution, but residual carbon still exceeded reliable CSIA thresholds. In contrast, aluminum oxide sorbent, exploiting surface complexation via phosphonic acid groups, performed better and proved more suitable for isotope analysis. Preliminary CSIA indicated no isotope fractionation during cleanup or early transformation, though at later stages, co-eluting products and residual glutamate impaired resolution and accuracy. These findings demonstrate the potential of carbon-CSIA for studying OP biotransformation, while emphasizing the need for more robust cleanup strategies to minimize matrix interferences.

6 General Conclusion and Outlook

Overall, this research has provided valuable insights into the biodegradability of APs and APPs under laboratory conditions. By investigating key factors such as substrate competition and mineral sorption, we have advanced our understanding of the biodegradation potential of compounds like glyphosate and AMPA, particularly in natural environments where these conditions are relevant. Although the biodegradation of glyphosate under P-limiting conditions has been extensively studied, our findings show that the presence of alternative P-sources — such as AMPA or AEP — can suppress glyphosate transformation. This suggests that microbial preference for other, more readily degradable P-sources may limit glyphosate degradation in complex environments. Interestingly, our experiments revealed that AMPA was more readily transformed by the tested bacterial strains, challenging common assumptions about its relative resistance to biodegradation.

Traditionally, sorption to mineral surfaces such as iron (oxyhydr)oxides has been considered a key factor in the accumulation of AMPA, as it was thought to reduce its bioavailability. In our study, we observed competitive sorption between glyphosate and AMPA, with glyphosate showing a stronger affinity for goethite. Although sorption processes influence the distribution of these compounds in soils, our results demonstrated that goethite did not hinder their biotransformation. Both glyphosate and AMPA remained bioavailable even when strongly sorbed, and transformation rates were unchanged compared to mineral-free controls. These findings show that biotransformation rates under the studied conditions were not determined by sorption affinity and that microbial processes effectively acted on both aqueous and sorbed phases.

Furthermore, this work also improved our understanding of the biodegradability of APPs. Besides the growing body of literature showing biodegradation in complex media matrices, our results revealed the flaw that transformation is driven abiotically by the presence of Mn(II). This calls for repetition of studies accounting for the interfering role of Mn(II). Our findings also imply that APPs can be more susceptible to abiotic breakdown because of Mn(II) or manganese oxides than bacterial involvement.

The data of cleanup and isotope analysis demonstrated that reliable isotope analysis of OP biotransformation is feasible, but requires further method refinement, particularly to handle late-stage transformation products. These developments are essential to better understand isotope effects during AP biodegradation, which remain underexplored despite the compounds' environmental relevance.

6 General Conclusion and Outlook

Outlook

The findings and hypotheses developed in this study open promising directions for advancing our understanding of A(P)P biodegradability. The observed dependence of glyphosate biodegradability on competing P-substrates such as APs represents only one aspect of it and can be further expanded to examine the effect of various P-containing compounds on it. Future work can broaden this perspective by systematically testing a wider range of P-containing compounds and evaluating how nutrient availability shapes degradation dynamics. Beyond P, the influence of different C-sources and the potential utilization of A(P)Ps themselves as C-substrates warrant further exploration. These questions are key to uncovering the true metabolic versatility of microbial communities facing A(P)Ps in diverse environments.

Furthermore, while this dissertation provides critical insights through pure-strain, laboratory-based experiments, the next step lies in moving toward greater ecological relevance. Real environments are shaped not only by isolated strains but by complex microbial communities where synergistic interactions, antagonism, and cometabolism strongly influence transformation processes. Including such communities in future experiments will bridge the gap between controlled laboratory conditions and natural systems. Similarly, incorporating additional mineral sorbents and, ultimately, real soil matrices will help better represent biodegradation processes held in environmental compartments composed of multiple interacting sorbents. This will provide a more accurate picture of how A(P)Ps behave in soils and sediments over long timescales.

In addition, this dissertation contributes to clarifying APP biodegradability by disentangling the interplay of abiotic and biotic reactions in common cultivation media driven by the presence of Mn(II). The next stage of research should be devoted to experimental designs that rigorously separate these processes, allowing biodegradability to be assessed with far greater certainty. Once these conditions are established, integrating isotope analysis will be crucial—not only to trace transformation pathways, but also to determine whether A(P)Ps such as glyphosate found in the environment exist as transformation products of APPs or by their direct release.

Ultimately, these future investigations will do more than resolve methodological questions: they will help clarify the environmental fate of a class of compounds whose persistence has long been underestimated. In light of recent findings that glyphosate and AMPA—both of major ecological concern—can emerge as breakdown products of APPs, it is now more urgent than ever to refine our knowledge. By expanding into more complex systems, applying advanced analytical tools, and connecting mechanistic insights to environmental scales, the

next generation of studies has the potential to reshape our understanding of A(P)P persistence and inform more effective environmental risk assessments and management strategies.

A Supporting information to chapter 2

Table A1. Media composition for the cultivation of the *Achromobacter insolitus* strain Kg 19 (VKM B-3295) (hereafter will be referred to as *A*. Kg 19).

Compound	**Empirical formula**	**Concentration**
Monosodium glutamic acid (glutamate)	$C_5H_9NNaO_4^+$	10 g L^{-1}
Ammonium chloride	NH_4Cl	2 g L^{-1}
Potassium sulfate	K_2SO_4	0.5 g L^{-1}
Magnesium sulfate heptahydrate	$MgSO_4$ * 7 H_2O	0.2 g L^{-1}
3-(morpholino)propanesulfonic acid (MOPS)	$C_7H_{15}NO_4S$	50 mmol L^{-1}
Sodium hydroxide for pH adjustment	NaOH (stock 1 mol L^{-1})	-
7-Vitamin solution		1 mL L^{-1}
Zinc sulfate heptahydrate	$ZnSO_4$ * $7H_2O$	20 mg L^{-1}
Calcium chloride hexahydrate	$CaCl_2$*6 H_2O	10 mg L^{-1}
Iron sulfate heptahydrate	$FeSO_4$ * $7H_20$	2.5 mg L^{-1}
Copper sulfate pentahydrate	$CuSO_4$ * $5H_2O$	2 mg L^{-1}
Manganese sulfate monohydrate	$MnSO_4$ * H_20	1 mg L^{-1}
Sodium molybdate	Na_2MoO_4	0.3 mg L^{-1}
Boric acid	H_3BO_3	0.06 mg L^{-1}
Nickel chloride hexahydrate	$NiCl_2$ * $6H_2O$	0.05 mg L^{-1}

Table A2. Media composition for the cultivation of the *Ochrobactrum pituitosum* strain GPr1-13 (hereafter will be referred to as *O*. GPr1-13).

Compound	**Empirical formula**	**Concentration**
Monosodium glutamic acid (glutamate)	$C_5H_9NNaO_4^+$	10 g L^{-1}
Ammonium chloride	NH_4Cl	5 g L^{-1}
Potassium sulfate	K_2SO_4	0.5 g L^{-1}

Magnesium sulfate heptahydrate	$MgSO_4$ * 7 H_2O	0.16 g L^{-1}
Calcium chloride dihydrate	$CaCl_2$*2 H_2O	0.08 g L^{-1}
3-(morpholino)propanesulfonic acid (MOPS)	$C_7H_{15}NO_4S$	50 mmol L^{-1}
Sodium hydroxide for pH adjustment	NaOH (stock 1 mol L^{-1})	-
7-Vitamin solution		1 mL L^{-1}

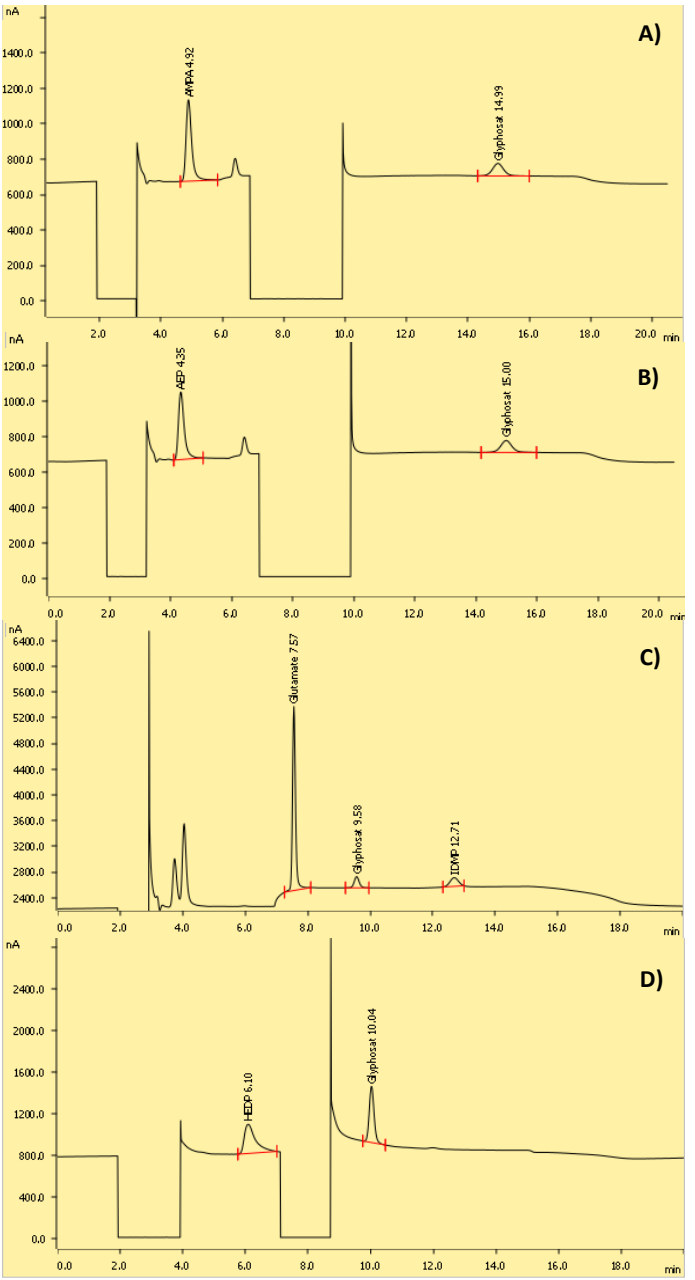
A)
nA
AMPA 4.92
Glyphosat 14.99
min
B)
AEP 4.35
Glyphosat 15.00
C)
Glutamate 7.57
Glyphosat 9.58
IDMP 12.71
D)
HEDP 6.10
Glyphosat 10.04

Figure A1. Exemplary chromatograms (retention time (R.T.) (min) versus current (nA)) of N-(phosphonomethyl)glycine (glyphosate) ((R.T.) 15.37 min) quantification in presence of (A) (Aminomethylphosphonate) AMPA (R.T. 5.40 min), (B) 2-aminoethylphosphonate (AEP) (R.T 4.35 min), (C) iminodi(methylene phosphonate) (IDMP) (R.T 12.71 min) or (D) 1-hydroxyethane-1,1-diphosphonate (HEDP) (R.T 6.10 min) as P-sources and glutamate as the carbon-source (R.T. 8.93) using ion chromatography with electrochemical detection (IC-ECD) with a flow gradient (see Tables S4 and S5).

Table A3. FlexiPAD detection method for quantification of all phosphonates tested as P-sources using IC-ECD.

FlexiPAD Detection method			
Duration (ms)	**Sum of duration (ms)**	**Starting potential (V)**	**Ending potential (V)**
370	370	0.0	0.0
150	520	0.0	0.25
110	630	0.25	0.25
120	750	0.25	0.0
50	800	0.0	0.0
40	840	-1.0	-1.0
60	900	0.6	0.6

Table A4. Flow gradient method used for the quantification of glyphosate, AMPA, AEP and glutamate using IC-ECD.

Time (min)	**Flow gradient (mL min^{-1})**	**Curve**
Start	0.4	
6.0	0.8	Step
17.5	0.8	Linear
18.0	0.4	Linear
20.5	0.4	Linear

Table A5. Flow gradient method used for the quantification of IDMP, HEDP but also of glyphosate when tested in parallel to IDMP or HEDP as P-sources.

Time (min)	Flow gradient (mL min^{-1})	Curve
Start	0.4	
7.0	1.2	Step
15.0	1.2	Linear
18.0	0.4	Linear
20.0	0.4	Linear

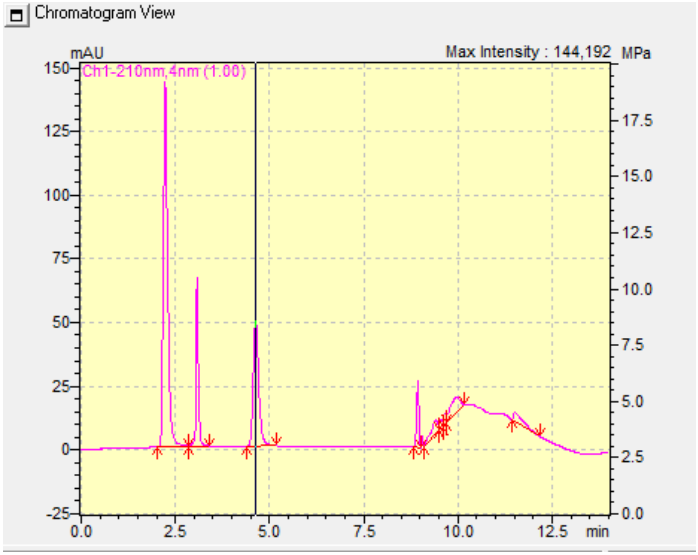

Figure A2. Exemplary chromatogram (retention time (R.T.) (min) versus absorbance units (mAu)) of phenylphosphonate (PPA) (R.T. 4.7 min) using HPLC-UV/vis with a flow gradient (see Table S6).

Table A6. Eluent gradient method used for the quantification of PPA by HPLC-UV/vis.

Gradient of eluent B (5 % water + 0.1 % H3PO4 in acetonitrile)		
Time (min)	**Gradient (%)**	**Curve**
Start	5	
5.0	5	
6.0	95	Linear
8.0	95	
8.5	5	Linear
14.0	5	

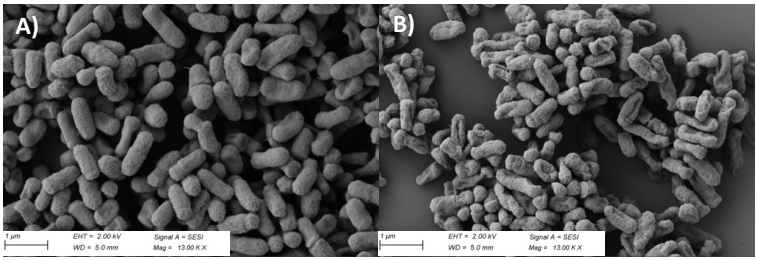

Figure A3. Scanning Electron Microscopy (SEM) images of (A) *A*. Kg 19 and (B) *O*. GPr1-13.

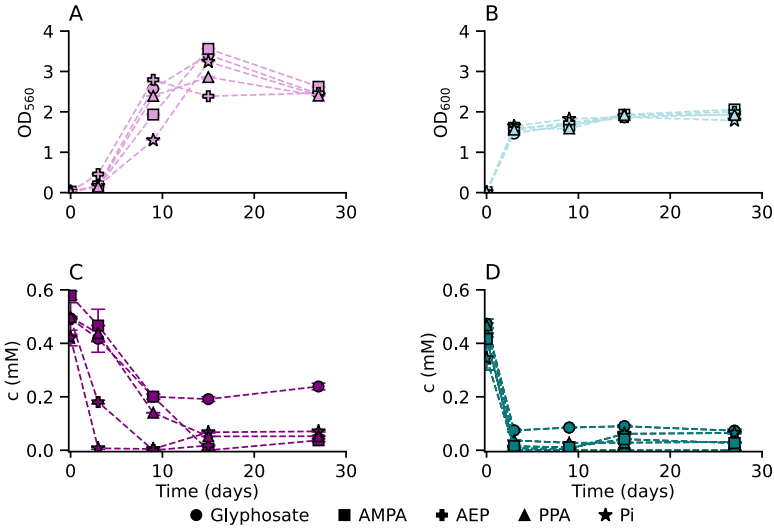

Figure A4. A, B) Optical density as well as C, D) concentration of glyphosate, AMPA, AEP, or inorganic phosphate (Pi) over time in cultures with *A*. Kg 19 (purple symbols) and *O*. GPr1-13 (green symbols). Glyphosate (circles connected by lines), AMPA (squares connected by lines), AEP (crosses connected by lines), PPA (triangles connected by lines) and Pi (stars connected by lines) were provided to the strains at 0.5 mM as sole P-sources. Error bars represent the standard deviation of duplicate cultures (if not visible, error bars are smaller than the data points)

Table A7. Summary of organophosphonate (OP) and Pi transformation rates by *A*. Kg 19 and *O*. GPr1-13 calculated either between day 0 and 3 (black color) or between 3 and 9 (brown color).

Transformation rates (mM day^{-1})		
Experimental setup	**Strain *A*. Kg 19**	**Strain *O*. GPr1-13**
Glyphosate	0.036 ± 0.001	≥ 0.133 ±0.009
AMPA	0.044 ±0.015	≥ 0.134 ±0.006
AEP	0.104 ±0.006	≥ 0.143 ±0.010
PPA	0.050 ±0.003	≥ 0.144 ±0.001
Pi	≥ 0.137 ±0.011	≥ 0.112 ±0.013

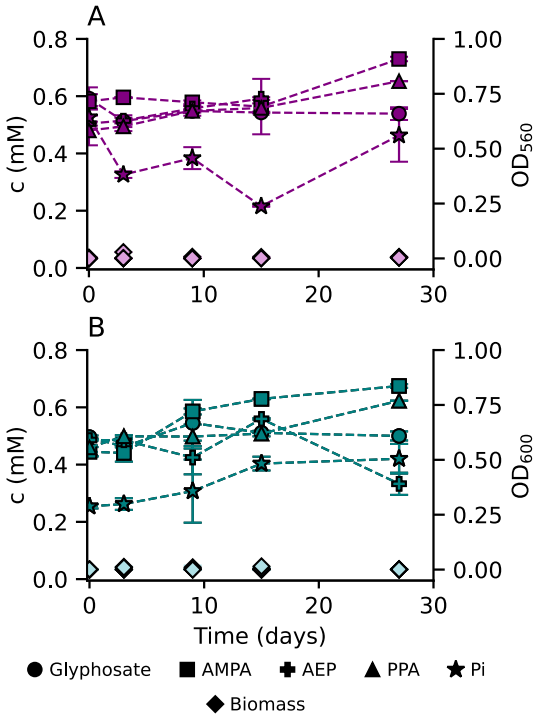

Figure A5. Glyphosate, AMPA, AEP, and Pi concentration in non-inoculated abiotic controls, and optical density over time in biotic P-free cultures. Glyphosate (circles connected by lines), AMPA (squares connected by lines), AEP (crosses connected by lines), PPA (triangles connected by lines) and Pi (stars connected by lines) were added at 0.5 mM in abiotic controls in media of A) *A*. Kg 19 (purple symbols) and B) *O*. GPr1-13 (green symbols). Diamonds represent optical density in biotic P-free controls of A) *A*. Kg 19 (purple symbols) and B) *O*. GPr1-13 (green symbols). Error bars represent the standard deviation of duplicate setups (if not visible, error bars are smaller than the data points).

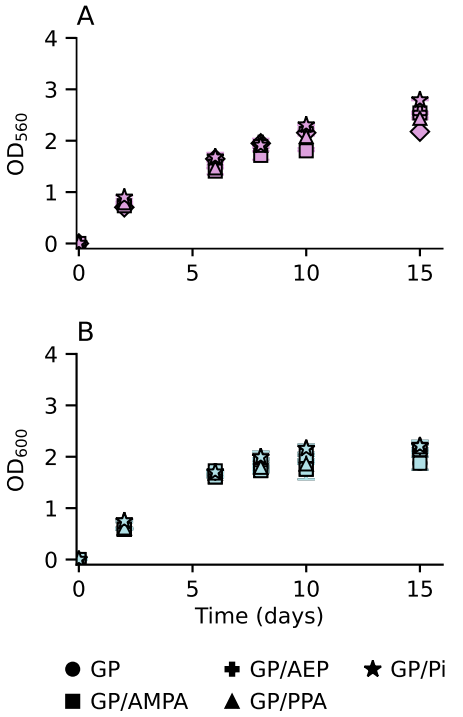

Figure A6. Optical density over time in competition experiments with A) *A*. Kg 19 (purple symbols) and B) *O*. GPr1-13 (green symbols). Glyphosate (GP) was either the sole P-source (c=0.5 mM) (circles) or provided in a mixture with equimolar concentrations (c=0.25 mM) of either Pi (stars), AMPA (squares), AEP (crosses), or PPA (triangles). Error bars represent the standard deviation of duplicate cultures (if not visible, error bars are smaller than the data points).

Table A8. Summary of organophosphonate (OP) and Pi transformation rates by *A*. Kg 19 and *O*. GPr1-13 calculated either between day 0 and 2 (black color) or between 2 and 6 (brown color).

Transformation rates (mM day^{-1})		
Experimental setup	**Strain *A*. Kg 19**	**Strain *O*. GPr1-13**
Glyphosate	Glyphosate = 0.098 ±0.006	Glyphosate = 0.077 ±0.004
Glyphosate + AMPA	Glyphosate = 0.023 ±0.004 AMPA = 0.093 ±0.001	Glyphosate = 0.051 ±0.003 AMPA = 0.080 ±0.003
Glyphosate + AEP	Glyphosate = 0.023 ±0.003 AEP ≥ 0.118 ±0.001	Glyphosate = 0.050 ±0.002 AEP ≥ 0.134 ±0.004
Glyphosate + PPA	Glyphosate = 0.026 ±0.003 PPA ≥ 0.121 ±0.001	Glyphosate = 0.058 ±0.005 PPA = 0.093 ±0.02
Glyphosate + Pi	Glyphosate = 0.036 ±0.002 Pi ≥ 0.143 ±0.008	Glyphosate = 0.059 ±0.006 Pi ≥ 0.148 ±0.008

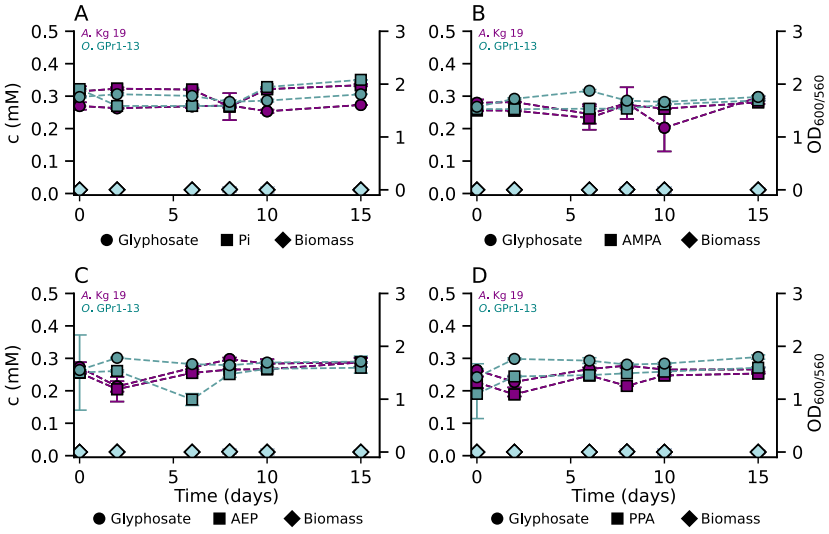

Figure A7. Glyphosate, AMPA, AEP, and Pi concentration in non-inoculated abiotic controls, and optical density over time in biotic P-free cultures. Glyphosate (GP) was added at 0.25 mM in parallel with equimolar concentrations of (A) Pi, B) AMPA, C) AEP, or (D) PPA. Diamonds represent optical density in biotic P-free controls, circles (connected by lines) represent glyphosate concentration, and squares (connected by lines) represent Pi, AMPA, AEP, or PPA concentration in non-inoculated abiotic controls. Abiotic and P-free controls were prepared in media used for *A*. Kg 19 (purple symbols) and *O*. GPr1-13 (green symbols). Error bars represent the standard deviation of duplicate setups (if not visible, error bars are smaller than the data points).

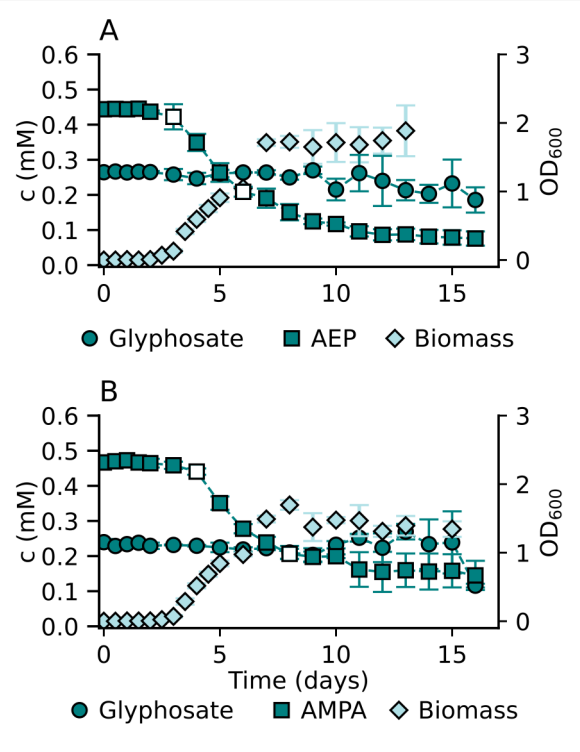

Figure A8. Glyphosate, AMPA, AEP concentrations, and optical density over time of *O*. GPr1-13. Glyphosate (GP) was provided at 0.25 mM in parallel with (A) AEP or (B) AMPA at c=0.5 mM. Diamonds represent optical density, circles (connected by lines) represent glyphosate concentration, and squares (connected

by lines) represent AEP or AMPA concentration. Data points marked with white symbols indicate the time points used to calculate the transformation rates of the OPs. Error bars represent the standard deviation of triplicate cultures (if not visible, error bars are smaller than the data points).

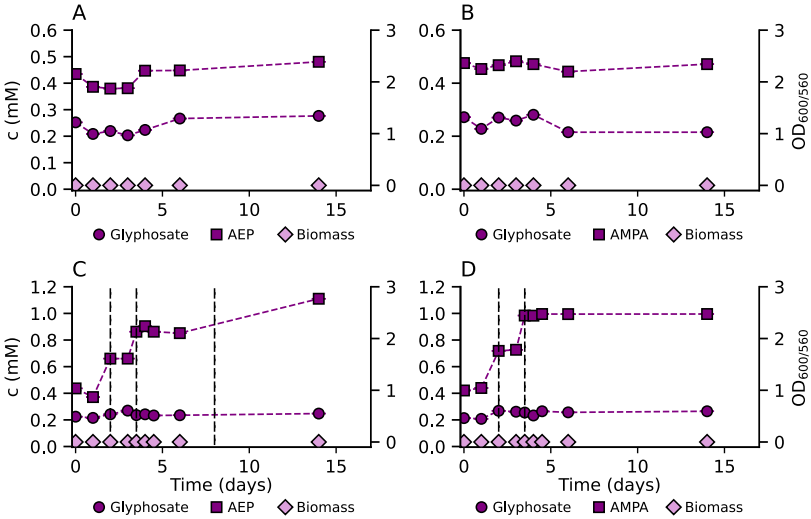

Figure A9. Glyphosate, AMPA, AEP concentrations, and optical density over time in spiking experiments in non-inoculated abiotic controls as well as in biotic P-free cultures. Glyphosate (GP) was added at 0.25 mM in parallel with (A), (C) AEP or (B), (D) AMPA. Diamonds represent optical density in biotic P-free controls, circles (connected by lines) represent glyphosate concentration, and squares (connected by lines) represent AEP or AMPA concentration. Dashed vertical lines indicate the days when controls were spiked with the respective compounds. After three pulses of AEP and two pulses of AMPA, the total concentrations of AEP and AMPA introduced were 1.25 mM and 1 mM, respectively. Abiotic controls were prepared in media used for *A*. Kg 19. Error bars represent the standard deviation of duplicates (if not visible, error bars are smaller than the data points).

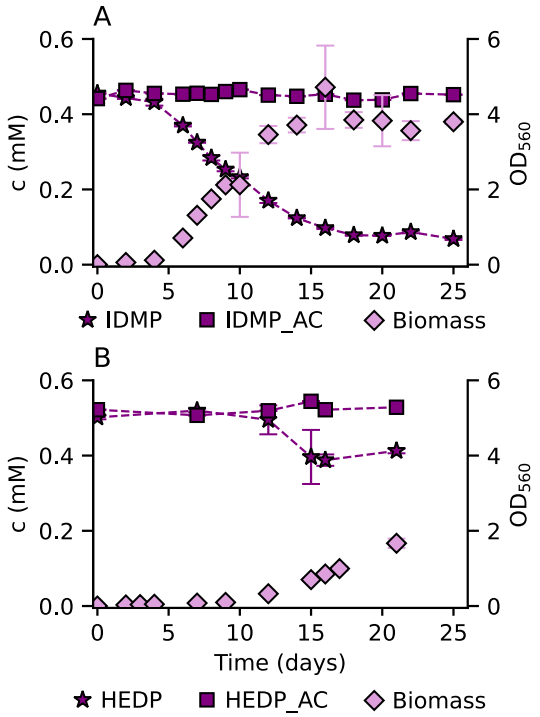

Figure A10. IDMP, HEDP concentrations, and optical density over time in experiments with *A*. Kg 19 as well as in non-inoculated abiotic controls (AC). A) IDMP and B) HEDP were provided at c=0.5 mM concentration. Stars (connected by lines) represent the concentration of IDMP or HEDP in cultures, and squares (connected by lines) represent the IDMP or HEDP concentration in abiotic controls (AC). Diamonds show optical densities of inoculated cultures. Abiotic controls were prepared in media used for *A*. Kg 19. Error bars represent standard deviation between duplicates (if not visible, error bars smaller than data points).

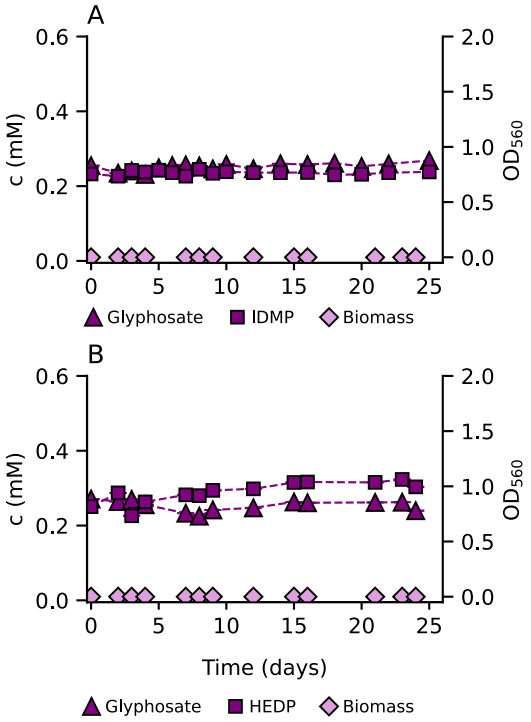

Figure A11. Glyphosate, IDMP, and HEDP concentration over time in non-inoculated abiotic controls. Glyphosate was added at c=0.25 mM in mixture with equimolar concentrations (c=0.25 mM) of A) IDMP or B) HEDP. Triangles (connected by lines) show glyphosate concentration and squares (connected by lines) represent IDMP or HEDP concentration. Diamonds represent optical density over time of A. Kg 19 in biotic P-free controls. Abiotic controls were prepared in media used for *A*. Kg 19. Error bars represent the standard deviation of duplicates (if not visible, error bars are smaller than the data points).

Table A9. Summary of OP transformation rates by *A*. Kg 19 and *O*. GPr1-13.

Transformation rates (mM day^{-1})		
Experimental setup	**Strain *A*. Kg 19**	**Strain *O*. GPr1-13**
Glyphosate	Glyphosate = 0.082 ±0.004	Glyphosate = 0.066 ±0.018
Glyphosate + AEP excess	Glyphosate = 0.106 ±0.026 AEP = 0.113 ±0.013	AEP = 0.071 ±0.009
Glyphosate + AMPA excess	Glyphosate = 0.061 ±0.006 AMPA = 0.039 ±0.001	AMPA = 0.059 ±0.002
Glyphosate + AEP spiking	AEP = 0.116 ±0.014	AEP = 0.073 ±0.009
Glyphosate + AMPA spiking	AMPA = 0.058 ±0.003	AMPA = 0.071 ±0.011
Glyphosate + IDMP	Glyphosate = 0.057 ±0.002 IDMP = 0.028 ±0.004	-
Glyphosate + HEDP	Glyphosate = 0.035 ±0.001	-

B Supporting information to chapter 3

Langmuir sorption isotherms

- Single adsorbate system

The Langmuir model is the classic mechanistic model for monolayer adsorption on homogeneous surfaces, characterized by saturation of sorption sites and can be described by the following equation:

$$c_{sorbed,i} = \frac{c_{sorbed,max,i} K_{L,i} c_{aq,i}}{1+K_{L,i} c_{aq,i}} \quad (1)$$

Where:

$c_{sorbed,i}$=amount adsorbed of compound *i* at equilibrium (mM g^{-1})

$c_{sorbed,max,i}$=maximum adsorption capacity of compound *i* (mM g^{-1})

$K_{L,i}$=Langmuir constant of compound *i* (L mM^{-1}) reflecting the affinity between the adsorbate and the surface of the sorbent

$c_{aq,i}$=equilibrium aqueous concentration of compound *i* (mM L^{-1})

- Multiple adsorbate system

The Langmuir model can easily be extended to scenarios where multiple compounds compete for the limited number of sorption sites.

$$c_{sorbed,i} = \frac{c_{sorbed,max,i} K_{L,i} c_{aq,i}}{1+(K_{L,i} c_{aq,i}+K_{L,j} c_{aq,j})} \quad (2)$$

$$c_{sorbed,j} = \frac{c_{sorbed,max,j} K_{L,j} c_{aq,j}}{1+(K_{L,i} c_{aq,i}+K_{L,j} c_{aq,j})} \quad (3)$$

Where i and j refer to the adsorbates (e.g., glyphosate and AMPA)

The normalized root-mean-square error (NRMSE) was employed to quantify the goodness of fit of the model, as defined by Eq. 4:

$$NRMSE = \frac{\sqrt{\frac{1}{N}\sum_{k=1}^{N}(y_{mod,k}-y_{ob,k})^2}}{y_{ob,max}-y_{ob,min}} \quad (4)$$

Where:

N=the number of observations

K=the observation indices

$y_{mod,k}$ and $y_{mod,k}$=the model predicted and observed values from eq. 1 and 3, respectively

$y_{ob,max}$ and $y_{ob,min}$=the maximum and minimum values of observation

NRMSE values range from 0 to 1. Values below 0.2 indicate strong agreement between predictions and observations.
Fitting was performed using python.

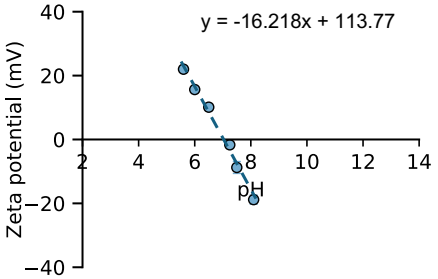

Figure B1. Zeta potential of goethite suspensions as a function of pH. The point of zero charge (pH_{pzc}) was determined to be 7.2 ± 0.1 from the zero-crossing of the zeta potential curve.

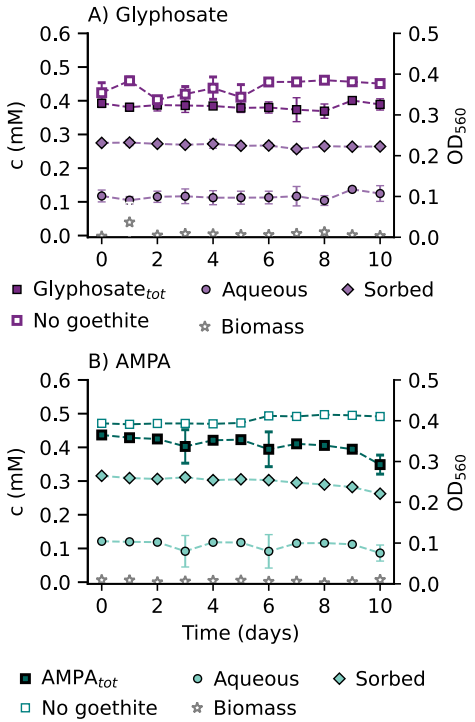

Figure B2. A) Glyphosate (purple symbols) and B) AMPA (green symbols) concentration when individually added in non-inoculated abiotic controls in the presence of goethite (28 g/L) at a concentration of 0.5 mM each. Circles (connected by lines) represent the aqueous concentrations, triangles (connected by lines) represent the sorbed concentrations, and squares (connected by lines) represent the sum of the aqueous and sorbed fractions. Open squares indicate glyphosate (purple symbols) and AMPA (green symbols) concentrations in non-inoculated abiotic controls without goethite. Open gray stars indicate optical density in biotic P-free controls with strain *A*. Kg 19 without goethite in presence of 0.5 mM A) glyphosate (purple symbols) and B) AMPA (green symbols). Error bars represent the standard deviation of triplicate setups (if not visible, error bars are smaller than the data points).

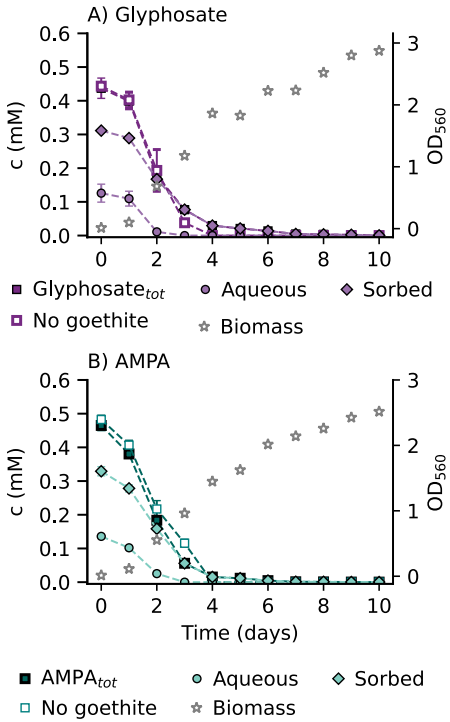

Figure B3. A) Glyphosate (purple symbols) and B) AMPA (green symbols) concentration when individually added in inoculated cultures with *A*. Kg 19 in the presence and absence of goethite (28 g/L) at a concentration of 0.25 mM each. Circles (connected by lines) represent the aqueous concentrations, triangles (connected by lines) represent the sorbed concentrations, and squares (connected by lines) represent the sum of the aqueous and sorbed fractions. Open squares indicate glyphosate (purple symbols) and AMPA (green symbols) concentrations in non-inoculated abiotic controls without goethite. Open squares indicate glyphosate (purple symbols) and AMPA (green symbols) concentrations in inoculated cultures without goethite. Open gray stars indicate optical density goethite-free setups inoculated with strain *A.* Kg 19 in the presence of 0.5 mM A) glyphosate (purple symbols) and B) AMPA (green symbols). Error bars represent the standard deviation of triplicate setups (if not visible, error bars are smaller than the data points).

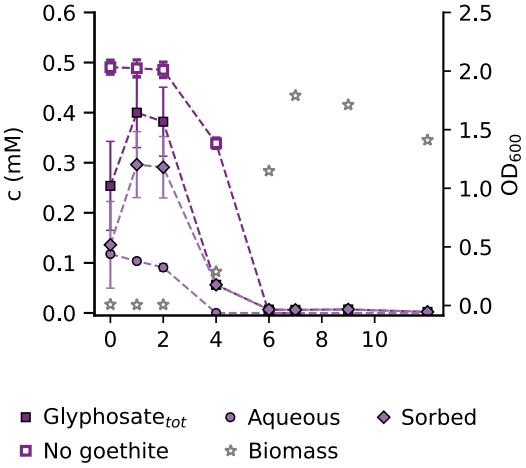

Figure B4. Glyphosate concentration when added in inoculated cultures with *O.* GPr1-13 in presence and absence of goethite (28 g/L) at a concentration of 0.25 mM. Circles (connected by lines) represent the aqueous concentrations, triangles (connected by lines) represent the sorbed concentrations and squares (connected by lines) represent the sum of the aqueous and sorbed fractions. Open squares indicate glyphosate concentrations in non-inoculated abiotic controls without goethite. Open squares indicate glyphosate concentrations in inoculated cultures without goethite. Open gray stars indicate optical density goethite-free setups inoculated with strain *O.* GPr1-13 in the presence of 0.5 mM glyphosate. Error bars represent the standard deviation of triplicate setups (if not visible, error bars are smaller than the data points).

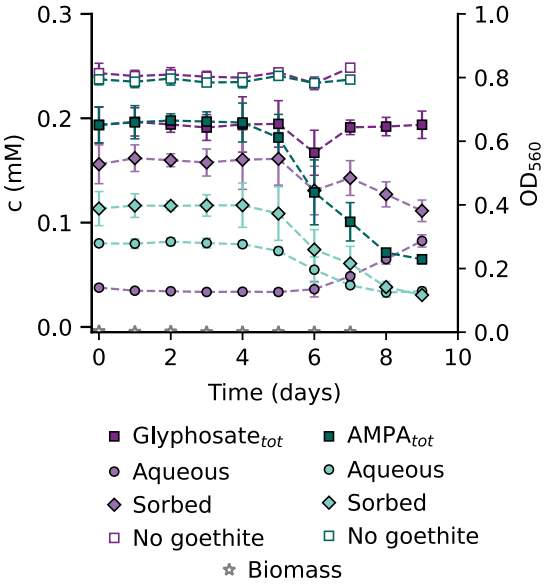

Figure B5. Glyphosate (purple symbols) and AMPA (green symbols) concentration when parallely added in non-inoculated abiotic controls in presence of goethite (28 g/L) at a concentration of 0.25 mM each. Circles (connected by lines) represent the aqueous concentrations, triangles (connected by lines) represent the sorbed concentrations and squares (connected by lines) represent the sum of the aqueous and sorbed fractions. Open squares indicate glyphosate (purple symbols) and AMPA (green symbols) concentrations in non-inoculated abiotic controls without goethite. Open gray stars indicate optical density in biotic P-free controls with strain *A*. Kg 19 wihtout goethite in presence of glyphosate (purple symbols) and AMPA (green symbols). From day 5 on, contamination was shown in the microcosm (dense pink cell pellet) which was associated with decreases in AMPA and glyphosate concentrations in non-inoculated abiotic controls. Error bars represent the standard deviation of triplicate setups (if not visible, error bars are smaller than the data points).

C Supporting information to chapter 4

Materials and methods

Setup of biodegradation batch experiments

Biotransformation experiments were performed with a rod-shaped bacterial strain *Achromobacter insolitus* strain Kg 19 (hereafter will be referred to as *A*. Kg 19) isolated from the Krasnodar region in Russia (45°03'10.8''N, 38°52'22.8''E) and obtained as freeze-dried culture from the Russian Centre of Microorganisms (VKM) (Tarlachkov et al., 2020). Pre-cultures were maintained in a carbon – and nitrogen–rich medium, buffered with 50 mM MOPS and supplemented with glyphosate as the sole P-source. For each experiment, a fresh inoculum was prepared by cultivating *A*. Kg 19 for 5 to 6 days, until a dense culture was obtained (optical density (OD) >> 1). Each experiment was initiated with the addition of 100 µL of a cell suspension to 100 mL of medium. The inoculum was prepared on the day the experiment was started as follows: 5 mL of the freshly growing culture was harvested and was subjected to centrifugation for 10 minutes at 7,000 rcf. The resulting cell pellets were washed twice by resuspension in centrifugation tubes using each time 5 mL sterile P-free medium. After the second washing step, the cell pellets were resuspended in 2.5 mL of the P-free medium, from which 100 µL was withdrawn and used as inoculum. All experiments were standardized to begin with a similar starting cell number, resulting in a cell density of approximately 10^6 cells mL^{-1}. The medium composition for *A*. Kg 19 ($Medium_1$) was comprised of: 10 (g/L) Na-glutamic acid as C-source, 2 (g/L) NH_4Cl as N-source, with 0.5 mM of the respective APP as P-source and was buffered at pH 7±1 with 50 (mM) MOPS. Additionally, the medium was supplemented with 1 mL/L of a 7-Vitamin solution, 0.2 g/L $MgSO_4$ x $7H_2O$, 0.5 (g/L) K_2SO_4, and a trace element solution with 2.5 (mg/L) $FeSO_4$ x $7H_20$, 10 (mg/L) $CaCl_2$ x $6H_2O$, 2 (mg/L) $CuSO_4$ x $5H_2O$, 0.06 (mg/L) H_3BO_3, 20 (mg/L) $ZnSO_4$ x $7H_2O$, 1 (mg/L) $MnSO_4$ x H_20, 0.05 (mg/L) $NiCl_2$ x $6H_2O$, 0.3 (mg/L) Na_2MoO_4 x $2H_2O$. For all biotransformation experiments 100 mL glass serum bottles, sterilized by dry heat at 180°C for 4.5 hours we used. the bottles continuously shaken on a rotary shaker at 150 rpm. Each culture was prepared under sterile conditions, filled with 100 mL of sterile medium, and adjusted to the desired OP concentration by adding a sterile-filtered stock solution prepared in the respective media. The serum bottles were sealed with sterile, oxygen-permeable cotton stoppers. The experiment was initiated by inoculating bottles with the living cells. Each experiment consisted of three living replicates, and three abiotic controls to assess potential interactions with the APPs and the medium.

Table C1. Media composition for the cultivation of the *Achromobacter insolitus* strain Kg 19 (VKM B-3295) (hereafter will be referred to as *A*. Kg 19).

Compound	**Empirical formula**	**Concentration**
Monosodium glutamic acid (glutamate)	$NaC_5H_9NO_4$	10 g L^{-1}
Ammonium chloride	NH_4Cl	2 g L^{-1}
Potassium sulfate	K_2SO_4	0.5 g L^{-1}
Magnesium sulfate heptahydrate	$MgSO_4 * 7H_2O$	0.2 g L^{-1}
3-(morpholino)propanesulfonic acid (MOPS)	$C_7H_{15}NO_4S$	50 mmol L^{-1}
Sodium hydroxide for pH adjustment	NaOH (stock 1 mol L^{-1})	-
7-Vitamin solution		1 mL L^{-1}
Zinc sulfate heptahydrate	$ZnSO_4 * 7H_2O$	20 mg L^{-1}
Calcium chloride hexahydrate	$CaCl_2 * 6H_2O$	10 mg L^{-1}
Iron sulfate heptahydrate	$FeSO_4 * 7H_20$	2.5 mg L^{-1}
Copper sulfate pentahydrate	$CuSO_4 * 5H_2O$	2 mg L^{-1}
Manganese sulfate monohydrate	$MnSO_4 * H_2O$	1 mg L^{-1}
Sodium molybdate	Na_2MoO_4	0.3 mg L^{-1}
Boric acid	H_3BO_3	0.06 mg L^{-1}
Nickel chloride hexahydrate	$NiCl_2 * 6H_2O$	0.05 mg L^{-1}

Table C2. Media composition for the cultivation of the *Ochrobactrum pituitosum* strain GPr1-13 (hereafter will be referred to as *O*. GPr1-13).

Compound	**Empirical formula**	**Concentration**
Monosodium glutamic acid (glutamate)	$NaC_5H_9NO_4$	10 g L^{-1}
Ammonium chloride	NH_4Cl	5 g L^{-1}
Potassium sulfate	K_2SO_4	0.5 g L^{-1}
Magnesium sulfate heptahydrate	$MgSO_4 * 7H_2O$	0.16 g L^{-1}
Calcium chloride dihydrate	$CaCl_2 * 2H_2O$	0.08 g L^{-1}
3-(morpholino)propanesulfonic acid (MOPS)	$C_7H_{15}NO_4S$	50 mmol L^{-1}

Sodium hydroxide for pH adjustment	NaOH (stock 1 mol L^{-1})	-
7-Vitamin solution		1 mL L^{-1}

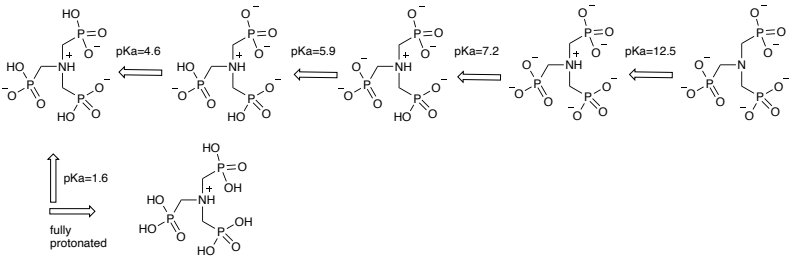

Figure C1: pH-dependent speciation of ATMP. ATMP acidity constants for an ionic strength of 0.1 at 25°C taken from Deluchat et al., (1997).

Results and Discussion

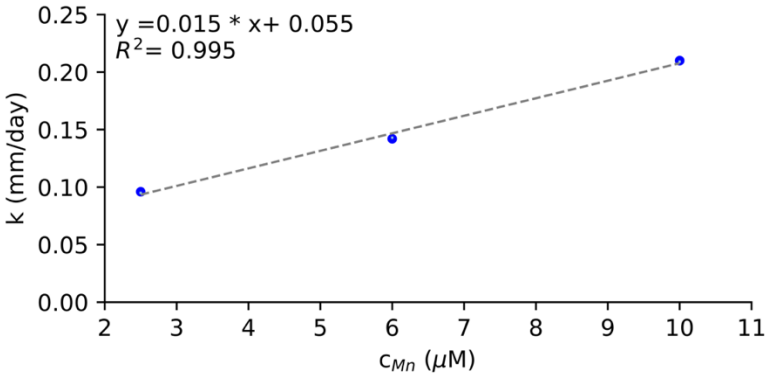

Figure C2: ATMP transformation rates as a function of Mn (II) concentration. The degradation rate increased linearly with Mn(II) levels, with measured rates of

0.096 ± 0.003, 0.142 ± 0.010, and 0.210 ± 0.006 mM day^{-1} for Mn(II) concentrations of 2.5, 6, and 10 µM, respectively. Symbols represent the calculated rates, and the dashed line indicates the linear fit.

Table C3. Formation constants for metal-EDTA complexes extracted from thermodynamic database in VisualMINTEQ (thermo.vdb).

Ion	**LogK**
Cu^{2+}	20.5
Zn^{2+}	18.0
Fe^{2+}	16.0
Mn^{2+}	15.6
Ca^{2+}	12.4
Mg^{2+}	10.6

The formation of these complexes can be represented generally by the equilibrium:

$$M^n + EDTA^{-4} = MEDTA^{n-4}$$

where:
$M^n = any\ metal\ cation$ (e.g., $Cu^{2+}, Zn^{2+}, Fe^{2+}$)
$MEDTA^{n-4} = the\ metal - EDTA\ chelate\ complex$

References

Deluchat, V., Bollinger, J. C., Serpaud, B., & Caullet, C. (1997). Divalent cations speciation with three phosphonate ligands in the pH-range of natural waters. *Talanta*, *44*(5), 897–907. https://doi.org/10.1016/S0039-9140(96)02136-4

Tarlachkov, S. V., Epiktetov, D. O., Sviridov, A. V., Shushkova, T. V., Ermakova, I. T., & Leontievsky, A. A. (2020). Draft Genome Sequence of Glyphosate-Degrading Achromobacter insolitus Strain Kg 19 (VKM B-3295), Isolated from Agricultural Soil. *Microbiology Resource Announcements*, *9*(17), 19–20. https://doi.org/10.1128/mra.00284-20

D Supporting information to chapter 5

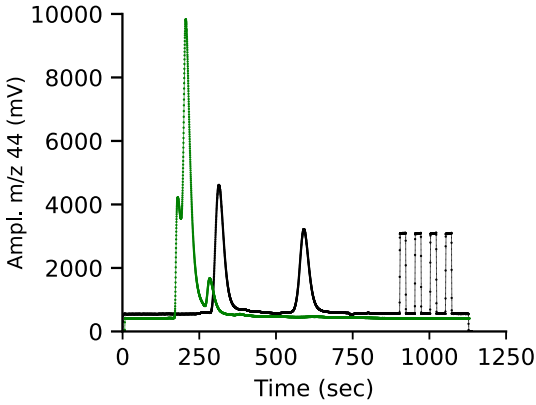

Figure D1. LC-IRMS chromatograms (amplitude, m/z 44 over time) of glyphosate standard 0.25 mM and 0.1 mM glutamate as well as MOPS 20 mM (external standard with green color) prepared in mQ. Glyphosate, glutamate and MOPS elute after approximately 600, 255 and 190 s, respectively using a Shodex IC NI-424 column (4.6 × 100 mm) at pH 3.1. The four peaks at the end of both chromatograms correspond to the CO_2 monitoring gas.

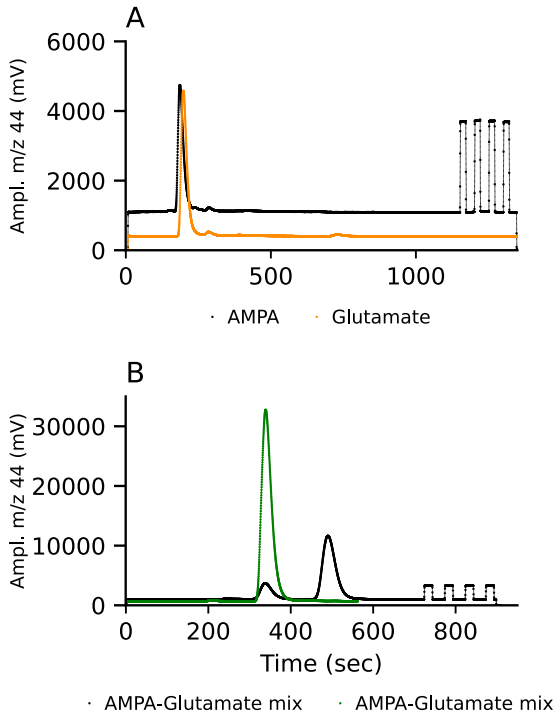

Figure D2. LC-IRMS chromatograms (amplitude, m/z 44 over time) of AMPA and glutamate under different separation conditions. A) AMPA (0.5 mM, black color) and glutamate (0.15 mM, external standard with orange color) on a Shodex IC NI-424 column. No chromatographic separation between the analytes can be achieved, with AMPA and glutamate eluting at approximately 186 s and 255 s, respectively. B) AMPA and glutamate (both 0.5 mM) and MOPS (external standard with green color) retention times on a Primesep column. Retention times for AMPA, glutamate and MOPS were at approximately 350, 456, and 340 s, respectively. Separation could be achieved only in unbuffered growth medium. The four peaks at the end of both chromatograms correspond to the CO_2 monitoring gas.

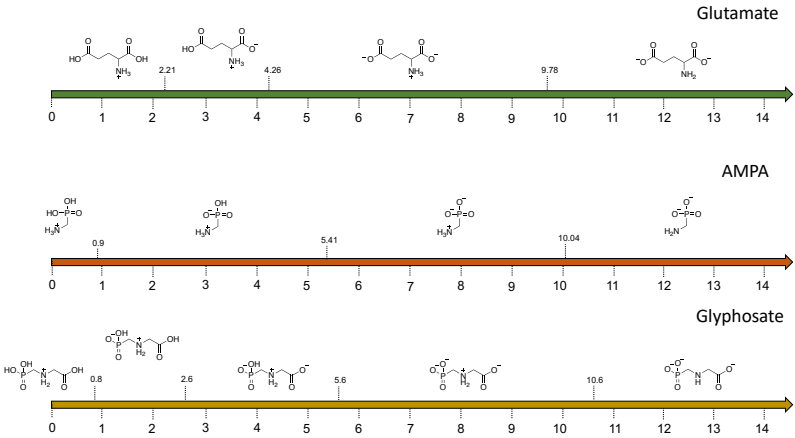

Figure D3. Speciation and pKa values of glyphosate (pKa values from Sprankle et al., 1975; Sidoli et al., 2016), AMPA (pKa values from Popov et al., 2001), and glutamic acid (glutamate, pKa values from Šarac & Hadži, 2021).

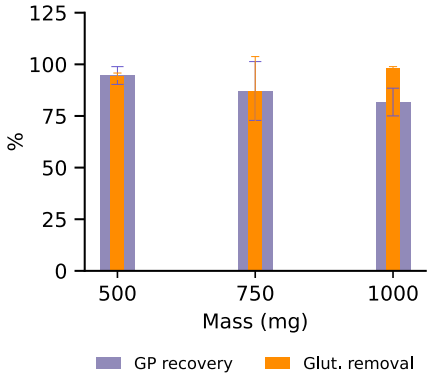

Figure D4. Effect of resin amount on glyphosate recovery and glutamate removal. Recovery of glyphosate and removal of glutamate following SPE-treatment with varying amounts (500-100 mg) of strong cation exchange resin (Dowex) at pH 1.5. All samples contained 0.05 mM glyphosate prior to treatment. Purple bars indicate glyphosate recovery, calculated by comparing nominal concentrations with those measured after treatment. Orange bars represent glutamate removal efficiency,

calculated as the percentage decrease between initial (nominal) and post-treatment concentrations. Error bars represent the deviation between duplicate samples.

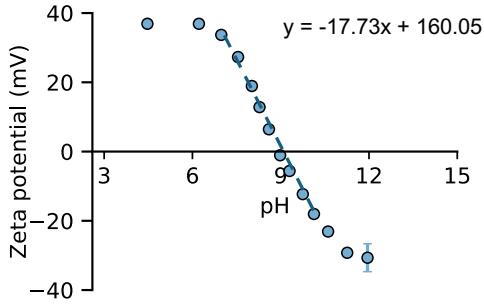

Figure D5. Zeta potential of A_2O_4 suspensions as a function of pH. The point of zero charge (pHpzc) was determined to be 9.0 ± 0.1 from the zero-crossing of the zeta potential curve.

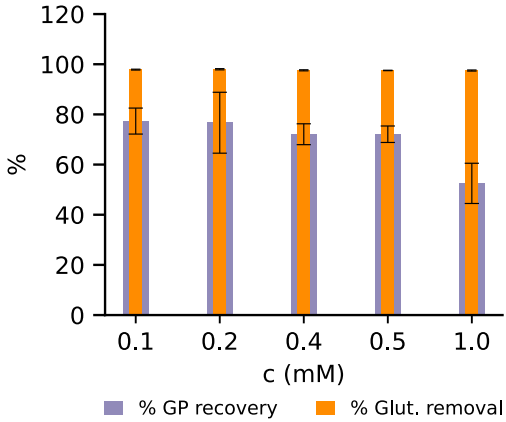

Figure D6. Effect of glyphosate concentration (0.1–1 mM) on glyphosate recovery and glutamate removal using 250 mg of Al_2O_3 sorbent after column-SPE. Purple bars show glyphosate recovery percentages, calculated by comparing nominal glyphosate concentrations to those measured post-cleanup. Orange bars indicate glutamate removal efficiency, expressed as the percentage decrease in glutamate concentration after treatment. Error bars represent deviations between duplicate samples.

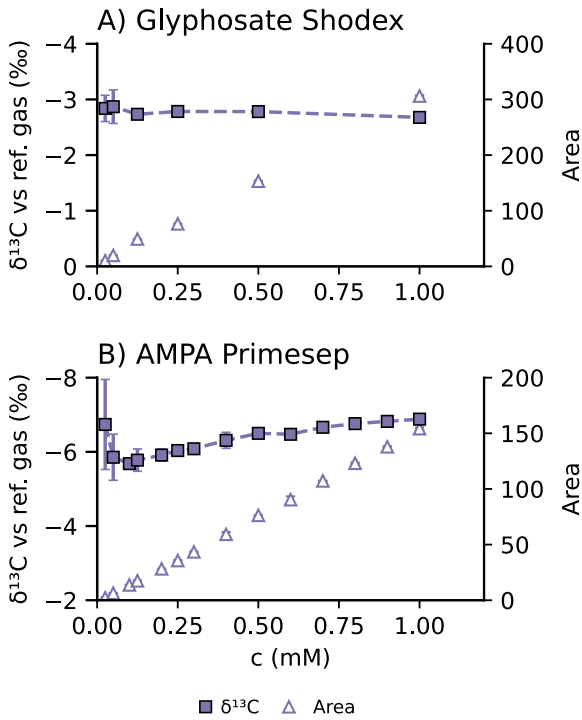

Figure D7: Linearity plots for (A) glyphosate (B) AMPA showing the dependency of the measured isotopic signature on the concentration and the amount of carbon on column, respectively. Glyphosate and AMPA were tested in a concentration range 0.0125 to 1 mM prepared in ultrapure water. Error bars correspond to the standard deviations of triplicate measurements.

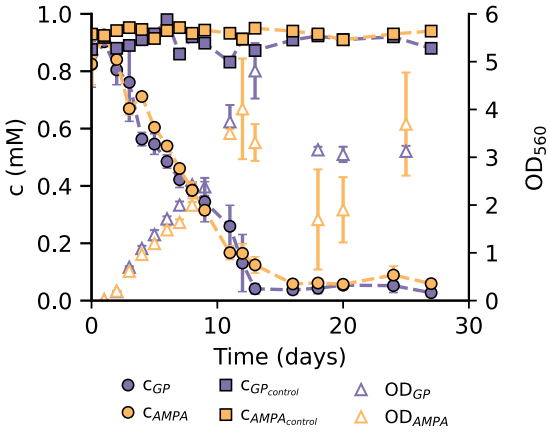

Figure D8. Changes in glyphosate and AMPA concentrations and optical density over time in the cultivation experiment with *A.* Kg 19. Glyphosate and AMPA were supplied as the sole phosphorus sources at 1 mM, and samples were subsequently treated with Al_2O_3. Circles connected by lines indicate the concentrations of glyphosate (purple) and AMPA (orange) over time in inoculated setups while squares represent concentrations is abiotic controls. Triangles represent changes in optical density (OD_{560}). Error bars show the standard deviation of triplicate measurements (if not visible, error bards are smaller than the symbols).

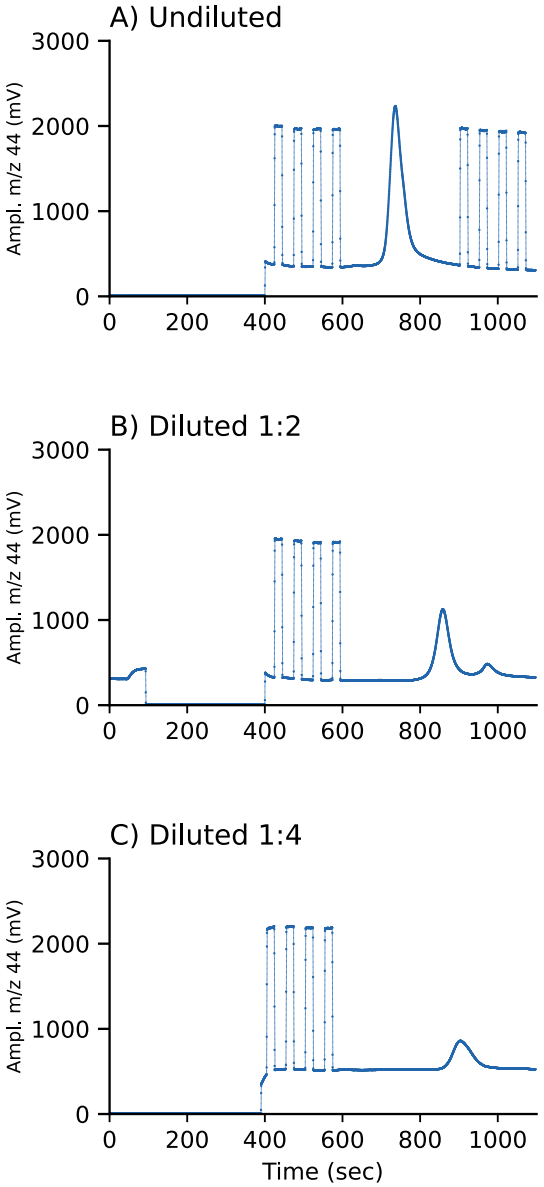
A) Undiluted
B) Diluted 1:2
C) Diluted 1:4
Ampl. m/z 44 (mV)
0
1000
2000
3000
0
200
400
600
800
1000
Time (sec)

Figure D9: LC-IRMS chromatograms (amplitude, m/z 44 over time) of glyphosate-containing samples from day 11 at varying dilution factors after Al_2O_3 cleanup. A) Chromatogram of the undiluted sample (c = 0.23 mM), with measured $\delta^{13}C_{glyphosate}$ value equal to 5.7765 ± 0.3642‰ (n = 3). B) Chromatogram of the same sample diluted 1:2 (c_final = 0.12 mM), showing two distinct of glyphosate and matrix. The $\delta^{13}C_{glyphosate}$ value was -0.664 ± 0.709‰ (n = 3). C) Chromatogram of a 1:4 diluted sample (c_final = 0.06 mM), displaying a clearly defined glyphosate peak with minimal matrix influence. The $\delta^{13}C_{glyphosate}$ value was −0.630 ± 0.122‰ (n = 3).

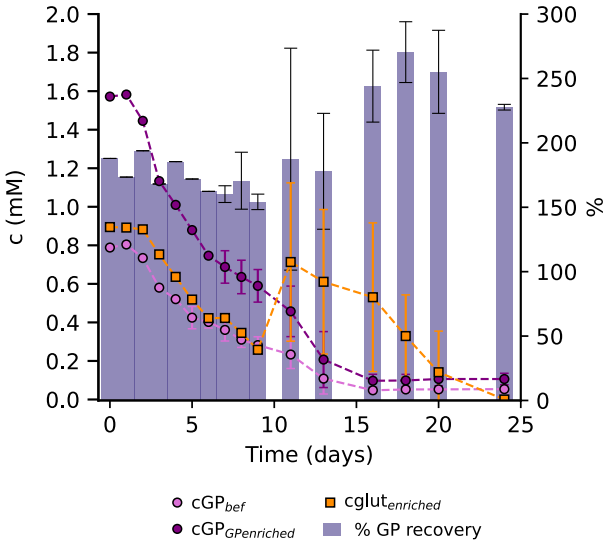

Figure D10. Transformation of glyphosate by strain *A.* Kg 19 and recovery following treatment with 250 mg Al_2O_3, including enrichment by elution with half the volume used for sorption. Purple circles (connected by lines) show glyphosate concentrations during the transformation experiment after Al_2O_3 cleanup, while pink circles represent glyphosate concentrations after cleanup and enrichment. Orange squares (connected by lines) indicate remaining glutamate concentrations following Al_2O_3 treatment. Purple bars show the percentage of glyphosate recovery, calculated by comparing nominal analyte concentrations to those measured after treatment. Error bars represent deviations between duplicate samples.

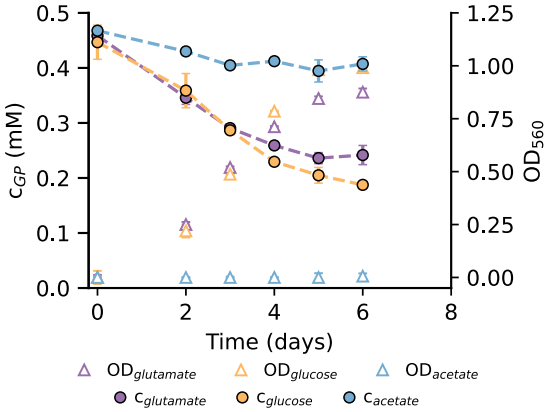

Figure D11. Changes in glyphosate concentration and optical density over time in cultivation experiments with *A.* Kg 19 using different carbon sources. Glyphosate was supplied as the sole phosphorus source at 0.5 mM. Circles connected by lines indicate glyphosate concentrations for each setup: glutamate (purple), glucose (orange), and acetate (light blue). Triangles represent changes in optical density (OD_{560}). Error bars show the standard deviation of triplicate measurements (if not visible, error bars are smaller than the symbols).

Acknowledgements

I would like to express my deepest gratitude to Prof. Stefan B. Haderlein for giving me the opportunity to conduct my PhD research within his group and laboratory. Thank you, Stefan, for being such a supportive supervisor! Your expertise, invaluable guidance, and continuous encouragement have been essential to the progress and completion of this work. I am truly grateful for your calming presence during challenging times and for never being denied resources or access to equipment, which ensured I always had the support needed for my experiments. Working under your supervision has been a truly rewarding experience.

I would also like to thank Prof. Peter Grathwohl for serving as the second reviewer of my thesis. I am also grateful for his contributions to my academic journey, as he first hosted me during my internship and kindly introduced me to his group, the department, and the Master's program in Applied and Environmental Geoscience. Further, I would like to thank Prof. Michaela Dippold as well as Prof. Christiane Zarfl for evaluating my thesis as members of my doctoral committee.

I would like to express special thanks to Dr. Philipp Martin, whose guidance and support profoundly shaped my research journey. Your deep knowledge was truly inspiring, and your structured, logical thinking—combined with your meticulous care for our analytical instruments—created a very reliable work environment. I am especially grateful for your encouragement during the first two years of my PhD, a time when the light at the end of the PhD-tunnel was still unseen.

Many thanks to Dr. Daniel Buchner for our collaboration, the ongoing interest in my work, the encouragement, and the generous support in providing student assistants. I am also grateful to Dr. Katharine Thompson for our collaboration and for always making time for me, even during your busiest periods. Special thanks to my MSc thesis supervisor, Dr. Johannes Scheckenbach, who introduced me to the field of glyphosate biotransformation, taught me essential techniques, and inspired me to continue developing this research topic. I hope the results reflect, at least in part, your original vision.

To my office mates—Dr. Anna Röhnelt, Ruoning Guo, and Jule Werner—thank you for creating such a pleasant atmosphere and for the friendly chats during breaks. I am especially grateful to Sara Wild for her cheerfulness and kindness, which made our group so welcoming. I would also like to thank the entire

Acknowledgements

Environmental Chemistry and Mineralogy working group, both former and current members, for fostering a collaborative and supportive environment. The open exchange of ideas, helpful discussions, and daily interactions made this journey not only productive but also truly enjoyable. Further on, I am also thankful to the MSc students—Martin, Tamara, and Larissa, as well as the BSc students Ellen and Teresa, who have worked with me for some time on these projects. It was wonderful to see your dedication and curiosity in action.

My sincere thanks go to all the dedicated technical staff at ZAG: Stepfanie Nowak, Bernice Nisch, Renate Seelig, Jana Geiselhardt, Björn Spranglewski, as well as Franzi Schädler and Lars Grimm—for always being ready to help with a cheerful smile. I also wish to thank Dr. Stefan Fischer and Dr. Michaela Wilsch-Bräuninger for performing the SEM imaging essential to my experiments.

A heartfelt and deeply grateful thank you goes to my family—my parents and my two sisters—who, even without fully grasping the challenges of this field, stood by me with unwavering support, love, and understanding throughout this journey. Despite the distance and the hardships, they made every effort to bridge the gap, visiting whenever they could, bringing warmth and comfort that helped me carry on.

To my closest friends, Despina and Eleni, who have long become my chosen family—words cannot fully express how grateful I am for your unwavering support and understanding throughout this journey. Although distance separated us, time was scarce, and our workloads demanding, your presence in my life never wavered—not for a single day. The joy of planning our summer breaks, even during the coldest winter days, always brightened my days. Thank you for standing by me, cheering me on from afar, and reminding me of who I am beyond the PhD. Most of all, thank you for sharing this wild and beautiful ride with me.

Finally, to my partner, Giorgos, thank you for being present and supportive, for clearing the shadows in my mind—even during times when your own PhD weighed heavily on you. Coming home after long days in the lab and finding you there was a true blessing, especially in moments when it felt like doors were closing. Your presence gave me strength and perspective when I needed it most!

This thesis would not have been possible without your involvement in the science and/or in my private life. Thank you all for walking this journey with me!

Acknowledgements

Acknowledgements